Development of a Next-generation Experimentation Robotic Vehicle (NERV) that Supports Intelligent and Autonomous Systems Research

Sean Marshall Baity

Thesis submitted to the faculty of the Virginia Polytechnic Institute and State University
in partial fulfillment of the requirements for the degree of

Master of Science
In
Mechanical Engineering

Dr. Charles F. Reinholtz, Chairman
Dept. of Mechanical Engineering

Dr. Alfred L. Wicks
Dept. of Mechanical Engineering

Dr. Robert H. Sturges, Jr., P.E.
Dept. of Industrial Systems Engineering
Dept. of Mechanical Engineering

December 9, 2005
Blacksburg, Virginia

Keywords: Unmanned Ground Vehicle, Autonomous Vehicle, Experimentation, System Integration, Robotic Vehicle Design, Mobile Robot Kinematic Design

Development of a Next-generation Experimentation Robotic Vehicle (NERV) that Supports Intelligent and Autonomous Systems Research

Sean Marshall Baity

ABSTRACT

Recent advances in technology have enabled the development of truly autonomous ground vehicles capable of performing complex navigation tasks. As a result, the demand for practical unmanned ground vehicle (UGV) systems has increased dramatically in recent years. Central to these developments is maturation of emerging mobile robotic intelligent and autonomous capability. While the progress UGV technology has been substantial, there are many challenges that still face unmanned vehicle system developers. Foremost is the improvement of perception hardware and intelligent software that supports the evolution of UGV capability.

The development of a Next-generation Experimentation Robotic Vehicle (NERV) serves to provide a small UGV baseline platform supporting experimentation focused on progression of the state-of-the-art in unmanned systems. Supporting research and user feedback highlight the needs that provide justification for an advanced small UGV research platform. Primarily, such a vehicle must be based upon open and technology independent system architecture while exhibiting improved mobility over relatively structured terrain.

To this end, a theoretical kinematic model is presented for a novel two-body multi degree-of-freedom, four-wheel drive, small UGV platform. The efficacy of the theoretical kinematic model was validated through computer simulation and experimentation on a full-scale proof-of-concept mobile robotic platform. The kinematic model provides the foundation for autonomous multi-body control. Further, a modular system level design based upon the concepts of the Joint Architecture for Unmanned Systems (JAUS) is offered as an open architecture model providing a scalable system integration solution. Together these elements provide a blueprint for the development of a small UGV capable of supporting the needs of a wide range of leading-edge intelligent system research initiatives.

Acknowledgements

The completion of this work would not be possible without the support of several people. I would first like to thank my wife Christina Baity for her assistance, thoughtful insight, and forbearance during the completion of this document. Her extraordinary understanding and patience has been invaluable as the pursuit of developing intelligent robots has consumed much of my time and energy. I would also like to express my deepest appreciation to my parents Paul and Debbi Baity for providing me with the opportunity and unconditional support to continue my education despite difficulty and hardship.

I would also like to express my gratitude to both Dr. Charles Reinholtz and Dr. Al Wicks. Both provided much appreciated technical discourse and sagacious advice with an uncommon youthful exuberance that afforded a uniquely stimulating and multi-faceted experience.

I would be remiss without mentioning my deep appreciation of my colleagues at Virginia Tech with their perpetually astounding collective ingenuity and remarkable skill. Particularly, I would like to thank Brett Gombar, Ben Hastings, and Andrew Bacha for their technical assistance during the long and arduous process of developing this work.

Finally, I would like to thank those, past and present, who have participated in the development of the autonomous vehicle technologies at Virginia Tech. Without their shared contributions, the work that I have pursued would be wholly impossible.

This work was supported by Army Research Development Engineering Command Simulation Technology Training Center (RDECOM-STTC) under contract N61339-04-C-0062.

Table of Contents

Index of Figures

Index of Tables

Index of Equations

1 Introduction

While there is undeniable potential for unmanned ground vehicle (UGV) mobile robotics, there is an arresting immaturity of supporting intelligent control and perception solutions. Although current state-of-the-art teleoperated vehicles do provide invaluable services, there is a strong aspiration and concerted effort to provide robotic UGV platforms with increasing levels of intelligence leading towards autonomous capabilities. In order to accomplish this task, increased research efforts of the unmanned systems research community must be adequately supported by hardware and mobility platforms that facilitate the development of the next generation breakthroughs in computing and intelligence algorithms.

1.1 Motivation

The motivation of this thesis is to outline the foundation of design and approach for the development of a small UGV that is capable of serving as a catalyst for the progression of the state-of-the-art in intelligent systems. The goal of the proposed design, rationale, and supporting research is to develop a thoughtfully considered unmanned ground vehicle that is capable of meeting the growing needs of the unmanned robotics research community at large.

Within this broad definition of design intent, there is a distinct need to investigate key elements of small UGV design in an attempt to develop the provisions for a largely applicable mobile robotic platform. Thoughtful and technologically relevant design of the physical robotic platform is essential to supporting leading-edge components and solutions fundamental to the development of autonomous capability. Further, scalable and open system architecture design and elemental integration schema provide the means for researchers to attain the latitude to seek new ideas and retain the capability to refine novel intelligent solutions.

The development of a design outline, including the kinematic design of a mobile robotic platform and a model system architecture schema, will provide the means for the creation of a small UGV capable of supporting experimentation and research in the area of unmanned systems.

1.2 Justification for the Next-generation Experimentation Robotic Vehicle (NERV)

The current Congressional mandate for the U.S. Army to field unmanned ground combat systems that comprise one-third of their total fighting force by 2015 is not unlike the optimistic Presidential proclamation of support for the ambition of sending man to the moon before the close of the 1960's [1]. Such a lofty goal, charged by diligent government backing, has ignited the development of unmanned systems for military applications. Emerging from this large-scale programmatic emphasis on the inclusion of unmanned systems are comprehensive development efforts focused on the creation of unmanned solutions for military applications. The primary goal of this development is to remove the soldier from dangerous situations through the extension of a soldier's own capabilities. However, robotic systems "need not operate in an actively hostile environment to perform a valuable high-payoff function" [2]. Apart from saving lives, the inclusion of robotic solutions into military operations seeks to automate the pervasively mundane tasks of military operations and to allow a soldier to perform the tasks for which they are trained to carry out. The result is that robotic systems, particularly unmanned solutions, provide for a more flexible and efficient military. Building upon long standing unmanned aerial vehicles (UAV) development and nearly 15 years of UGV research, the military is determined to develop UGV technology and is poised to integrate intelligent ground vehicles into the fabric of military operations.

Although there is a great initiative to support UGV development within the military, there are also many other areas where unmanned ground systems hold the very real promise of becoming ubiquitous productive contributors [3]. The current development of unmanned vehicle technologies through well-supported government programs will undoubtedly prove to be the catalyst for large scale integration of unmanned systems within the private sector. In fact, projections of the impact of the current 2005 U.S. $150 billion Future Combat Systems (FCS) initiative indicate a tremendous explosion in robot markets for domestic use [4]. A 2005 United Nations study indicated that the military initiative towards unmanned vehicles at all levels will increase the rate and amount that unmanned technologies will enter daily life. The report cited the continued growth of industrial robots and the maturation of the home market including unmanned robots for both entertainment and service. Analysis of funding for the FCS market indicates that the $1.7 billion dollar government based program will expand to nearly $6 billion by 2010 as unmanned technologies are rolled into service and continue to prove invaluable in the field [5]. With this in mind, there is little question that unmanned systems are a key element to the future to both military and civilian interests.

With the projection of the expanding consumer marketplace for unmanned systems, the inevitable research efforts supporting this growth will not be relegated to defense interests alone. While this potential proliferation of unmanned systems into civilian applications will no doubt be supported by the maturation of fundamental technologies resulting from government initiatives, commercial research endeavors will be needed to meet the projected consumer interest. This leads to the conclusion that the potential market for unmanned intelligent vehicle system spans multiple sectors and will require vast research resources to attempt to meet the prospective demands [6]. This broad movement towards unmanned systems development is supported by the desire to remove people from the dull, dirty, and dangerous aspects of everyday life.

In either a military or civilian venue, intelligent unmanned vehicle systems will prove to be a vital aspect to many future technology development programs. Acknowledging this increasing emphasis on providing intelligent unmanned systems, the Joint Robotics Program (JRP) Master Plan for 2004 outlines the four main methods by which the JRP will posture itself for future success [7]:

- Evolving UGV systems as user requirements change
- Ensuring that autonomous capability can be inserted into current force systems
- Developing second generation programs
- Continuing to advance the intelligence of unmanned systems

Based upon these four objectives, it is notable that the primary focus of the JRP methods for meeting the rapidly evolving service requirements for unmanned ground systems centers upon providing autonomous capability. Further, the JRP acknowledges that the integration of leading technology from a variety of contributors will be a monumental and essential task as future systems are developed. The JRP directed Joint Architecture for Unmanned Systems (JAUS) working group facilitates this multi-developer approach through the creation of a technology independent standard for system development and integration known as the aims to facilitate multi-point development efforts [8].

As a result of the historical progression of unmanned ground vehicle systems technology through military channels, there has been a distinct emphasis of mobility platform designers to meet the needs of the armed forces. While the resulting platforms are adept at meeting the demands of field commanders and have proven capable in the rugged

environment commonly encountered on the battlefield, they have done so with support extensive long-term development programs fueled by substantial government funding. The resultant of these research efforts are extremely robust mobility platforms that are either prohibitively expensive for or restricted from use by most civilian interests. Additionally, commercially available robotic platforms are generally developed to meet a specific market segment such as the small tracked teleoperated UGV mobility platforms for Military Operations in Urban Terrain (MOUT) or urban search and rescue. Such targeted design and mission profile often limits the effective transferal of such vehicles in other areas of research and development. For example, a small teleoperated tracked platform, while being more than adept at negotiating difficult urban terrain, is ill-suited for long distance travel applications. Additional characteristics that limit the application of such teleoperated vehicles to a broader range of research programs are the lack of available power, limited operational range between operator and vehicle, and limited speed. Further complicating the application of commercially available unmanned platforms within research is that the concern for proprietary protection often the leads to technologies that are built upon a closed system architecture that thwart any attempt to expand the vehicle's capabilities.

This closed-architecture approach and limited capability of current small UGV platforms poses a substantial obstacle for those researchers who are striving to develop the next-generation of intelligent systems. Being without accessible UGV platforms on which real-world experimentation and testing inhibits the ability to efficiently and effectively investigate progressive research topics. To address this need, many academic and commercial efforts have responded in three distinct ways: 1) Retrofit or repurpose traditional manned vehicle platforms to become unmanned, 2) develop custom mobile robots as research test-beds, or 3) attempt to up-fit an earlier generation unmanned system. While all three methods do provide a means to develop a suitable mobility platform, they do so often at high cost with prolonged development cycles and at the expense of possible future functionality.

Complicating matters further, the development of a mobility platform may lie outside the scope of a particular research group's expertise, time constraints, or mission statement. For example, various groups focus on the development of intelligent software and algorithms while not developing a specific platform on which to test their product outcomes in real-world settings. Such organizations include university programs, commercial software developers, and military organizations charged with developing such technologies as autonomous navigation simulations, cooperative communication or adaptive networking protocols, and cooperative mission behaviors. The requirements for a robotic platform in such a context are

generally geared towards a specific research application, often carried out in controlled environments, where a single key technology concept is demonstrated and matured. This consigns such organizations to search for a viable platform on which to apply their technology when real-world experimentation is required.

There is the additional difficulty of integrating the results of such efforts amongst the research community. With respect to the challenge of integrating robotics research with the end goal of developing intelligent vehicle systems, David Kortenkamp reports that through discussions at several technical meetings, unmanned robotics researchers identified four main issues that needed to be addressed [9]. These issues, in order of identified importance, are:

1. Researchers must have a consistent way of describing the problems they are addressing.

2. Researchers must be able to measure the effectiveness of various robotics components in different environments and situations.

3. Researchers must be able to exchange components and should easily integrate outside components on their hardware and in their environments.

4. Researchers must have the support of funding agencies to do integration research and to distribute their results.

Furthermore, Kortenkamp notes that while many robotic solutions may be developed; there is little value to a potential user if there is no means to differentiate the performance with regards to the potential end application situation. The implication of this observation being that development of a standard baseline unmanned vehicle platform is essential to the progression of the state-of-the-art.

In response to this increasing and pressing need to support the growth in unmanned system technologies, the development of a Next-generation Experimentation Vehicle (NERV) mutually suited to supporting military, industrial, and commercial research efforts will serve to enable a more effective and broadly successful expansion of UGV technologies. To be successful such a system must display attributes that focus on the needs of researchers at various levels. This includes addressing the procurement, development, and performance obstacles associated with currently available small UGV mobility platforms. Further, acknowledging the fact that not all development work need be carried out on the final

application mobility platform to be valuable to the progression of unmanned technologies. Rather, a standard small UGV platform for intelligent systems design would provide uniformity on which comparisons can be made and conclusions can be drawn in a more effective and efficient manner. In total, unmanned system developers stand to benefit from the use of a well developed open architecture platform that is scalable in the ability to meet a variety of mission profiles.

1.2.1 Customer Defined Needs

A targeted approach to meet the needs of a system developer at an experimental level hinges upon the engineering and practical value of an NERV solution. Building upon the customer opinions derived by Kortenkamp, the NERV must be able to display the following fundamental attributes in order to meet the needs of the ever expanding unmanned systems community:

- Provide a stable and reliable platform supporting the implementation of a variety of technologies that meets or exceeds performance standards characteristic of current UGV systems.
- Support an effective integration of various current and future technologies to support the progression of intelligent systems
- Enable multi-disciplinary research through a cost effective, open-architecture solution.

To further investigate the needs for an improved UGV system, a survey was carried out to gather information on the current opinions regarding UGV design, capabilities and implementation. The survey was conducted via a free web-based survey service provided by Virginia Tech and administered to a variety of current and potential small UGV users, designers, and researchers. The questions aimed to provide insight on the respondent's personal level of general familiarity with UGV technology and polled the respondent for opinions on desirable features of a small UGV in the context of a research environment. A copy of the survey form and a summary of question results are detailed in Appendix A.

Admittedly, it is difficult to collect statistically significant data regarding the performance of current UGV platforms. This is due mainly to the limited pool of individuals who have a working knowledge of unmanned systems. In contrast to the surveys and customer data collected supporting the development of discrete engineered consumer products such as toothbrushes and automobiles, the average individual may have never seen

a UGV or may have such a limited experience that articulating specific opinions and needs may be difficult at best. It is often then necessary to rely on formulating customers needs through extrapolation and interpretation. This leaves the developer to define a solution based upon often limited and nebulous customer input. While this is a common method of developing customer needs into initial product specifications during the design process [10], the task of developing an improved solution becomes difficult without comparative or experienced based user input. However, there is a requisite need to develop a design need baseline formulated from the opinions of UGV users.

This lack of a suitable sample set is further complicated by the lack of continuity in the design and function of UGV platforms. The design of small unmanned ground vehicle has yet to converge to a standard conceptual design on which performance and satisfaction can be based. This convergence is demonstrated by the current form an automobile. Currently, cars are designed where nearly all models have four wheels that ride on rubber tires, have doors, a steering wheel, gasoline internal combustion engine, radio, air conditioning, and can achieve highway speed by means of the transmission of mechanical power to two or four drive wheels via a multi-speed gearbox. This generalized concept allows potential and current customers to provide design feedback in a specific context and with a particular frame of reference. Without such a foundation, ambiguities and "what if" scenarios often overshadow the task of deriving customer responses. While this conceptual design ideology may or may not be a desirable within the context of unmanned systems, there is no doubt that there is a lack of a well defined reference frame when a comparative effort of UGV platforms is attempted.

Therefore, it was essential that the survey created to provide insight into the needs of customer needs for UGV technologies within the research community is focused upon a particular application and provide a means to assess the respondent's level of familiarity with the systems. In addition, allowances for free response permit relevant knowledge and experience to be considered to account for the varied applications and respondent involvement with UGV technology.

In total, 56 respondents contributed to the results presented in Appendix A. The respondent pool was comprised of primarily unmanned system researchers, both in industry and academia, with 98 percent of the respondents having heard of UGV technology and 80 percent ranking their familiarity with UGV technology as average or better. The majority, 68 percent, of the respondents also had a practical hands-on experience operating a small unmanned ground vehicle. When the respondents were asked if they felt as though currently

available small UGVs met the needs of unmanned systems researchers, the response was indecisive as 39 percent selected “somewhat” and an equal amount were “not sure”.

The survey revealed that the majority of the respondents were primarily familiar with (i.e. observed or operated) three commercially available small UGV platforms: the PackBot by iRobot (32 %), the Talon by Foster-Miller (21 %), and the Matilda by MESA Associates (46 %). The results were skewed however towards the vehicles either developed or operated by the Virginia Tech Unmanned Systems research group. These vehicles included the Matilda with 46 percent of the respondents identifying a familiarity with the platform. In addition, 20 percent identified other familiar small UGV platforms such as the Intelligent Ground Vehicle Competition and DARPA Grand Challenge vehicles developed at Virginia Tech. This level of familiarity with specific Virginia Tech UGV technologies is a result of the respondent pool of the survey being comprised of people who were all involved with or familiar with the unmanned systems work at Virginia Tech.

With regards to the design of a small UGV, 91 percent of the respondents indicated that an open system architecture would be a desirable or required feature for UGV researchers. In addition, 83 percent indicated that it would be desirable or required to base such an open system on an industry standard communication protocol. When asked to identify the sensor and payload devices that would be required to be included on a small UGV research vehicle the results predominately identified five key sensor groups: visual and audio feedback, obstacle detection, localization devices such as GPS and INS, reconnaissance devices, and mechanical manipulators. The devices that were identified with the most frequency as being essential elements to the design of a small UGV were technologies that could directly support teleoperation or autonomous navigation capabilities. The inclusion of weapons or mission specific payloads such as nuclear, biological, and chemical (NBC) detectors or cable spoolers were not identified as being fundamentally essential to the design of a small UGV by the majority of the respondents.

As far as features and operational capabilities presented to the survey participants as possible options for inclusion into the design of a small research UGV, the results indicated that each option presented would be desirable to the majority of the respondents. This wide-ranging and indecisive response may be in part attributed to the general tone and ambiguous phrasing of the question. The non-specific and general phrasing of the questions regarding vehicle capabilities without the inclusion of an explicit supporting hypothetical scenario may have led the respondents to indicate that a small UGV research platform should have the ability to do everything and go everywhere. However, the result could also

lend support to the assertion that small UGV design lacks converging design concepts that leads to the attitude that each UGV technology should be all and do all.

Survey responses indicate that differentially drive wheels, skid or tank steered vehicles and Ackermann steering methods were the preferred technologies for a small UGV platform. With regards to the question of wheels or tracks, 73 percent of the respondents indicated that the selection depended directly on the application. Moreover, 23 percent favored wheels over tracks outright. A vehicle runtime of four to eight hours and a top speed of approximately 10 miles per hour were identified by the respondents as the preferred performance characteristics of a small research UGV. If batteries were used as the primary power source for a small UGV, the respondents overwhelmingly preferred removable and rechargeable battery packs.

The survey results indicated that the primary focus for unmanned systems research should be the development of improved algorithms. In addition, the respondents highlighted power sources, software protocols, and sensor technology as being key focus areas of research investigation. Perhaps this feeling of the need to focus on intelligent software and sensor solutions rather than mobility and vehicle platforms was best articulated by a single respondent's final comments on the survey form,

> *"… there needs to be a major paradigm shift towards a focus on software. How often have we gone "to see a robot"… what is there to see? It is just a drive-by-wire vehicle. The software is what makes the machines unique."*

Echoing this sentiment towards an increased focus on intelligent systems, autonomous capabilities were identified as a critical requirement to the future of unmanned systems by 80 percent of the respondents. Further, 66 percent indicating that there is a distinct requirement for standards by which autonomous solutions can be compared and validated.

Justification for the development of the NERV platform is rooted in the needs of the unmanned systems research community. While the task of developing the requirements for such a flexible and scalable UGV solution is indeed difficult, there is a distinct and dire need to support the development of the emerging autonomous technologies. The outline for a novel solution for an experimentation robotic vehicle that supports intelligent and autonomous vehicle systems research can be developed supported by the increasing needs for

research and applying the requirements identified through the customer defined needs assessment survey.

1.3 NERV Mission Profile

It is often the case that UGV system development, notably the development of autonomous systems, attempts to chase the elusive "intelligent and autonomous" target [11]. That is to say, designs of autonomous systems have often attempted to be the "end all" intelligent solution and have been forced to later redefine project goals. A prudent and overt definition of specific design intentions and goals are vital to the successful progression of a design.

Supporting the development of the NERV, the explicit definition of an intended goal must be defined. The subsequent design of the NERV will be predicated upon the mission profile outlining the intended use and application.

The mission profile of the NERV can be defined through the description of three key elements: (1) setting, (2) objectives, and (3) functionality.

1.3.1 Setting

An operational setting for mobile robotics is the general domain of operation for the vehicle platform. Figure 1 details the contributing factors of an operational setting for a mobile robotic platform. In order to better qualify operational settings, boundaries for the operational domain must first be established. Generally, the boundaries of the operational setting define a subset of a larger domain. The choice of the operational region is contingent upon mission objectives and vehicle functionality. Supporting this choice is the categorical assessment of the operational setting in the context of vehicle deployment. A broad analysis of terrain constituents and composition allows for the selective determination of what type of terrain profiles best support the NERV mission.

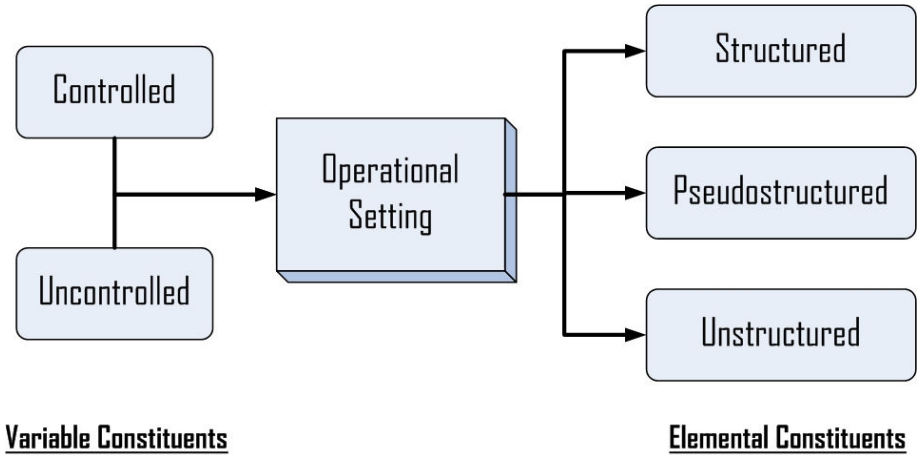

Figure 1: Contributing factors to the operational setting of a mobile robot

The setting can be described by two categories of constituent factors. The first category is the variable constituents that describe the degree to which setting parameters are altered or controlled by humans for the purpose of meeting a specific mission profile. The second category is the elemental constituents that comprise the physical realm of the operational setting. The elemental parameters of the operational setting describe the general makeup of the terrain including surface conditions, obstacle geometry, and overall predictability of the environment. Generally, robotic platforms are developed for, and applied to, a specific setting composition in order to achieve effective results. It is therefore beneficial to develop a means to classify operational settings in order to outline the NERV operational setting in the context of an overall platform mission profile.

Operational settings for research robotics can be generally categorized as being either controlled or uncontrolled terrains. Controlled terrains are generally man-made or restricted environments where the terrain has been altered or where influencing factors are mitigated to meet specific needs thereby controlling domain variables. This controlled approach is the general means of developing an operational setting for robotic research to ensure significant experimental results.

Figure 2: An example of a controlled environment for robotic navigation [12]

Uncontrolled terrains are regions where vehicles operate where no attempt has been made to control natural environmental variables. This category would encompass most real-life situations where operators of vehicles have little to no control over what they may encounter or be required to navigate. Specific examples include navigation in highway traffic, off-road travel, or battlefield operations. With the increased variability inherent in an uncontrolled environment there is the demand for the increased ability to negotiate a wider variety of terrain situations and a distinct need to incorporate more advanced sensory solutions to the baseline robotic platform achieve acceptable operation.

Figure 3: Uncontrolled rugged desert terrain [13]

Overall terrain compositions can be further refined with the determination of the predominate arrangement of obstacles and general surface conditions within the environment. The definition of terrain composition is not analogous to terrain classification

where terrain elements are identified as specific objects through sensory analysis of the surrounding environment. Rather the elemental constituents of a setting are descriptions of the overall composition of the terrain and the predictability of such a composition. These elemental constituent categories are structured, pseudostructured, or unstructured terrain arrangements.

Structured terrain consists of obstacles that are of a predictable nature and lacking in non-linear dynamic characteristics. Surface conditions are generally constant without random discontinuity and of a simple planar nature. Appropriate navigation actions within a structured domain can be based upon a priori knowledge of the expected obstacle geometry and make up. This predictable arrangement of the terrain components allows the use of case specific mobility solutions and sensor arrangements tailored to the specific cases within the structured terrain. Examples of structured environments are shown in Figures 4 through 6. Navigation within a maze or hallway can be generally considered a structured environment as obstacles and pathways adhere to very predictable standards making the environment inherently structured. Figure 6 depicts a robotic vehicle that is attempting to overcome a set of stairs. Stairs can be considered structured terrain elements as the majority of stairs characteristics such as tread width, riser height, and material adhere to standard convention. The resultant robotic platform and sensor systems developed for structured settings are generally functionally limited or display diminished capability if applied to a situation that is not congruent with intended structured operational setting.

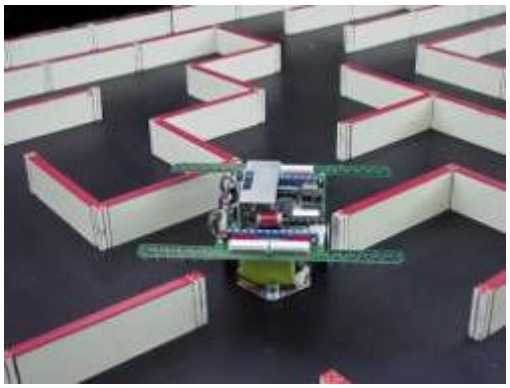

Figure 4: A maze is an example of a highly structured environment [14]

Figure 5: Structured indoor navigation [15]

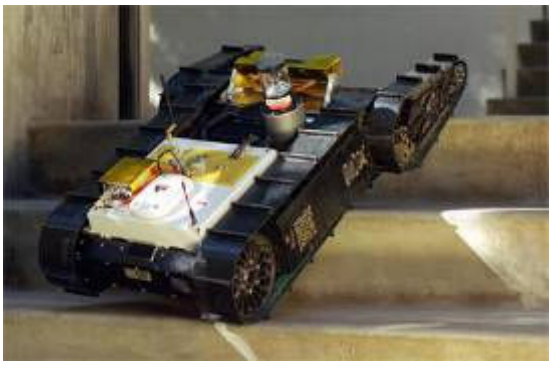

Figure 6: Stairs are considered structured terrain elements [16]

Conversely, unstructured terrain is generally a random collection of obstacles where assumptions relating to the composition of the terrain are difficult or impossible to determine prior to deployment. Surface conditions are generally highly discontinuous with multi-planar interactions. Randomness introduced within a setting by the inclusion of non-linear dynamic obstacles is an unstructured phenomenon that adds to the complexity of an operational setting. An example of unstructured terrain is rubble from a collapsed building as shown in Figure 7 or where surface topography is generally random or unknown such as off-road travel. Unstructured terrain requires a robotic platform to achieve a high degree of mobility to negotiate and avoid such random obstacles. This places a demand on the locomotive and sensory elements of a robotic design. In general, this adds complexity and cost with the expanded demands on the robotic platform's capabilities.

Figure 7: Rubble is a prime example of an unstructured environment [17]

There is however the question of scale when considering the application of terrain composition descriptors. The scale of the robotic platform relative to the surrounding elements in the environment affects the determination of if the operational setting conditions can be considered as being either structured or unstructured. Figure 8 depicts a common commercially available PackBot teleoperated UGV platform negotiating a field covered in part by randomly distributed rocks. With consideration to the relative scale of the platform depicted in the figure, the rocks certainly comprise an unstructured surface condition for the vehicle. However, this collection of rocks would be considered part of a generally structured surface for a larger M1A2 Abrams tank shown in Figure 9. The tank could easily overcome the obstacles that would be unstructured and difficult terrain for the much smaller PackBot platform. This then leads to the conclusion that the definition of setting composition is based in part on the relative scale of interaction between the vehicle platform and the discontinuities present in the setting. While standards for the assignment of a scale factor are not generally developed, the author suggests a simple relation between obstacles size and a mobility platform form factor criteria. A simple ratio between parameters such as wheel diameter and obstacle diameter or height would provide a quantitative assessment of the impact of an obstacle.

Figure 8: Rocky terrain can be considered to be unstructured for a small UGV [18]

Figure 9: M1A2 Abrahams tank [19]

An amalgamation of the structured and unstructured terrain is the pseudostructured environment. This is the most predominate and most appropriate case for most outdoor mobile robotics within the research community. This is because of the general overall applicability of a terrain that consists of some structured and unstructured content. The pseudostructured case describes most real-world situations that mobile robotics may encounter during operation of tasks such as autonomous navigation. Examples of a pseudostructured environment would be operation on a desert road, Figure 10, where the structured road path is surrounded by unstructured terrain at either side with the possibility of non-linear dynamic obstacles. Figure 11 highlights a section of the Southwest Research Institute's small robotic vehicle test-bed that includes pseudostructured operational setting on which experimentation and testing is carried out on various robotic platforms.

Figure 10: Pseudostructured desert road environment [20]

Figure 11: Southwest Research Institute's small robotic vehicle test-bed [21]

Another example of a controlled pseudostructured environment was the course constructed at the California Motor Speedway in Fontana, California for the 2005 DARPA Grand Challenge National Qualification Event (NQE). The NQE course covered both paved and unpaved sections of the speedway grounds and included obstacles and corridors that simulated the features that would be presented to the autonomous competitors in the Grand Challenge race in the Mojave desert. The course developed for the NQE was a GPS defined course measuring approximately 2.2 miles in length and served as the qualification

benchmark by which the finalists for the DARPA Grand Challenge race were selected. Although the course was designed to be traversed by pick-up or SUV sized vehicles, a small UGV platform could have easily negotiated the course; albeit at a speed that would be slower than a full-sized counterpart. The course included defined waypoint gates that the vehicle must pass through while avoiding simulated cattle gates, phone poles, rugged terrain, parked cars, and tank traps. However, despite these discontinuities the course surface was predominately asphalt or maintained grass. In addition, the course included a 90 foot tunnel that obscured GPS communications to add to the complexity of the navigation solution. The NQE course was controlled by DARPA personnel that were responsible for maintaining the course, publishing common route coordinates, and ensuring the safety of those observing the action as well as for the vehicles themselves by removing as much variability within the scope of the NQE event as possible.

When considering the scale and application of the NERV, the platform would be employed within the scope of a controlled outdoor environment to support autonomous systems experimentation and research. In addition, the general composition of the environment would best be a pseudostructured terrain, where the demands on basic mobility and sensory technology would best simulate real-world situations while not requiring extreme mobility capabilities.

Knowing that the NERV is aimed to meet the needs of the unmanned ground vehicle research community and that the platform is to be within the small unmanned ground vehicle classification (i.e. a gross vehicle weight between 5 and 500 pounds), it is possible to then consider the effect of scale on the vehicle. This leads to the generalization of the ideal setting for NERV operation. This controlled pseudostructured environment would be described as a generally flat open area that contains obstacles in various regions that may be of a structured or unstructured nature. The NERV would not generally be capable of negotiating over highly unstructured regions and would aim to avoid such obstacles and remain within the most structured region that is possible. This situation would be indicative of road or path following operation where moving off the structured roadway would lead to the introduction of unstructured surface conditions. As a singular example, the field shown in Figure 12 would provide a suitable operational setting for research and experimentation for the NERV platform as the generally structured grass and road surfaces include unstructured elements such as the dilapidated fence.

Figure 12: Pseudostructured environment suitable for the NERV platform [22]

1.3.2 Objectives

The NERV is aimed towards meeting the needs of researchers through supporting experimentation of leading-edge intelligent technologies. However, all experiments are not created with equal purpose [23]. D.S. Alberts states within "Code of Best Practice: Experimentation", that experiments can be categorized into three general areas that generally correlate the experiment motivations to the timeframe of the development cycle.

- Discovery Experiments
- Hypothesis Testing Experiments
- Demonstration Experiments

A generalized product development path, as shown in Figure 13, outlines the progression of unmanned systems technology from initial technology conception based upon customer needs to the fielding of a practical real-world solution. Highlighted in the figure is the relationship of the three types of experimentation with the development path.

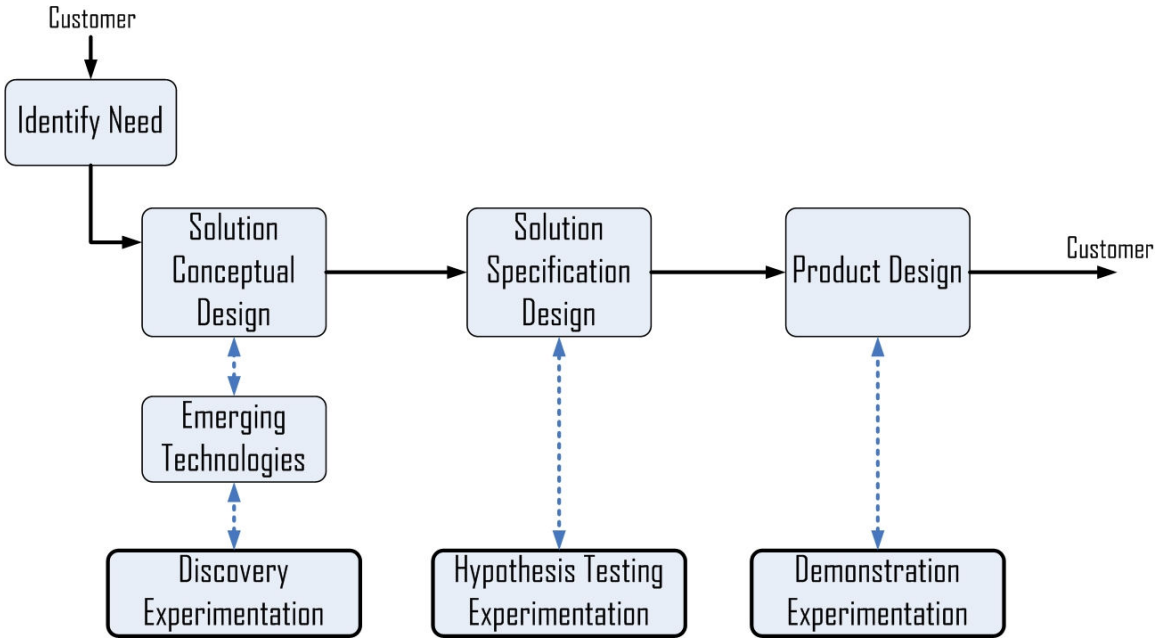

Figure 13: Generalized development path for unmanned systems technology

Discovery experiments occur early in the development cycle and are employed to investigate novel technologies or operational concepts. Often, as Alberts explains, discovery experiments lack the scientific rigor in order to fully develop cause and effect relationships. The result being that such experiments do not offer conclusive evidence of the long-term efficacy of the technologies under investigation.

Hypothesis testing experimentation occurs once a technology matures to a point where specific predictions can be made regarding anticipated performance. Alberts points out that scientific control is of utmost importance during hypothesis testing as this type of experimentation is designed to demonstrate convincing evidence of cause and effect, not just that the technology works. With regards to the developers of the technologies under examination, this type of experimentation offers the chance to gain valuable insight into technology and leads to the ability to effectively refine a design.

Demonstration experiments focus on proof of operational feasibility and occur late in the development cycle. This is often an experiment environment where the technology is sufficiently mature to provide a demonstration of a functional system that is integrated to a point where a potential customer or funding agency can make the decision on the future course of the development effort.

The objectives of the NERV mission are based upon the desire to be congruent with the intentions and goals of the researchers who employ the use of the platform. Acknowledging that the NERV will be designed to be a broadly applicable solution predicated upon the needs of the research community at large, the aim of the NERV primary mission objective is to attempt to meet the needs of unmanned systems researchers during the discovery and hypothesis testing experimentation efforts. While the NERV will no doubt exhibit capabilities that would allow for the demonstration experimentation of technologies, it is envisioned that the NERV platform will support the development of products and technologies that will be finally applied at a scale that exceeds the NERV platform capabilities. This necessitates that the NERV must be capable of meeting a wide variety of needs with mission objectives remaining broad in scope in an effort to support the UGV research community at large. In actuality this is a difficult proposition and has been the downfall of many a design to be, and do, everything at once. However, the definition of specific objectives for the NERV mission profile will serve to guide the NERV design and application.

Considering the context within the scope of a technology development path, the mission objective of the NERV in application can be summarized as a singular principle goal:

- *To provide small UGV platform functionality that facilitates real-world discovery and hypothesis experimentation*

1.3.3 Functionality

In a broad sense, the functionality of the NERV mission is based upon (1) mobility, (2) capability, and (3) interoperability. The functional characteristics detailed throughout the design presented within this work will be centered upon these three points with particular attention to the NERV mission objective and setting.

Mobility will primarily be determined by the NERV mission setting as previously described. It will also consider the intended capability and interoperability of the NERV. The mobility of the NERV will be optimized for the intended application and not aimed to be a solution for specific applications outside the scope of the UGV research community such as urban search and rescue or military operations. The underlying assumption for the mobility design of the NERV is that the development of mobility platforms is a well examined and matured area of study. It is accepted that the transfer of technologies to alternate vehicle platforms with mission specific or improved mobility is assumed to be practical and feasible.

Capability refers to the modes by which the NERV can be operated. The baseline NERV vehicle will have the ability to be teleoperated from a remote location where a human operator provides all cognitive processing. Moreover, the NERV will have the progressive means to expand it capabilities to include semiautonomous and autonomous functionality. This layered approach to NERV capability defines a modular approach to system architecture and integration. The approach of developing the NERV with modular capability provides for the ability for the vehicle to exhibit scalability and flexibility in an effort to support the wide range of potential application. Concurrent with an objective review of the current state of UGV research, the NERV will strive to achieve increased UGV autonomy by way of directly supporting a diligent and concerted effort to develop the state-of-the-art in such areas [24].

Interoperability will be a key point for the NERV platform design supporting the modular capability. This functionality will be supported by an open architecture design that allows for the transferal and engagement of the NERV to a variety of missions. While the NERV will be able to be a fully functional stand-alone UGV, it will also have the ability to integrate within a network of other devices. This will include the ability to accept the inclusion of additional hardware and software within the vehicle's onboard systems as well as networking to other vehicles and devices.

1.3.4 Current Research Needs

Presently, there are several known research efforts that would benefit from the functionality of the NERV platform. While the end resultant of the research may or may not utilize the NERV mobility platform or be a UGV at all, the open and scalable system architecture supports development capabilities to meet the varying demands of these research endeavors.

1.3.4.1 Joint Unmanned Systems Test, Experimentation, and Research Site

The Joint Unmanned Systems Test, Experimentation, and Research (JOUSTER) site is a government funded research initiative that is tasked with a two part mission [25]:

1. To provide a flexible, low-cost, responsive experimentation facility to supplement current sites.

2. To act as an independent agent in defining standard tests and test protocols for unmanned vehicles systems and subsystems that quantify performance in a controlled environment.

In specifically addressing the JOUSTER mission statement, it is desirable to evaluate the effectiveness of various sensor systems as they pertain to unmanned intelligent vehicle development. JOUSTER is also tasked with the development of benchmarks for the evaluation of the effectiveness of unmanned system navigation strategies. Additionally, JOUSTER is focused on the development and validation of the Joint Architecture for Unmanned Systems (JAUS) which serves as a technology independent communication protocol for the unmanned systems community [26].

Currently supporting the maturing JAUS protocol, JOUSTER has developed a JAUS test-bed UGV that provides a platform on which JAUS interoperability and functionality can be demonstrated. This test-bed vehicle is based upon a small tracked UGV designed with the intention of serving the military as a teleoperated inspection vehicle. However, shortcomings of this teleoperated platform limit the application of the platform in autonomous vehicle systems research. A lack of closed loop drive control, limited mobility over some terrains, short runtimes leading to confined operating range, and lack of component interoperability prohibit the platform from completing long term autonomous system experimentation. While JOUSTER research is focused on developing add-on systems that can provide extended autonomous capabilities to legacy teleoperated platforms, there is a distinct need to provide a platform that exhibits capabilities suited to the development of test and evaluation methods for JAUS, autonomous navigation solutions, and sensor hardware.

1.3.4.2 Smart Farming

Another known research application is the development of intelligent autonomous agriculture solutions that improve the efficiency and effectiveness of farming operations while striving to reduce environmental impact. Previous development efforts geared towards agriculture have focused on developing such technologies as autonomous tractors that harvest fields and autonomous helicopters that carry liquid sprayers to distribute pesticides and fertilizers. While many efforts have been underway to develop these drone type applications, the concept proposed by researchers at Virginia Tech is to develop actively investigative autonomous farming solutions that can provide valuable data leading towards not only the ability to accomplish day-to-day tasks in a more efficient manner but also to provide information leading towards more effective and systemic crop maintenance.

The primary need is to develop autonomous sensors and systems that can provide relevant ground-truth data such as soil conditions, plant health, and pest infestation to the agriculture researchers. To accomplish this task a suitable UGV platform with the mobility to move through fields of crops and the flexibility to provide sensor system interoperability is

desired to facilitate the development of this "smart" farming technology. A well-developed UGV that provides scalable capability and that is available as an off-the-shelf development platform would expedite the experimentation and proof-of-concept demonstrations requisite to this emerging research endeavor.

1.3.4.3 Active Acoustic Source Identification and Localization

An effort ongoing at Virginia Tech sponsored by the Office of Naval Research (ONR) is focused on the development of technologies that are capable of identifying, localizing, and tracking acoustic sources in a real-world environment. Conceptually, this effort would provide an autonomous UGV that is instrumented with an array of microphones capable of directionally locating an acoustic noise source. The UGV would then assimilate the suspected noise source direction with the known UGV global location and purposely maneuver to develop a global location of the known noise source. The UGV would then be capable of relaying this information to other interested parties and then be able to dynamically track the acoustic target.

The need of this research effort is for an autonomous UGV that is capable of performing the maneuvers required to identify, localize, and track a dynamic target. Moreover, the UGV must be capable of both mechanically and logically integrating the specific acoustic sensory equipment payloads developed to accomplish this mission.

1.3.4.4 Collaborative UAV-UGV Behaviors

Future applications of autonomous robotic systems will no doubt require collaborative interactions between intelligent platforms. An ongoing initiative is to develop collaborative techniques that team an UGV with a UAV to accomplish a task that would be difficult for each independent entity to perform on its own. Examples of missions that would benefit from air-ground teaming would be autonomous reconnaissance and the identification of threats within a battlefield such as landmines. Meeting these objectives would be made more effective with the collaborative efforts of an air platform capable of providing information relevant data to the UGV that would be adept at close-up inspection and ground-truth information.

The demands on the UGV would be to display the capability autonomous navigation and providing a sufficient platform on which inspection and neutralization payloads could be implemented. In addition, the UGV must be able to seamlessly communicate with the aerial counterpart as well as to upper level command and control.

1.3.4.5 Tactical Behavior Development

Currently, the task of autonomous point-to-point navigation of a UGV while avoiding obstacles is a well researched area with numerous examples of the demonstration of this capability [27] [28] [29]. However, the application of an UGV within a military operation that demonstrated near-human capabilities would require much more than the ability to follow a road or path. The inclusion of tactical behaviors that would provide autonomous in situ decision making capabilities is essential to the success UGV technology not only in the military but in the commercial sector as well. While the task has historically been to achieve autonomous navigation while avoiding the bushes and remain in the center of the road, the requirements of real-world applications often dictate that the UGV operate amongst the bushes choosing the best path based upon the threat of possible detection by the enemy. This is a problem not only of developing an extremely up to date and detailed map of the vehicle's surroundings but also developing the means of generating awareness of the system to the surroundings and how to best use the environment to achieve a tactical advantage.

An example of the problem of tactical behavior would be the autonomous re-supply of a forward operations base. An autonomous UGV convoy is following a road towards the base loaded with essential materiel. The convoy would travel along the road while maneuvering to minimize their visibility to potential points of observation by the enemy. This implies navigating a path that considers potential sight-lines and ambush points. Adaptive tactical capabilities would be necessitated when the lead vehicle in the convoy detects that the bridge crossing a large river on the planned route been destroyed. The UGV collective would cooperatively search for an alternate route by utilizing updated sources of information acquired through onboard sensor systems or outside sources such as an UAV platform. Once an alternate route is acquired the moves to the new location, updates the planned route, and crosses the river.

While the end application of this type of technology would be best implemented on off-road capable military mobility platforms, the development of these navigation algorithms within a real-world setting can be conducted through the utilization of an NERV platform. While the NERV may not be able to navigate across extremely rugged terrain, the intelligence and mobility capabilities of the NERV would allow the vehicles to support research addressing the development and demonstration the intelligent autonomous behaviors needed to accomplish such tactical missions.

2 Current Small UGV Solutions

An examination of currently available small unmanned ground vehicle platforms is necessary to continue the development of a design criteria baseline for the development of the NERV. An invaluable resource available to the unmanned robotics research community is the Tech Database maintained by the Space and naval Warfare Systems Command (SPAWAR), San Diego (SSC San Diego), a leader in the Department of Defense (DoD) robotics development since the early 1980's [30]. This database contains relevant unbiased information relevant relating to not only UGV and UAV robotic platforms but also relevant data on sensory and software solutions implemented by the unmanned systems community. Therefore, the Tech Database is an ideal source by which an overview survey of current small UGV solutions can be established.

To develop an accurate baseline for the design of the NERV platform, a product survey database of basic performance characteristics can be derived from the fusion of up-to-date information provided by UGV manufacturers and the informational assets of the SPAWAR Tech Database of small UGV platforms. Manufacturer information was collected via web based product specification resources found at the product websites and through telephone conversations with technical sales representatives. The result is a compilation of basic performance information pertaining to the various platforms is detailed in the tables presented in Appendix B. Relevant specifications for individual UGV products contained in the survey database include:

- Vehicle Name and Manufacturer
- Availability: Commercial-off-the-shelf or Prototype
- Base platform cost
- Physical parameters: length, width, height, weight
- Primary Control Mode: Teleoperated or Autonomous
- Communications link technology and operational range
- Method of locomotion: Wheels or Tracks
- Method of steering: Skid, Differential, Omni-directional, or Ackermann
- Primary operation theater: Indoors or Outdoors
- Power source technology
- Maximum runtime
- Maximum speed
- Maximum payload
- Ground clearance

While all due diligence was afforded during the compilation of this product summary database there are several platforms that all information could not be located due to a lack of published information and proprietary limitations. In addition, there is a pervasive difficulty when trying to collect, decipher, and compare performance specifications of UGV platforms resulting from a lack of standardization of testing methods and performance benchmarks. These difficulties presented during the information collection process prevent significant performance comparisons between mobility platforms. As a result, the product summary database is ill-suited to the task of deriving specific design metrics and target performance specifications for the NERV. Rather, the database is a valuable resource to gain insight into the current capabilities and design solutions leading to a generalization of acceptable performance thresholds that would provide a progression of the state-of-the-art in small UGV design.

For the purposes of the product summary database, a small UGV is characterized by a gross vehicle weight of between 5 and 500 pounds. A total of 66 UGV platforms, from 25 manufacturers, were included in the survey. Of the 66 UGV platforms, 49 can be considered commercial-off-the-shelf (COTS) items available for purchase by the general research community. The remainder can be classified as prototype level vehicles where there exists as singular or limited number of platforms and are not to a level of development to market the vehicle.

All of the vehicles within the survey were primarily teleoperated. Some of the more advanced platforms incorporated autonomous capability by allowing simple station following or operator assistance functionality. However, none of the vehicles currently have the ability to perform complex autonomous navigation.

The average cost of the platforms was $28,319. This number however is rather misleading as several factors lead to difficulties in developing an accurate average cost for vehicle platforms. The accuracy of available pricing data was often suspect. Secondly, the lack of congruence between system capabilities often skewed the average cost towards the lower end of the scale. Pricing data was often more readily available for the more inexpensive vehicle platforms as these are generally produced in higher quantities and are available through distributors to a larger market. Perhaps the most difficult aspect of formulating an accurate cost estimate for a small unmanned vehicle is how to include the variety accessories that are required to operate the vehicles. The case that often arises is where the requisite operator control unit or control software is just as expensive as the robot itself compounding the difficulty in developing a comparison base for vehicle cost. This

added cost extends to add-on sensor devices to extend capability, varying communication radio configurations, different lengths of communication tethers, and software development kits that allow you to interface with the vehicle. With such a variety of vehicle configurations it is difficult to determine a authoritative base cost comparison.

The average weight of the vehicles surveyed within the small UGV weight class was roughly 43.75 kg (96.5 lbs). This shift to the lower end of the 2.3 kg to 226.8 kg (5 lb to 500 lbs) weight class is no doubt due to the desire to make small unmanned ground vehicles that are man-transportable, conserve energy, and of a form factor that allows easy access to confined unstructured terrain.

The survey also provided some insight into the prevailing physical locomotion configurations of small unmanned ground vehicles. The percentage of vehicles that utilize wheels as their primary form of vehicle-to-ground interaction was 68.2 percent, while 30.3 percent vehicles utilize tracks as their primary form of locomotion. However, 55.6 percent of the wheeled vehicles utilize a four-wheel, skid steer type of design that is used by the tracked vehicles. In total, 66.7 percent of the vehicles utilize a skid steer design. This is most likely due to the simplicity of implementing the differential type drive as well as the improved stability compared to a two drive wheel and single caster differentially steered vehicle. Other forms of vehicle heading control were also represented such as omni-directional wheels, Ackerman steering, and vehicle body articulation. Together these alternate forms of steering control comprised 10.6 percent of the vehicle platforms in the survey. The lack of popularity of these designs can be attributed to the increased mechanical and control complexity required to implement such mobility solutions.

Other data points collected, such as maximum runtime, payload, and speed, for each robot platform were often highly dependent on operating conditions. Such performance characteristics are by far the most difficult values to assess and compare without standards by which these variable can be judged. This difficulty is manifested in varying values presented in product literature and other published works. An example is the payload capacity of the ATRV-mini produced by iRobot Corporation. The company data sheet specifies that the max payload for the vehicle is 9.1 kg (20 lbs) while the SPAWAR Tech Database lists the maximum payload as 51.28 kg (113 lbs). The SPAWAR value was undoubtedly collected through experimentation and user feedback while the iRobot product literature was certainly intended to provide a nominal payload where other performance factors such as speed and runtime could be optimized. While neither value appears to be

unreasonable for the ATRV platform, there is a noticeable disconnect between the methods by which these values are collected and reported.

2.1 Leading Small UGV Platforms

Through the broad survey of small unmanned ground vehicles it was apparent that four platforms were popular choices for research UGV platforms and best provided a benchmark on which the NERV development could be referenced. The rapidly expanding and yet immature field of mobile robotics and unmanned vehicles has limited the extent of scholarly literature specifically detailing small UGV platform design and performance. This challenge coupled with the propensity for platforms to be developed upon proprietary solutions leads to a limited base upon which to develop a scholarly review of extant technologies. Therefore, the database developed from product literature and online content pertaining to vehicle design and performance are the primary source for developing a sketch of the leading currently available small UGV platforms.

The PackBot created by the iRobot Corporation and the Talon created by Foster-Miller Incorporated are two of the most widely used teleoperated vehicles small UGV platforms. This is due in large part by the successful adoption of these platforms in use within the U.S. Military supporting troops in combat [31]. An emerging platform within military applications is the Dragon Runner UGV developed by Carnegie-Melon University. In contrast to the PackBot, Talon, and Dragon Runner platforms that are geared towards military applications, the Pioneer3-AT small UGV produced by ActivMedia Robotics, is developed for and widely applied in leading research applications.

The iRobot PackBot is arguably the current standard for small, robust, teleoperated robotic vehicles [32]. Appealing industrial and mechanical design, durable construction, and exceptional capability are the hallmarks of the PackBot platform and set it apart from the other offerings within the small UGV community. The base PackBot platform weighs 18 kg (39.7 lbs) and measures 69.2 cm in length by 41 cm wide by 18.3 cm tall (27.2" by 16.14" by 7.2"). The PackBot is a tracked vehicle that utilizes rigid rubber tracks to gain traction and to steer the vehicle. This drive system powered by either nickel-cadmium (Ni-Cd) or nickel-metal hydride (Ni-MH) battery cells allows the vehicle to achieve an advertised maximum speed of 13.31 km/h (8.27 mph), carry a maximum payload of 16 kg (35 lbs), and offers a runtime of two to twelve hours depending on operating parameters. The PackBot is controlled by a portable OCU that can operate the vehicle at a distance of 1000 meters (3208 feet) line-of-sight utilizing a digital 2.4 GHz radio frequency link. The OCU measures 35 cm in length by 45.7 cm width by 21.5 cm height (14.6" by 18" by 18.5"), weighs 20 kg (45 lbs),

and provides the ability to run for a maximum of four hours via integrated and standardized proprietary PackBot battery packs or to run via an external power source.

The most defining physical features of the PackBot are the articulated tracked flippers that extend from the front of the vehicle that allow the vehicle to alter the platform center-of-gravity and apply localized traction to overcome obstacles. The design of the PackBot mobility platform and control systems has been tailored to military and law enforcement operations where durability and maintainability are essential characteristics. The base PackBot platform is offered in three primary system variants: the PackBot Scout, the PackBot Explorer, and the PackBot EOD. Each platform offers a different suite of sensors to accommodate the intended application. The PackBot Scout is the most basic variant including only fixed mount video cameras. The PackBot Explorer provides extended capability by mounting the visual inspection equipment at the end of an articulated head that allows the operator to maneuver the head without repositioning the vehicle platform. The PackBot EOD or Explosive Ordinance Disposal variant includes a manipulator arm that provides a gripper device to interact with suspected explosive devices. All of the variants within the PackBot family can accept payloads that expand capabilities such as a cable spooling device that provides a tethered link to the PackBot to enable operation out of line-of-sight. Figure 14 details the PackBot EOD variant with cable spooler mission payload.

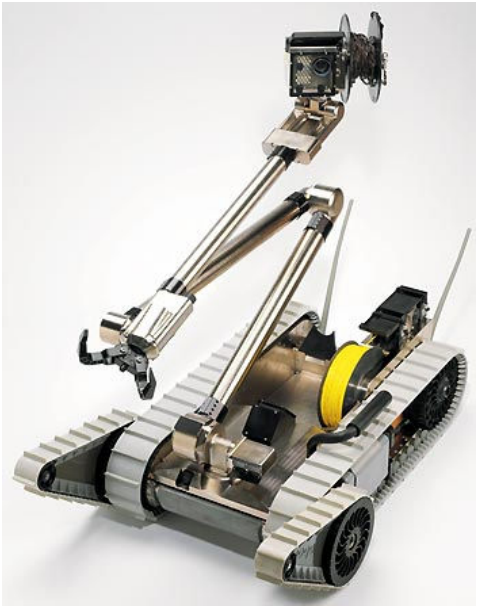

Figure 14: iRobot PackBot with EOD manipulator and cable spooler [33]

Expanding the capabilities of the PackBot family of teleoperated vehicles, a recently developed version of the PackBot demonstrates industry leading autonomous capability geared towards urban reconnaissance. Such capabilities are obstacle detection and avoidance, street following and mapping, and video logging. The stated goal is to have a fully functional prototype by the fall of 2005 and transition this technology into a payload than can transform any PackBot system into a fully autonomous system [34].

The Talon Unmanned ground vehicle produced by Foster-Miller, shown in Figure 15, is another example of a teleoperated UGV that has been used extensively in military and civilian applications. The Talon is a battery powered, track based mobile platform that has been specifically designed for irregular and challenging terrain [35]. The base vehicle platform weighs 39 kg (85 lbs) and has a footprint of 86.4 cm length by 57.2 cm wide by 27.9 cm tall (34" by 22.5" by 11") with sufficient onboard lead acid or lithium ion (Li-Ion) battery power to achieve a runtime between one and four hours depending on operating conditions. The vehicle and some payload functions are controlled remotely by an OCU via a radio frequency link. The OCU provides four hours of runtime via a standard military specification battery (BA-5590/U or equivalent) and weighs 15 kg (33 lbs). It is noteworthy that while the Talon OCU utilizes a standard military battery, the batteries used to power the Talon platform are not a standard military specified battery. The batteries do provide power to achieve an advertised top speed of roughly 7.7 km/h (4.8 mph) and a maximum payload of 136 kg (300 lbs).

Figure 15: Foster-Miller Talon with the gripper manipulator payload [36]

The Talon platform can accept a variety of additional payloads that expand the vehicle's capability to meet specific mission objectives. The Foster-Miller website lists the following non-lethal payloads [37]:

- Gripper manipulator
- Smoke dropping module
- Breaching tool
- Generation III night vision camera
- Nuclear, Biological, and Chemical (NBC) sensors
- UXO/countermine systems/sensors

The base platform of the Talon can utilize such additional payloads to address specific mission objectives. Figure 16 highlights some of the functional variants of the Talon. At this point in time, there are no published reports that Foster-Miller researchers plan to develop the COTS Talon to include autonomous capability.

Figure 16: Talon family of variants [38]

The Talon is currently the only mobile robotic platform that is certified by the Department of Defense (DoD) for remotely controlled live firing of lethal weapons [39]. The weaponized Talon platform is known as the Special Weapons Observation Reconnaissance Detection System (SWORDS) and is shown in Figure 17. The SWORDS platform can accept a variety lethal weapons including the M16 rifle, M82A1 (50-cal), and a 40 mm grenade launcher.

Figure 17: SWORDS Talon platform with mounted weapon [40]

The Dragon Runner small UGV, shown in Figure 18, was developed at the Robotics Institute of Carnegie Mellon University under government funding from the Marine Corps Warfighting Lab and the Office for Naval Research (ONR) [41]. The 7.3 kg (16 lb) teleoperated Dragon Runner platform measures 39.4 cm in length by 28.6 cm width by 12.7 cm height (15" by 11.5" by 5"). The Dragon Runner is designed to be a man-portable surveillance robot that can be dropped or thrown into dangerous situations as highlighted in Figure 19. The chassis includes a non-active, invertible suspension designed to allow the Dragon Runner to operate regardless of resulting platform orientation after tossing the vehicle. The Dragon Runner is unique among the current small UGV product offerings in that it is a small UGV that utilizes Ackermann style steering and can achieve speeds of nearly 32.2 km/h (20 mph).

Figure 18: The Dragon Runner small UGV [42]

Figure 19: A "toss" test at the Southwest Research Institute [43]

The Dragon Runner is controlled by a 3.2 kg (7 lb) OCU shown in Figure 20 that incorporates a small ambidextrous controller that resembles a video game controller. This controller is noteworthy for the fact that the OCU is not carried within a large case like that utilized for the baseline PackBot or Talon small UGV systems. The Dragon Runner is still a prototype small UGV system and is currently being refined through field trials with deployed troops [44]. The control is the Dragon Runner is designed to extend the capabilities of a solider to perform surveillance and reconnaissance as well as sentry duties. Motion and audio sensors will allow the Dragon Runner to stand watch and alert the operator if an anomaly is detected. Other mission payloads can be used to provide lethal and non-lethal force as well as Nuclear/Biological/Chemical (NBC) detection.

Figure 20: Dragon Runner with OCU [45]

In contrast the PackBot, Talon, and Dragon Runner small UGVs, the Pioneer3-AT (P3-AT) platform manufactured by the ActivMedia Robotics Company shown in Figure 21, is a platform that is not tailored to military applications. Rather, the P3-AT is a robotic

platform that is designed to provide a research platform that is capable of operating inside of outside the laboratory. The P3-AT utilizes an embedded controller that links into a variety of sensors to allow for autonomous operation and autonomous algorithm development. The base software included with the P3-AT allows a vehicle fitted with the proper sensory equipment to accomplish basic autonomous functions such as localizing position, develop path plans, and to wander. In addition to this autonomous functionality, the P3-AT can be teleoperated by remote connection.

Figure 21: ActivMedia Robotics Pioneer3 -AT vehicle platform [46]

The P3-AT is advertised as an all-terrain small UGV that utilizes four driven wheels in a skid steer drive configuration to maneuver both indoors and out. However, in contrast to the weather-resistant platforms developed for military use, the P3-AT is not water tight or weather resistant. The base P3-AT weighs 12 kg (26.5 lbs) and measures 50 cm in length by 49 cm wide by 26 cm tall (19.7" by 19.3" by 10.2"). The onboard batteries provide a maximum runtime of six hours, a maximum speed of 2.52 km/h (1.56 mph), and maximum payload of 30 kg (66.1 lbs). The P3-AT does not require a specific OCU device. The vehicle can be controlled via a radio or tether connection by any computer that is running the ActivMedia controller software.

2.2 Previously Successful UGV Platforms at Virginia Tech

Small unmanned ground vehicles have been developed at Virginia Tech with a similar mission profiles to the proposed NERV. The Autonomous Vehicle Team at Virginia Tech have been developing platforms for nearly a decade for entry into the Intelligent Ground Vehicle competition (IGVC) with the intention to meet the goals of the competition and serve as research vehicles that support the progression of intelligent autonomous capabilities. While these platforms are designed to excel at the IGVC, they do possess

qualities that make them suitable research platforms. Their small size, fully autonomous capability, and reliability are keystones to their successful application within a research context. Although these vehicles are exceptional vehicles, they are designed with a specific competitive goal in mind and often lack the flexibility and ease of use functionality that is required in order for different organizations outside of the system developers to quickly and effectively operate the vehicles to support research. In addition, the durability and maintainability often become issues due to the fact that they are produced within a nine month development cycle; from concept to competition in a single academic year. This short development time frame often induces trade-offs within the design process to expedite completion while sacrificing long term platform integrity. Despite these short comings, the Virginia Tech UGV platforms developed for the IGVC are a logical reference on which the design of a NERV platform can be based.

2.2.1 Overview of the IGVC

The Intelligent Ground Vehicle Competition is an inter-collegiate student design competition where engineering students from around the world conceive and field practical autonomous unmanned ground vehicles [47]. The IGVC aims to provide a competitive arena in which students can field their designs in order to accomplish common tasks. These events include the Autonomous Challenge, the Navigation Challenge, and the Design Competition. Although the IGVC was initially designed as a student design competition, the practical application of the technology as well as the uniqueness of the research supporting the design intelligent robotics has proven the IGVC to be an exceptional arena in which the next-generation of autonomous technologies has and continue to be fostered. In fact, the research implications wrought by this unique competition has been used a case study for autonomous robotics development and research [48]. In addition, the design process and results of the IGVC leverage some leading industry hardware and develop systems engineering practices that are applicable to the broad range of UGV development efforts [49].

The objective of the Autonomous Challenge is for a fully autonomous ground vehicle to negotiate an outdoor obstacle course. The course must be completed within a prescribed time while staying within a defined speed limit and avoiding obstacles on the track [50]. Performance is based upon speed and ability to negotiate through the complex terrain without contacting obstacles or boundaries.

The objective of the Navigation Challenge is to autonomously travel from a starting point to a number of target destinations (waypoints or landmarks) and return to the initial

starting position, given only a map of the target position coordinates. The performance is based upon speed and accuracy.

The Design Competition is focused on the evaluation of the engineering process that each design team followed to create their vehicle. The vehicle design judging is performed by a panel of expert judges familiar with the field of autonomous unmanned vehicle systems. Teams produce formal written and oral presentations to document the vehicle design.

2.2.2 Virginia Tech UGV Platform – Gemini

One of the most successful platforms ever developed at Virginia Tech for the IGVC is a novel small and fully autonomous UGV known as Gemini [51] [52]. In addition to winning top honors in every competitive category at the 2005 IGVC, Gemini is the only vehicle design to date that has won the IGVC design competition two years in a row. This was accomplished by the continuation and refinement of a practical system architecture based upon a stable platform that supported the successful application of intelligent software. Gemini was created alongside a sibling autonomous vehicle Johnny-5 and spawned the design of a third vehicle Polaris. All three systems make use of similar kinematic, power, and sensor solutions that support intelligent and autonomous navigation capabilities. The recent competitive successes of the Gemini, Johhny-5, and Polaris vehicles are detailed in Appendix C.

2.2.3 Mobility Platform – Gemini

The fundamental design of Gemini is a two-body articulated platform that provides zero-radius turning capability along with exceptional stability on uneven terrain. Gemini's four-wheel configuration and aggressive stance provide for a stable vehicle platform. Gemini offers the mobility afforded by three wheel vehicle platforms while exhibiting the stability indicative of four wheel platforms. The two degree-of-freedom articulated joint enables the vehicle to maintain four points of contact and allows Gemini to conform to uneven terrain; it functions essentially as a suspension without springs. The keys to this enhanced performance lie in the drive system and in the two degree-of-freedom joint connecting the front and rear platform. Independent motors drive the two front wheels while a vertical axis of rotation between the body sections allows the front platform to pivot relative to the non-driven rear platform as detailed in Figure 22. The steering pivot point is centered directly between the front wheels, allowing the front platform to turn about its center (a zero-radius turn) without moving the rear platform. Steering is accomplished by driving the two front wheels at different velocities. A second axis of rotation between the body sections allows the front body to roll relative to the rear body as demonstrated in Figure 23. This allows Gemini

to keep all four wheels on the ground on extremely uneven terrain. Since the pitching motion between the front and rear is constrained, the rear platform gives the front platform stability in the fore and aft direction, which allows the front platform to have only two wheels.

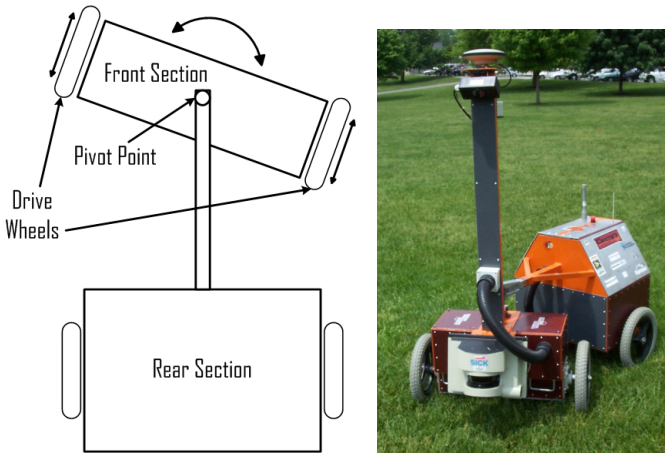

Figure 22: Detail of the steering method of Gemini

Figure 23: The unique mobility provided by the two degree-of-freedom articulated platform

The desire to minimize the twisting of interconnecting cables restricts the continuous execution of zero-radius turns of the front section. The photo in Figure 22 demonstrates the practical limit of roughly 90° on the rotation of the front section relative to the rear. However, the degree of mobility and drive symmetry afforded by the implementation of differentially driven wheels allows Gemini to move in any direction from a fixed starting point despite the rotational limits.

The Gemini platform weighs 134.7 kg (297 lbs) and measures 91.4 cm (36") wide, 157.5 cm (62") long, and 182.9 cm (72") tall. The maximum speed of the Gemini platform is five miles per hour as dictated by the IGVC rules.

2.2.4 Power System – Gemini

The Gemini platform is a completely battery operated with eight lead acid absorbed glass mat (AGM) batteries providing 56 amp-hours of electrical capacity. This system is integrated into the chassis of the vehicle and can be recharged through a rear AC power port that interfaces with an onboard microprocessor controlled battery charging system. This electrical system provides nearly six hours of runtime at full operational capability with all systems onboard the vehicle engaged and the vehicle operating at the specified maximum speed of five miles per hour.

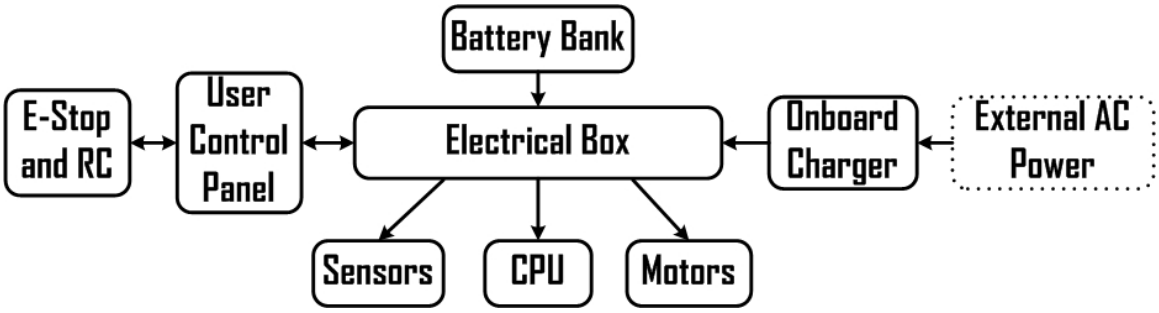

Figure 24: Gemini power system schematic

2.2.5 Systems Integration – Gemini

The integration of sensors and computing elements onboard Gemini allows for the fully autonomous as well as teleoperation capabilities. The system architecture of Gemini is detailed in Figure 25 and highlights the primary sensory and computing elements utilized in the design of the vehicle. The use of industry standard communication protocols streamlined the integration process and provided for fault tolerant communication pathways between the essential elements required for fully autonomous operation.

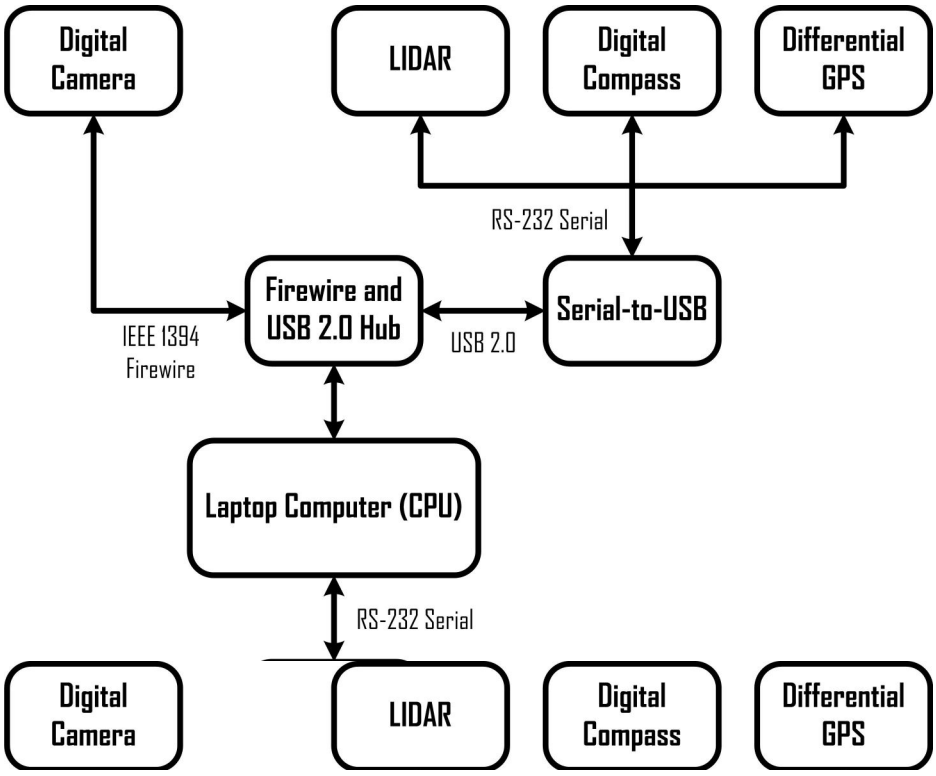

Figure 25: System Architecture for Gemini

3 Design of the NERV Platform

The development of the NERV is based upon addressing the need of the unmanned systems community for an effective and efficient UGV platform that can readily facilitate the development of the next generation of intelligent systems. The target application of the NERV is to assist researchers in the experimental stage of solution development where real-world proof-of-concept is essential. The vision of the NERV application is based upon meeting the needs of developers where mobility over controlled terrain, platform effectiveness, and cost efficiency are paramount.

With consideration to the developed mission profile for the NERV, the goals of the platform design can be summarized as follows:

- Target the design of the mobility platform to provide sufficient stability and maneuverability in the context of research and experimentation.

- Provide increased performance capabilities with respect to current small UGV platforms within the context of a research and experimentation.

- Supply an innovative forward-looking, technology independent, systems integration methodology to facilitate the extended technological relevance of the NERV platform.

Regarding capability levels of unmanned ground vehicles, The Committee on Army Unmanned Ground Vehicle Technology categorizes UGVs into one of four classifications based upon platform capability [53].

- Teleoperated Unmanned Ground Vehicle (TUGV)
    - *An operator provides all cognitive processing at a distance with a communications link providing on-board sensor feedback that allows visualization of the TUGV's situation.*
- Semi-Autonomous Preceder-Follower (SAP/F-UGV)
    - *Has the ability to autonomously navigate from point A to point B, following a leading agent, while avoiding obstacles.*
- Platform-Centric Autonomous Ground Vehicle (PC-AGV)

        - *A vehicle that has the ability to perform an assigned complex mission by itself. This type of UGV would be equivalent to a comparable manned vehicle in the scope of the desired abilities.*

- Network-Centric Autonomous Ground Vehicle (NC-AGV)

    - *Basically a PC-AGV in a networked environment where information and task assignment is received over a network.*

For the NERV to be on par with the currently available platforms, basic teleoperation capability must be an included feature of the design. Building upon this base line capability, the NERV will provide means to progressively implement levels of autonomy within the original framework and systems integration. The NERV will be capable of TUGV operation as a baseline with add-on accessories providing the scalable abilities of the SAP/F-UGV, PC-AGV, and the NC-AGV. This progressive expansion of the vehicles capabilities will be supported through a thoughtful development of scalable system architecture.

This scalable system architecture begins with a foundation schema on which the design of the entire NERV system is developed. A modular and multi-layered approached detailed in Figure 26 is the top level view of the NERV design. The design of the NERV platform will be based upon this multi-level structure and detailed in the following sections. The emphasis of the design presented will be on the formulation of the theory behind the design rather than the specifics pertaining to component specifications. The result being an outline of the design of a vehicle system, that can be implemented in whole or in part on a variety of platforms, that is independent of specific technologies and products.

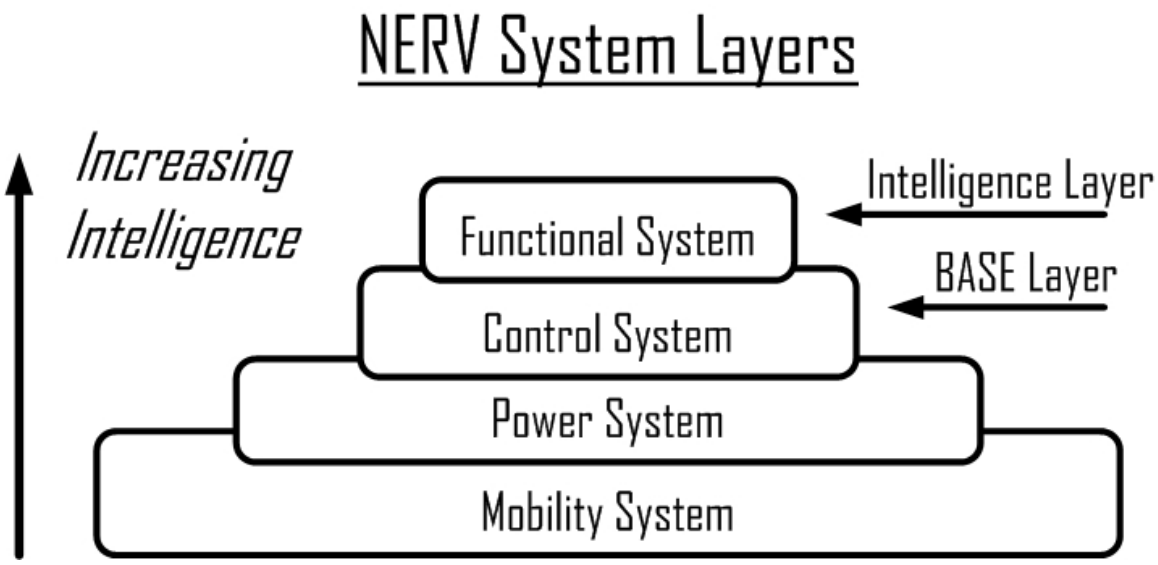

Figure 26: NERV system integration overview

The system integration of the NERV begins with the mobility system of the vehicle. This is the foundation on which all of the other systems within the vehicle will be supported. As described within the context of the proposed design, the mobility system includes the kinematic design of the vehicle. However, it forgoes the inclusion of other mobility concerns such as the frame and power train design. This omission is due to the aforementioned emphasis on technology independent design and the assumption that alternative mobility solutions can be readily developed. The power system level builds upon the mobility system to provide means to reliably distribute power throughout the vehicle and to all associated components.

The control and functional systems are the layers through which human controllers or autonomous capabilities dictate the behavior of the vehicle. The control system is the low level controller that controls vehicle position and motion as well as provides the communication interface to the functional system. The functional system is the top most layer that contains the higher level functionality of the vehicle including teleoperation, autonomous, and mission specific capabilities.

3.1 Mobility System

Benoit Mandelbrot through his analysis of fractals explained one condition of nature in which the structural complexity was self-similar over all dimensions [54]. The implication of this conclusion is that an unmanned ground vehicle of fixed dimensions will most assuredly be unable to negotiate over all terrain. With this is mind, it is apparent that there

is no UGV design that is effective in every situation. Durrant-Whyte in a critical review of the state-of-the-art autonomous land vehicles points out that given realistically achievable mobility requirements, there is little doubt a suitable vehicle platform can be designed to meet those needs as the development of mobility platforms is a well understood field [55]. The application of these observations to the design of the NERV mobility platform indicates that given a specific mission profile a mobility platform can be developed with performance capabilities sufficient to meet the needs presented.

It follows that an effective design of an NERV must then consider the intended use and application of the technology. As previously noted, the NERV platform will serve as a research test-bed on which intelligent systems can be developed at the experimental level. Extending the assertion of Durrant-Whyte, the assumption supporting the mobility design of the NERV is that intelligent technologies developed and refined at the experimental level on a specific mobility platform are readily transferable to alternate operational scenarios beyond the scope of the baseline NERV mobility platform capabilities. The primary goal of the NERV is then, in the context of vehicle maneuverability and mobility, to provide adequate performance that will enable the development of intelligent systems irrespective of total-terrain mobility.

3.1.1 Kinematic Design

While there are numerous kinematic designs of robotic mobility platforms, the design progression of intelligent ground vehicles at Virginia Tech has highlighted the effectiveness of two particular kinematic arrangements in scenarios similar to the proposed NERV application. Both designs achieve zero turning radius capability by means of two co-axial differentially driven wheels. In addition, these example kinematic designs have proven mutually successful at the Annual Intelligent Ground Vehicle Competition [56]. As noted in the NERV mission profile specification, the IGVC is an accurate approximation for the pseudostructured terrain on which the NERV platform is intended to excel.

The first design is a three-wheeled platform that utilizes two differentially driven wheels to provide maneuverability. The third wheel in this configuration is a caster wheel which provides support as the vehicle maneuvers over terrain. This three wheel design allows for zero radius turning providing for improved maneuverability of the vehicle platform over Ackermann style vehicle platforms. A diagram of this type of kinematic platform is shown in Figure 27.

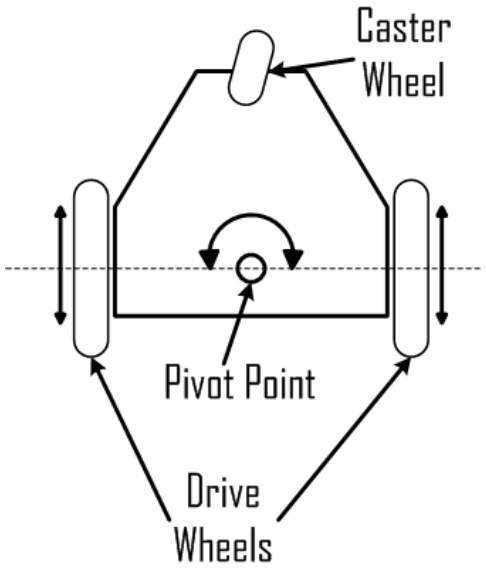

Figure 27: Three-wheeled differentially driven mobility platform

The second mobility platform is a four-wheeled design that utilizes an articulated interconnecting joint to allow a front a rear section to maneuver in tandem. This design was developed at Virginia Tech with the Gemini platform. This design again uses two differentially driven wheels to provide maneuverability of the vehicle. In essence, the rear section of the four-wheeled configuration is analogous to the caster wheel in the three-wheeled configuration.

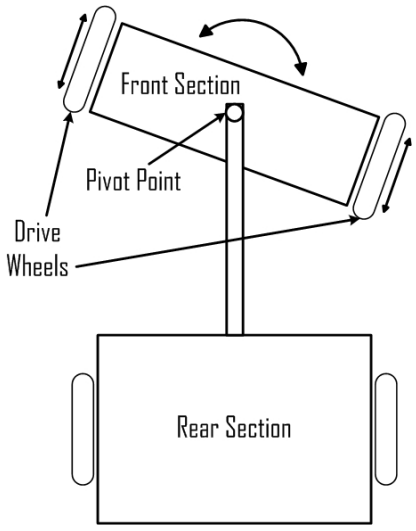

Figure 28: Four-wheeled differentially driven mobility platform

Of the two designs, the four-wheeled two-body articulated platform provides for increased vehicular stability while maintaining excellent maneuverability. The two-body articulated design also incorporates a two-degree-of-freedom joint that serves as the interconnection between the two sections. This joint allows the two vehicle sections to twist and turn relative to each other. With consideration to the analysis presented by Mandelbrot, the way in which living organism confront the variability in terrain is by the utilization of the multiple degrees-of-freedom [57]. The addition of the second degree-of-freedom between the forward and rear sections of the Gemini Platform adds to the vehicle's ability to traverse over variable terrain. In the case of the Gemini platform, the second degree-of-freedom allows the vehicle to maintain contact of all four wheels on the ground during operation. For traditional Ackerman type vehicles, such as automobiles, this fundamental requisite for proper locomotion has been achieved through the use of spring and damper suspension systems which attempts to force the wheels to remain in contact with the ground surface. The second axis of rotation of the Gemini platform accomplishes this task of maintaining four points-of-contact without the need for springs.

The simple yet capable four-wheeled Gemini-type platform is then an exceptional platform concept on which the NERV can be developed. The proven success of the two-body design in situations congruent with the NERV mission profile as well as the stability and maneuverability afforded by the novel design lead to the adoption of this platform design as the conceptual basis for the NERV.

3.1.1.1 Tracks versus Wheels

In the context of military operations, mobility is a measure of a system's freedom of movement and average speed or travel time over a given piece of terrain [58]. The debate over the best mobility platform, wheeled or tracked vehicles, has been an ongoing and fiercely contested issue. This is no more apparent than in the context of the progression of the United States Military as it develops the next generation of combat technologies. At the forefront, is the ongoing controversy over the development of the 19-ton, eight-wheel drive Stryker armored combat vehicle developed by General Dynamics Land Systems. Although the Stryker vehicle is perceived as inadequate compared to traditional tracked vehicle for overland travel through sand, mud, or snow; the Stryker does provide military planners with the benefits of a greater top speed, better fuel economy, and improved deployment times. Proponents of the Stryker platform point out the logistical benefits of operating wheeled platforms while detractors highlight the platform's decreased mobility over aggressive terrain and vulnerability to immobilization by destroying the rubber tires as a reason for

wheels not being acceptable solutions. Despite the debate, the speed and flexibility benefits of a wheel based mobility platform are indicative of the current Department of Defense aim to field a lighter and more responsive force to address needs across the globe.

Moreover, the current development of the primary UGV platform for the Future Combat Systems (FCS) is fraught with similar deliberation. The FCS program focuses on integrating unmanned and autonomous systems into a cooperative role along side the soldier. With no clear dominant mobility technology emerging through nearly a century of development, there is little doubt that the debate over the use of wheels or tracks will most likely continue to remain unresolved. How then can this question be answered in order to best decide which technology to employ on the NERV?

The resolution of this discussion may lie in the example set by the agriculture and construction industries. Both wheeled and tracked platforms are employed with success with consideration to both task effectiveness and economy of application. The key to the successful implementation of wheeled or tracked vehicles is based upon selective application of the technology [59]. It is generally acknowledged by those who employ both wheeled and tracked platforms that each technology offers distinct benefits over the other. Therefore, the proper solution can best be determined through thoughtful consideration the intended application and evaluation of each platform technology in context [60]. With this in mind, the development of the NERV should adequately address the question of building the vehicle upon a tracked or wheeled chassis. This analysis should be assessed based upon the intended application, proposed mission profile, and specific design goals.

Predominate in the small unmanned ground vehicle market are vehicles that have a continuous track based mobility platform. Figure 29 highlights an example of a PackBot tracked platform developed by iRobot. Such tracked vehicles have proven adept at negotiating highly discontinuous terrain and have the ability to traverse obstacles that would defy most wheeled mobility platforms of the same vehicle size class. The use of continuous tracks for the small unmanned ground vehicle is most likely the result of careful attention to the intended use of the vehicle. As these robots are generally designed for use in urban search and rescue (USAR) and military operations in urban terrain (MOUT), tracks afford these small platforms the ability to traverse difficult terrain often encountered in the field such as rubble, steps, and gaps. With such operations, it is often a question of only finesse rather than speed and obstacle avoidance common to overland mobility such as roadway navigation. This is an essential characteristic as these vehicles are often applied in

situations where obstacles need to be directly overcome, rather than avoided, to accomplish the mission.

Figure 29: iRobot's PackBot utilizes a track system [61]

Tracked vehicles utilize the concept of differential drive operation, often referred to a "tank-steer" or "skid-steer". This method of steering a vehicle is applied by driving each track of the vehicle at differing velocities. Driving both of the tracks forward, with the left track moving at a greater velocity, will yield an arced vehicle forward path in a right hand turn. A left hand turn is achieved in a similar manner by driving the right track at a faster velocity than the left. A key feature to this design is the ability of a platform to have a zero-turning radius, allowing the vehicle to pivot in place to change orientation within its own overall length.

However, small tracked vehicles are somewhat inefficient for the purposes of most experimental situations where ground conditions could be traversed equally well by either tracks or wheels. Skid or "tank" steered tracked vehicles provide exceptional mobility over irregular terrain but sacrifice efficient use of power, potential top speed, and maneuverability responsiveness [62]. Tracked vehicles utilizing the skid-steer method require a large amount of power due to the lateral sliding of the track contact surface across the ground during the process of turning. This is even more of a concern when tread grousers, often employed to increase frictional interaction between the ground surface and the treads, become entangled in ground obstructions such as rocks or thick grass. This skidding interaction with the ground and ground discontinuities is also the direct primary cause of treads being thrown from the drive system causing the vehicle to be wholly

immobilized. Drive tracks being thrown from small unmanned vehicles is a common problem failure mode and one that is often a catastrophic failure causing a mission to be aborted.

The heavy use of power for turning resulting from the sliding of tracks across the ground is less of a concern with wheeled skid-steer vehicle as tires display a much smaller cross-section that is required to slip across the surface of the ground as the vehicle turns or pivots. This reduction in sliding cross-section achieved through the use of wheels provides the ability for wheeled vehicles to achieve changes in direction with some savings in the required applied power to execute a turning maneuver. However, the use of skid-steer mobility platforms, like those shown in Figure 30, still requires the wheels to slide across the surface of the ground.

Figure 30: Small mobile research robots that use skid-steer wheels [63]

Beyond the drawback of increased power consumption for a skid-steer vehicle platform, there is an issue with the reduction in ground-truth localization. The introduction of the often unquantifiable sliding characteristic of a skid-steer vehicle limits the ability to accurately track the ground effector interaction and determine a current absolute vehicle state. To track the relative or absolute position change of a vehicle, wheel odometery is often used to localize a vehicle. Odometery techniques are based upon the assumption of little to no wheel or track slippage. Generally, these assumptions are wholly impractical when

applied on a device such as a skid-steer small UGV where ground slippage is a normal aspect of operation.

The benefits of a zero turning radius can be achieved through the use of differentially steered wheels that are arranged coaxially as shown in Figure 31. This configuration does not necessitate the degree of slip across the ground, characteristic of skid-steer platforms, in order to maneuver.

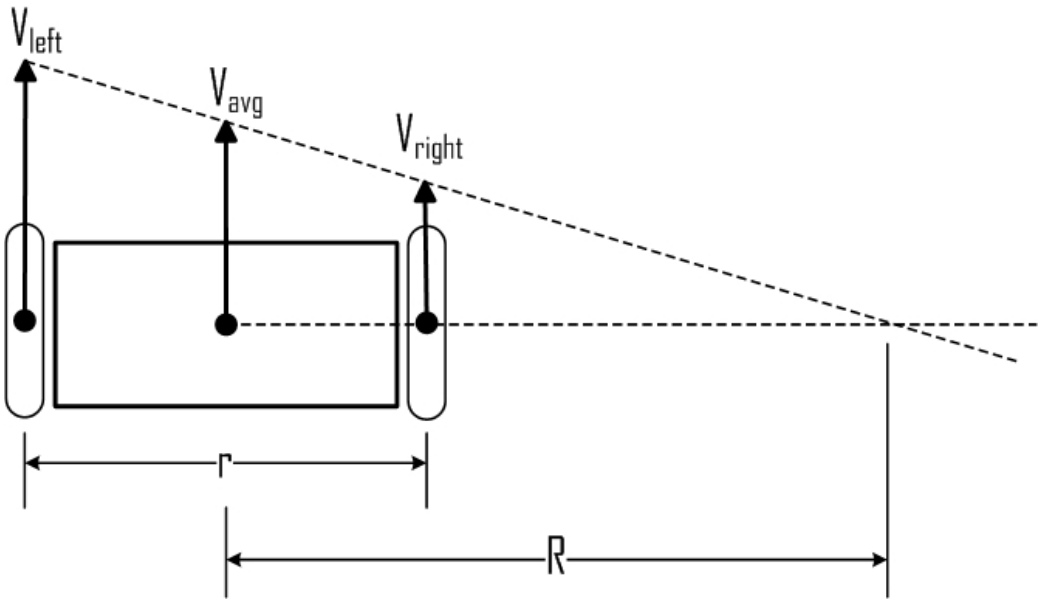

Figure 31: Schematic representation of coaxially oriented differentially driven wheels with R being the vehicle turning radius

Moreover, traditional tank tracks used on large military platforms utilize hydraulically assisted independent wheel suspension to support the tracks as they operate. This provides the benefit of allowing the flexible tracks to effectively contour to the ground surface beneath the tread providing increased traction through increased ground contact as shown in Figure 32. However, the use of tracks on small man-portable or man-packable UGVs often is employed without the use of such complex suspension systems common on their larger counterparts. This use of rigid tracks offsets the mobility advantage of conventional suspension tracks ability of following the ground or obstacle contour [64]. It is also noted that the operation of lightweight UGVs with tracks are prone to increased amounts of wheel slippage during operation causing the vehicle to lose tractive efficiency [65]. This is due mainly to the implementation of rigid tracks or systems where the track

travel is limited and the vehicle cannot overcome obstacles without lifting the entire track off of the ground and reducing the contacting track surface as shown in Figure 33.

Figure 32: Model of a tank suspension overcoming an obstacle [66]

Figure 33: A rigid track system encountering a discontinuity [67]

A large benefit of the utilization of a tracked vehicle is the inherent benefit of low ground pressure. The load distribution over the track contact area provides for a lighter vehicle footprint than if wheels are implemented on a vehicle of the same weight. The minimization of ground pressure is beneficial as a vehicle can avoid becoming mired in loose or non-cohesive terrain such as mud, sand, or snow. This increased mobility over poor terrain surfaces has been a traditional justification for the use of tracked mobility platforms in military operations where heavily armored vehicles must traverse a variety of off-road terrain in all-weather conditions.

The use of tracks for the purposes of decreasing ground pressure becomes less of a concern for vehicles of the size and weight of small unmanned ground vehicles. Adequately minimal ground pressures for the navigation of poor terrain are achievable with either tracked or wheeled platforms due to the decreased overall platform weight.

According to the relationship between ground pressure and the ability to traverse a wide variety of terrains, if a wheeled vehicle can achieve a low ground pressure nearing that of a tracked vehicle, a wheeled vehicle can have the same mobility success over a wide variety of ground surfaces [68]. It is suggested that vehicle ground pressure and soil strength are primary indicators of vehicle mobility [69]. With this in mind, when applied with consideration to terrain mobility based upon ground pressure, wheels can achieve similar mobility over difficult terrain. Within the scope of a small unmanned ground vehicle, this is an attainable objective as vehicle weight can be minimized and wheel footprint can be altered to achieve an acceptable ground pressure rating.

Furthermore, research into the mechanisms and rates of failure in unmanned ground vehicles of varying size classes, has concluded vast preponderance of platform failures have been directly related to failure of tracks systems [70]. The study also concluded that wheeled platforms applied in similar USAR and MOUT field applications had a lower occurrence of ground effector related failures. The study highlighted that thrown tracks were the primary cause of failure with tracked platforms while obstructions in the track mechanisms were often the root cause of failure.

There is no doubt that tracked vehicles can operate in situations where wheeled vehicles would be incapable. There is also no question that wheeled platforms offer benefits over tracked vehicles where USAR and MOUT type operations are not the primary focus for a small unmanned ground vehicle. Much of the current research into robotic UGV platforms focuses on the development of vehicles that display a greater level autonomy and can operate at higher speeds. With consideration to these issues in light of the NERV mission profile, it is apparent that a wheeled vehicle would be an ideal solution. The increased operating speeds, improved efficiency, and improved reliability offered by a coaxially differentially driven wheeled platform is well suited for supporting experimental development of intelligent systems within a controlled pseudostructured environment where mobility over highly unstructured terrain is not required.

3.1.2 Kinematic Model

The development of a planar kinematic model for the four-wheel driven two-body articulated Gemini-type robotic platform will detail the maneuverability capabilities of the proposed NERV design as well as provide insight to the mechanics of the NERV platform that will support increased system control and capabilities. For the purposes of this analysis, second degree of freedom that allows the front section to roll relative to the rear section will be neglected.

The analysis of the two-body articulated, Gemini-type, robotic platform begins with the development of a global model of the kinematic construction of the vehicle as shown in Figure 34. The model of the vehicle is developed as a rigid body on wheels that operates exclusively on a horizontal inertial plane. There is an assumption of no wheel slip and a singular point of contact between the wheels and the ground. The notation and terminology used throughout the analysis process is based upon the methods presented by Siegwart and Nourbakhsh [71].

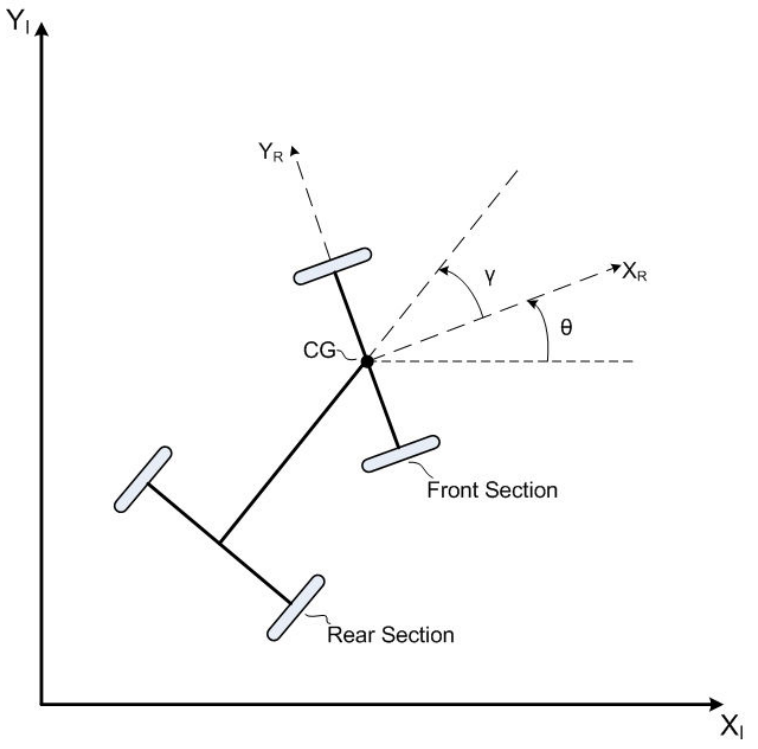

Figure 34: Kinematic representation of the two-body articulated mobile robotic platform.

The model consists of two distinct members: a front section and a rear section. Each section includes two fixed wheels that are orientated coaxially. The front and rear section pivot relative to each other about the point *CG*. The vehicle pose within an inertial frame can be defined by two angular measurements and the location of the point *CG*. The angle between the robot frame ($X_R - Y_R$) and the inertial frame ($X_I - Y_I$) is defined as θ. The angle γ, between the robot coordinate frame attached to the front section of the vehicle and the rigid connecting rod of the vehicle, provides the internal body angle between the front and rear sections.

Global parameters defining the location and orientation of the front section of the vehicle with respect to a global inertial frame of reference can generally be expressed as a vector including the x and y positions of the point *CG*. In addition, a third level of dimensionality θ indicates the angular displacement of the robot coordinate frame relative to the z-axis of the inertial frame that lies orthogonally to the $X_I - Y_I$ plane. The angle γ can be considered as a parameter internal to the vehicle and can addressed independently.

$$ {}^{I}\xi_{CG} = \begin{bmatrix} X \\ Y \\ \theta \end{bmatrix} \qquad (1) $$

The derivative of the position vector results in a composite linear and angular velocity vector that defines the motion of the front section of the vehicle within inertial space.

$$ {}^{I}\dot{\xi}_{CG} = \begin{bmatrix} \dot{X} \\ \dot{Y} \\ \dot{\theta} \end{bmatrix} \qquad (2) $$

With the general development of the notation and layout of the vehicle model, the analysis of the two body articulated robotic vehicle is a two step process: (1) analysis of the front section of the vehicle and (2) analysis of the rear section based upon the results of motion of the front section of the robot. The end result of the analysis of the vehicle platform is to be able to determine the expected position and pose of the vehicle given the front wheel velocities and an initial pose. The ability to calculate the desired rear wheel velocities based solely on body position and front wheel speed allows the vehicle configuration to operate with four powered wheels with motion dependent upon the simple motion of the differentially driven front section. The analysis methodology of the kinematic model is shown in Figure 35

and highlights the iterative nature of the analysis that will lead to the ability to develop a model of vehicle motion as a function of time.

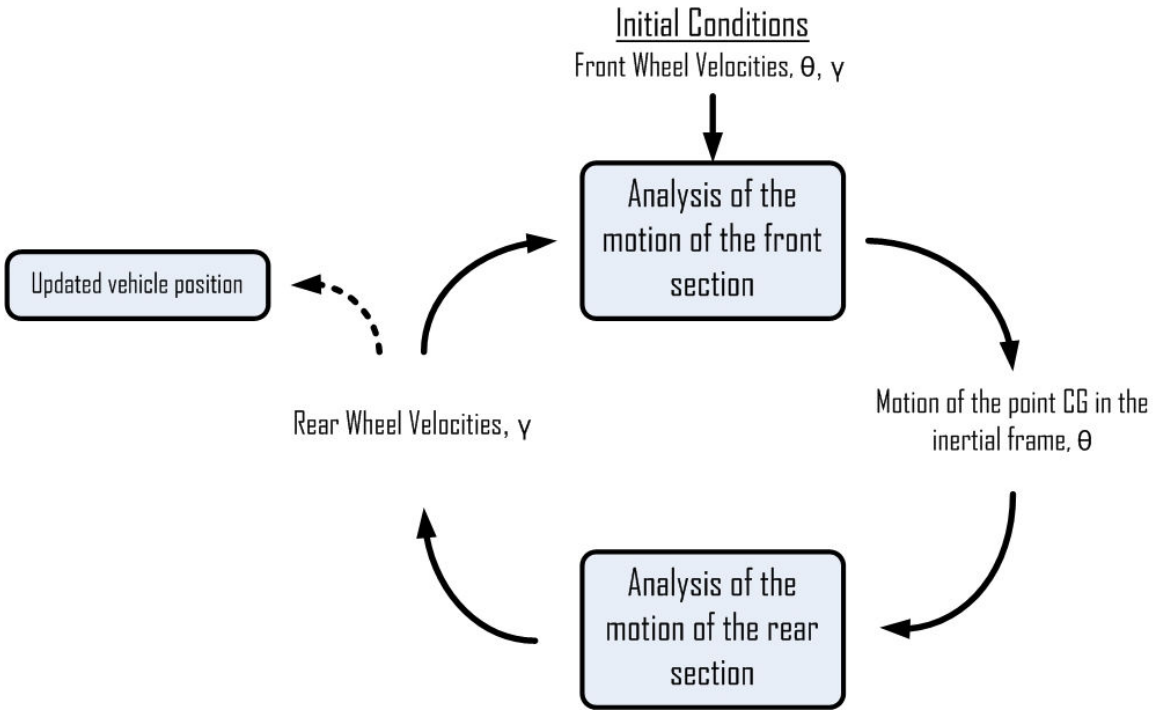

Figure 35: Kinematic analysis methodology

To begin the analysis of the two bodied vehicle, a model of the front section of the vehicle must be developed that will be able to provide the motion of the point *CG* in inertial space as a function of the variables contained within the ${}^{I}\dot{\xi}_{CG}$ vector. The kinematic model , generalized in Figure 36, of the front section is based upon the fixed wheel constraint equations for a differentially driven robot as presented by Siegwart et al [72]. The wheel coordinate frames (X_W – Y_W) for each wheel are oriented so that a positive rotation of the wheel results in a positive motion along the X_R axis.

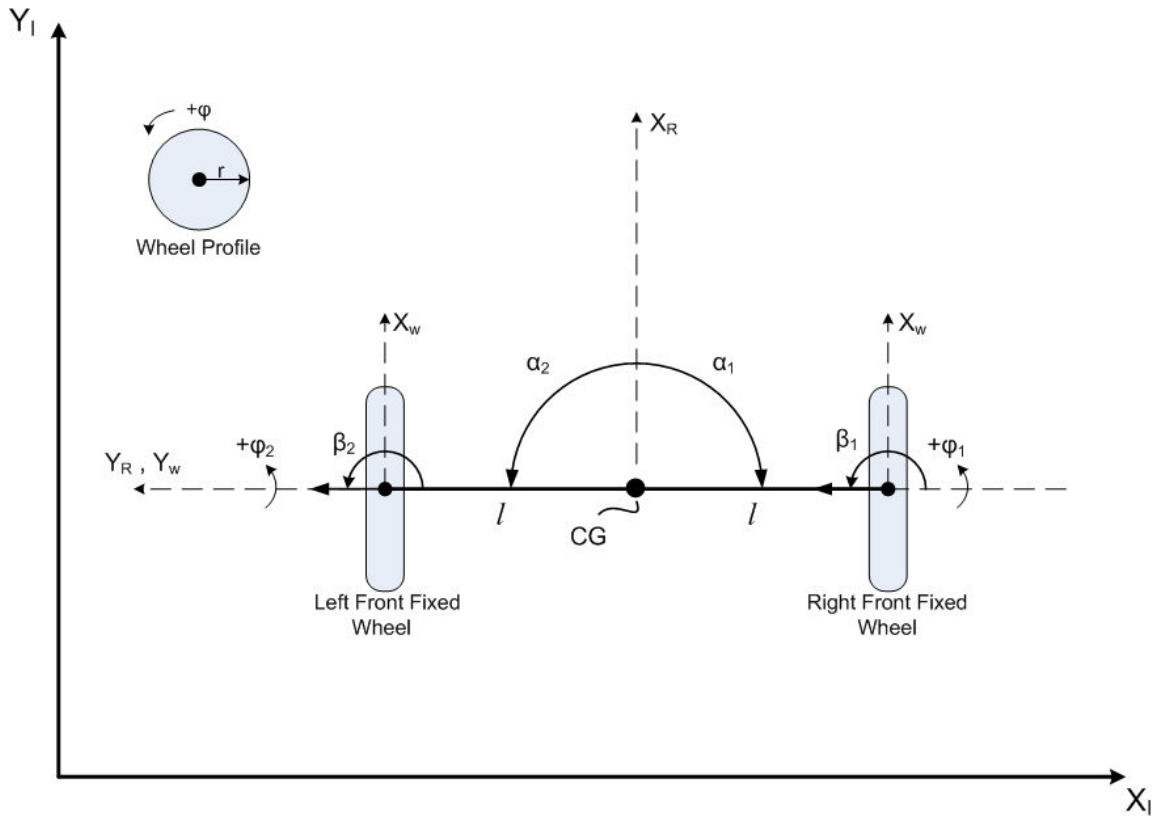

Figure 36: Kinematic model of the front section

For a fixed standard wheel (e.g. a wheel without the ability to steer), the motion of the wheel is dictated by a rolling constraint and a sliding constraint. The rolling constraint detailed by Equation 3 enforces that all the motion along the direction of the wheel plane must be accompanied by an appropriate amount wheel spin so that there is pure rolling at the contact point.

$$\left[\sin(\alpha+\beta) \quad -\cos(\alpha+\beta) \quad (-l)\cos\beta\right]R(\theta)\dot{\xi}_I = r\dot{\varphi} \qquad (3)$$

With the assumption of no slip of the wheel, Equation 4 enforces a sliding constraint on the fixed wheel and ensures that the component of the wheel's motion orthogonal to the wheel plane will be zero.

$$\left[\cos(\alpha+\beta) \quad \sin(\alpha+\beta) \quad (l)\sin\beta\right]R(\theta)\dot{\xi}_I = 0 \qquad (4)$$

With both wheels on the front section of the vehicle being of a fixed configuration, aggregate matrices of the sliding and rolling constraints can be developed using the notation

developed in Figure 36 and the matrix elements of Equations 3 and 4 for the rolling and sliding constraints of a fixed wheel. The rolling constraints for both the left and right fixed wheel on the front section are shown in Equation 5 and the composite of the sliding constraints are shown in Equation 6.

$$J_1 = \begin{bmatrix} \sin(\alpha_1 + \beta_1) & -\cos(\alpha_1 + \beta_1) & (-l)\cos(\beta_1) \\ \sin(\alpha_2 + \beta_2) & -\cos(\alpha_2 + \beta_2) & (-l)\cos(\beta_2) \end{bmatrix} \tag{5}$$

$$C = \begin{bmatrix} \cos(\alpha_1 + \beta_1) & \sin(\alpha_1 + \beta_1) & (l)\sin(\beta_1) \\ \cos(\alpha_2 + \beta_2) & \sin(\alpha_2 + \beta_2) & (l)\sin(\beta_2) \end{bmatrix} \tag{6}$$

The values for α and β developed for the model of the front section of the vehicle are listed below in Table 1. The value for l is a constant value based upon vehicle construction.

Table 1: Values for alpha and beta for the front section

Variable	**Value**
α_1	$\frac{-\pi}{2}$
α_2	$\frac{\pi}{2}$
β_1	π
β_2	0

It is notable that with the configuration of the fixed wheels on the front section of the vehicle in a parallel and coaxial construction, the result of Equation 5 is only a single independent equation.

Additionally, Equation 6 comprises the resulting wheel velocities for the two wheels. The value of $\dot{\varphi}$ represents the rotational velocity of the wheel and r is the radius of the wheel.

$$J_2\dot{\varphi} = \begin{bmatrix} r_1 & 0 \\ 0 & r_2 \end{bmatrix} \begin{bmatrix} \dot{\varphi}_1 \\ \dot{\varphi}_2 \end{bmatrix} \qquad (7)$$

Fusing Equations 3, 4, 5, 6 and 7, yields the following expression:

$$\begin{bmatrix} J_1 \\ C \end{bmatrix} R(\theta) \left({}^{I}\dot{\xi}_{CG} \right) = \begin{bmatrix} J_2\dot{\varphi} \\ 0 \end{bmatrix} \quad (8)$$

The rotation matrix mapping coordinates from the robot frame to the inertial frame of reference is defined as:

$$R(\theta) = \begin{bmatrix} \cos(\theta) & \sin(\theta) & 0 \\ -\sin(\theta) & \cos(\theta) & 0 \\ 0 & 0 & 1 \end{bmatrix} \quad (9)$$

Rearranging Equation 8, it is then possible to determine the instantaneous motion of the point *CG* in the inertial frame based upon the geometry of the vehicle construction and the speed of the two front wheels. The resulting expression is shown in Equation 10.

$${}^{I}\dot{\xi}_{CG} = R(\theta)^{-1} \begin{bmatrix} J_1 \\ C \end{bmatrix}^{-1} \begin{bmatrix} J_2\dot{\varphi} \\ 0 \end{bmatrix} \qquad (10)$$

For the analysis of the rear section of the vehicle, it is desirable to determine the wheel velocities of the rear wheels based entirely upon the wheel velocities of the front wheels and the body angle between the front and rear sections. To accomplish this, the results of Equation 10 for the motion of the point *CG* on the front section will be used as the input to the analysis of the rear section of the vehicle. The point *CG* is common between the two sections and represents the point of rotation between the two bodies. The kinematic model of the rear section is shown in Figure 37 and is an extension of the concepts utilized in the analysis of the front section of the vehicle. This adaptation of the concepts allows a similarly straightforward analysis of the rear section that is the inverse of the front section problem. Where the analysis of the front section of the vehicle determined the motion of body in the inertial frame reference the point *CG* based upon wheel speeds, the analysis of the rear section will determine the resultant wheel speeds of the rear wheels based upon the motion of point *CG* in the inertial frame. The robot coordinate frame ($X_R - Y_R$) is carried over

from the analysis of the front section of the vehicle and provides a means to create a reference angle, γ, between the front section and rear section of the vehicle.

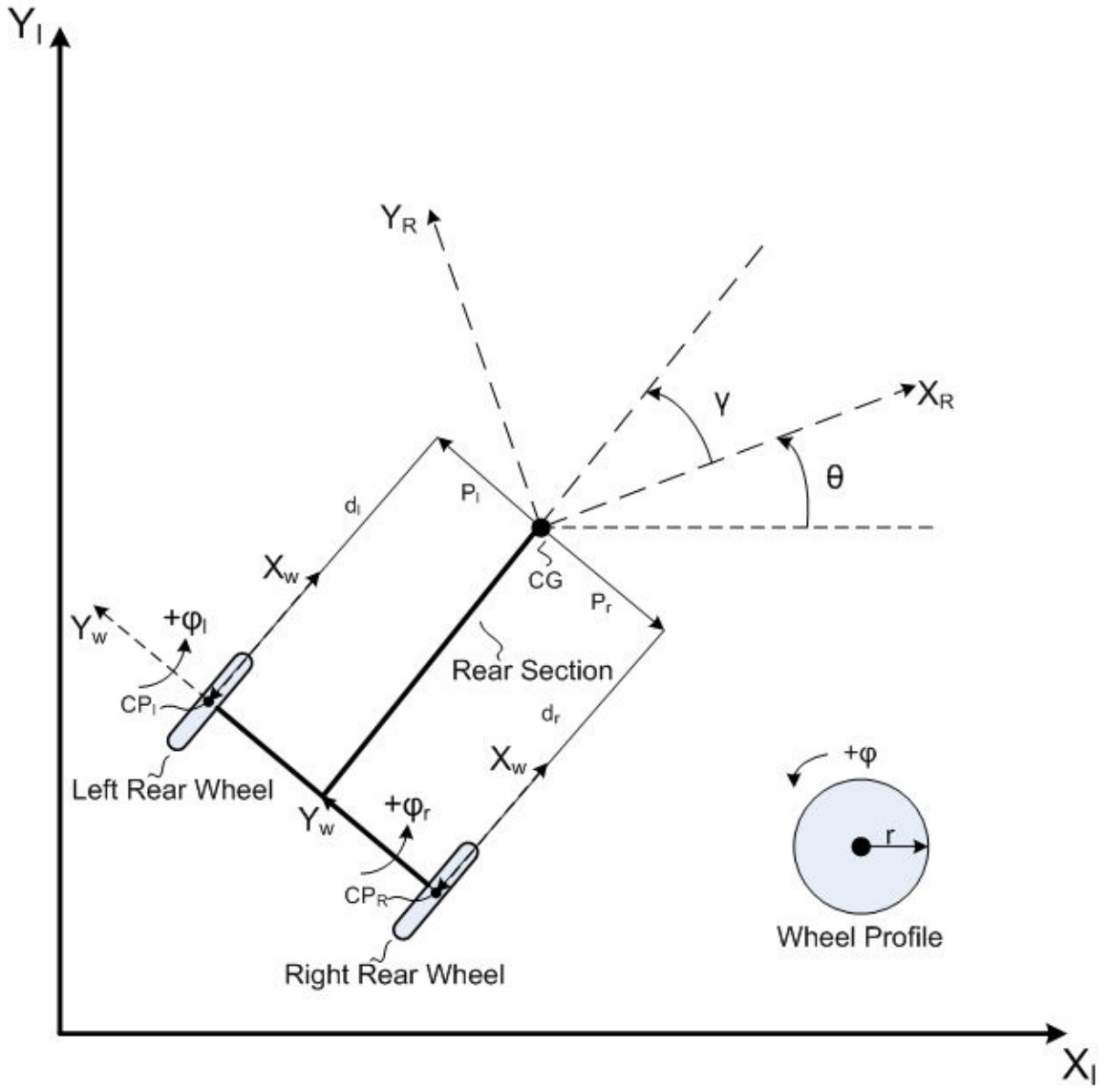

Figure 37: Kinematic model of the rear section of the two-bodied vehicle

To begin the analysis of the rear section of the vehicle, Equation 11 defines the contact point of the left rear wheel in the global reference frame. The analysis will develop the kinematic equations for the left rear wheel of the vehicle and then apply the results to provide additional equations for the right rear wheel.

$$ {}^{I}\vec{P}_{CPl} = \begin{bmatrix} X \\ Y \end{bmatrix} + P_l j e^{j(\gamma+\theta)} - d_l e^{j(\gamma+\theta)} \qquad (11) $$

The derivative of the position of the contact point yields the velocity of the contact point of the left rear wheel shown in Equation 12.

$$ {}^{I}\vec{V}_{CPl} = \begin{bmatrix} \dot{X} \\ \dot{Y} \end{bmatrix} - P_l(\dot{\gamma}+\dot{\theta}) e^{j(\gamma+\theta)} - d_l j(\dot{\gamma}+\dot{\theta}) e^{j(\gamma+\theta)} \qquad (12) $$

Equation 13 represents the unit vector of the axis of rotation for the left rear wheel. The positive value of the axis is determined to yield a positive motion along the x-axis of the robot coordinate frame for a positive wheel rotation.

$$ {}^{I}\vec{Y}_{Wl} = j e^{j(\gamma+\theta)} = \begin{bmatrix} -\sin(\gamma+\theta) \\ \cos(\gamma+\theta) \end{bmatrix} \qquad (13) $$

The dot product of the vector of the axis of rotation vector and the velocity of the contact point must be equal to zero, otherwise the wheel would be able to slide perpendicular to the motion plane of the wheel. Equation 14 represents the sliding constraint for the rear wheels of the vehicle.

$$ {}^{I}\vec{Y}_{Wl} \circ {}^{I}\vec{V}_{CPl} = 0 \qquad (14) $$

The dot product yields an equation for the angular velocity $\dot{\gamma}$ of the rear section relative to the front section. Equation 15 utilizes the physical constants of the vehicle construction and the values of the inertial position ${}^{I}\xi_{CG}$ and motion ${}^{I}\dot{\xi}_{CG}$ vectors obtained from Equation 10 utilizing the initial conditions provided by the vehicle pose.

$$ \dot{\gamma} = \frac{1}{d_l}[-\dot{x}\sin(\gamma+\theta) + \dot{y}\cos(\gamma+\theta) - d_l\dot{\theta}] \qquad (15) $$

Equation 16 is the expression for the unit vector for the motion plane of the left rear wheel.

$$ {}^{I}\vec{X}_{Wl} = e^{j(\gamma+\theta)} = \begin{bmatrix} \cos(\gamma+\theta) \\ \sin(\gamma+\theta) \end{bmatrix} \qquad (16) $$

The dot product of the unit vector of the motion plane for the rear wheel and the velocity of the contact point yields the wheel velocity. Equation 17 defines the rolling constraint for the rear wheel.

$$ {}^{I}\vec{X}_{Wl} \circ {}^{I}\vec{V}_{CPl} = \dot{\phi}_l r_l \quad (17) $$

Working through Equation 17 with the initial condition ${}^{I}\xi_{CG}$ values of the vehicle pose, the motion vector ${}^{I}\dot{\xi}_{CG}$ obtained from Equation 10, and with the value of $\dot{\gamma}$ from Equation 15, the resultant is an expression detailed by Equation 18 for the rotational velocity of the left rear wheel.

$$ \dot{\phi}_l = \frac{1}{r_l}[\dot{x}\cos(\gamma+\theta) + \dot{y}\sin(\gamma+\theta) - P_l(\dot{\gamma}+\dot{\theta})] \quad (18) $$

This solution easily transfers to the right rear wheel of the vehicle as the construction of the vehicle is symmetric. For the right rear wheel the position of the contact point is defined as Equation 19.

$$ {}^{I}\vec{P}_{C\,\mathrm{Pr}} = \begin{bmatrix} X \\ Y \end{bmatrix} - P_r j e^{j(\gamma+\theta)} - d_r e^{j(\gamma+\theta)} \quad (19) $$

The derivative of Equation 20 the position results in an expression representing the velocity of the contact point for the right rear wheel.

$$ {}^{I}\vec{V}_{C\,\mathrm{Pr}} = \begin{bmatrix} \dot{X} \\ \dot{Y} \end{bmatrix} + P_r(\dot{\gamma}+\dot{\theta})e^{j(\gamma+\theta)} - d_r j(\dot{\gamma}+\dot{\theta})e^{j(\gamma+\theta)} \quad (20) $$

In accordance with the convention for establishing the unit vector representing the motion plane of the wheel for the left rear wheel, the right rear wheel utilizes the same definition as developed in Equation 16. The dot product of the unit vector representing the motion plane of the right rear wheel and the velocity of the right rear wheel contact point again is equal to the rotational velocity of the wheel.

$$ {}^{I}\vec{X}_{Wr} \circ {}^{I}\vec{V}_{C\,\mathrm{Pr}} = \dot{\phi}_r r_r \quad (21) $$

The result of Equation 21 yields an expression that represents the rotational velocity of the right rear wheel in terms of the global velocity and angular position of the front section of the vehicle as well as the rate of angular displacement of the body angle between the front and rear sections of the vehicle.

$$\dot{\phi}_r = \frac{1}{r_r}[\dot{x}\cos(\gamma+\theta) + \dot{y}\sin(\gamma+\theta) + P_r(\dot{\gamma}+\dot{\theta})] \qquad (22)$$

The expression for $\dot{\gamma}$ is a constant for both wheels due to the fact that the wheels are in a coaxial configuration. This allows the result from Equation 15 to be used to solve for the rotational velocity of the right rear wheel via Equation 22.

3.1.3 Kinematic Computer Simulation

With the theoretic kinematic model of the two-body vehicle developed, a computer simulation can be created. A simulation was created using Matlab script files to provide a simple means to perform the calculations and provide visual feedback of the results for verification and display. The simulation uses initial conditions that define the initial pose of the vehicle and physical constants of the vehicle construction to provide a predicted path of the vehicle in the inertial frame based solely on the front wheel velocities. This process is generally outlined in the diagram shown in Figure 35 and implemented via the architecture defined in Figure 38. The Matlab code that implements the simulation is detailed in Appendix D.

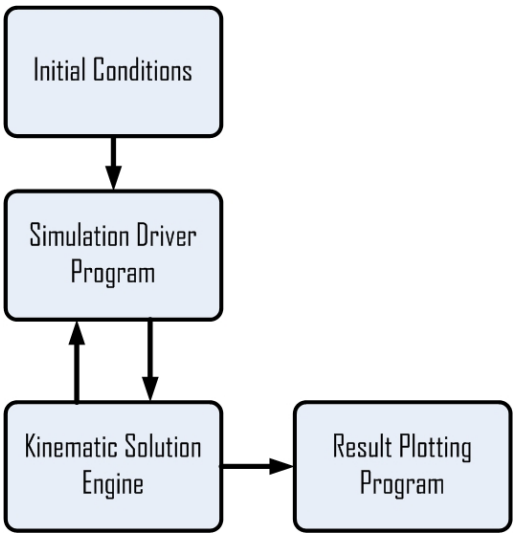

Figure 38: Kinematic simulation program architecture

The user defined inputs to the simulation are detailed below in Table 2. These inputs define the initial conditions of the vehicle and simulation parameters. The front wheel speeds are notably the only variable factor within this group of initial conditions. The result is the ability to not only model the predicted path of the two-body vehicle for a specific pose given constant wheel speeds of the front wheels but, also to change the wheel speeds dynamically through the simulation yielding a more complex path model.

Table 2: Input values to kinematic computer simulator

Parameter	Description	Type
$\dot{\varphi}_1$	Rotational velocity of the front right wheel	Variable
$\dot{\varphi}_2$	Rotational velocity of the left front wheel	Variable
CG	Initial starting point of the vehicle referenced to the center of	Constant
R_1	Radius of the front right wheel	Constant
R_2	Radius of the left front wheel	Constant
R_R	Radius of the right rear wheel	Constant
R_L	Radius of the left rear wheel	Constant
l	Distance between front wheels and center point of rotation CG	Constant
d	Distance between CG and rear axle	Constant
p	Distance between rear wheel and midpoint of rear axle	Constant
θ	Initial angle of rotation between front body and inertial space	Constant
γ	Initial angle of between the front and rear sections	Constant
Δt	Time step to use in the simulation	Constant
t	Total simulation length	Constant

For the purposes of demonstrating the results of the kinematic computer simulation, an arbitrary vehicle design is used to generate the simulation results. The parameters used for demonstration results are detailed in Table 3. Values for the initial angles that define the pose of the vehicle as well as the wheel velocities will be altered to define the case that is to be analyzed using the simulation.

Table 3: Arbitrary design and simulation parameters used for demonstration examples

Parameter	Value	Units
CG	[0,0]	meters
R_1	0.1	meters
R_2	0.1	meters
R_R	0.1	meters
R_L	0.1	meters
l	0.25	meters
d	0.5	meters
p	0.25	meters
Δt	0.1	seconds
t	5	seconds

The running the simulation yields a projected path plot that includes a representation of the body members of the two-body robotic platform. The results for the simple case of an arbitrarily constructed vehicle with constant front wheel speeds of $\dot{\varphi}$ = 10 radians per second and having initial pose defined by $\theta = \pi/4$ and $\gamma = 0$ is shown in Figure 39. The result is the vehicle moving in a straight forward direction relative to the initial pose in the inertial frame.

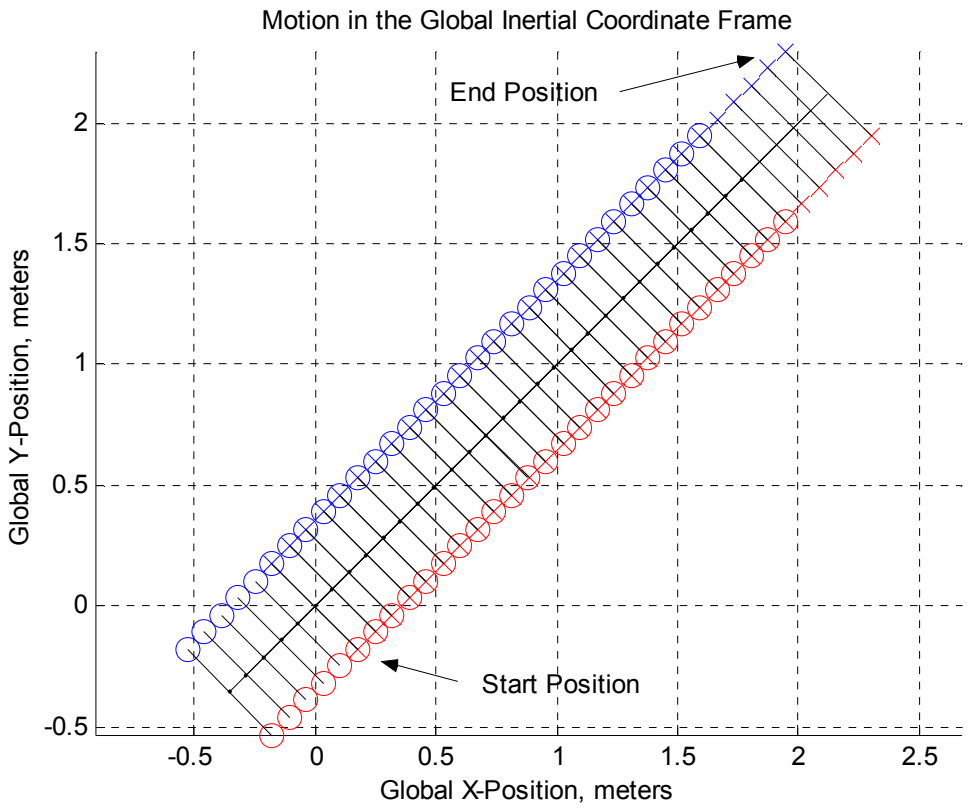

Figure 39: Simple case of predicted vehicle path. Red denotes the right side of the vehicle and blue the left. X's indicate the front wheels and O's indicate the rear wheels.

The result of the simulation with the same initial pose but wheel speeds of $\dot{\varphi}_1 = 10$ radians per second and $\dot{\varphi}_2 = 5$ radians per second, is shown in Figure 40.

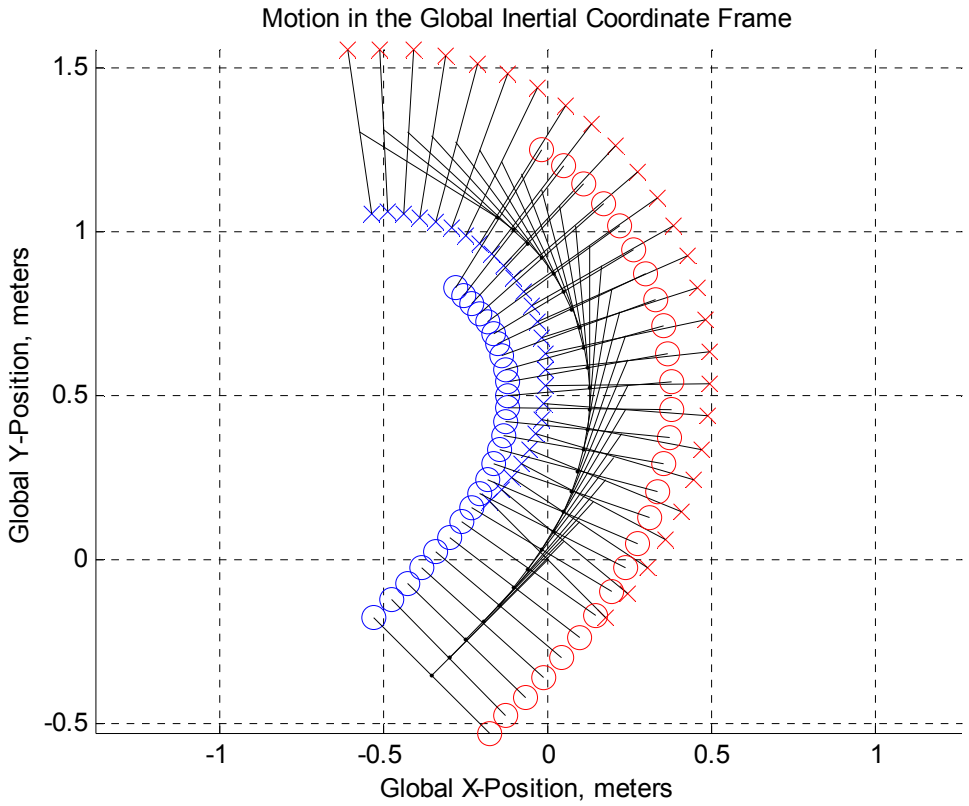

Figure 40: Predicted path for the same initial pose as Figure 39 but with differing front wheel velocities.

For another example of the vehicle motion, consider the pose of the vehicle where $\theta = \pi/2$ and $\gamma = \pi/2$ and both wheel velocities are equal at $\dot{\varphi}$ = 10 radians per second. The resulting path is detailed in Figure 41 with the simulation total time extended to five seconds to highlight the tendency towards a steady state operation.

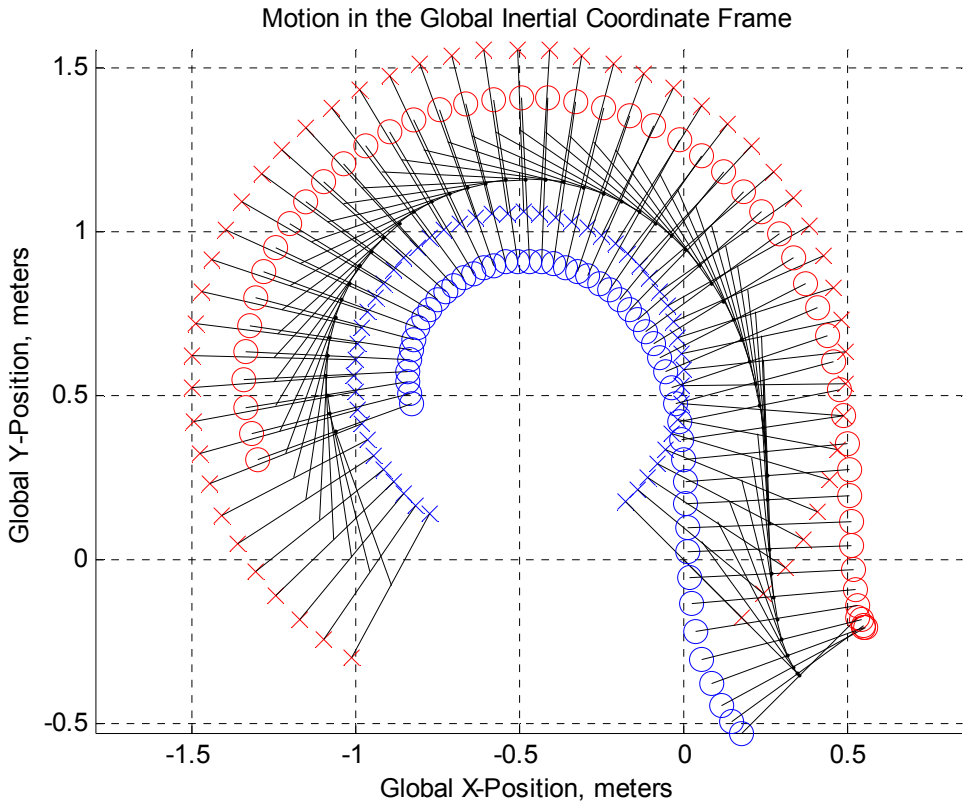

Figure 41: Predicted path of vehicle motion highlighting the tendency of the rear section to seek equilibrium with the front section of the vehicle.

For the example motion shown in Figure 41 it is of interest to plot the value of γ as a function of time. As the vehicle moves from an initial position, the constant front wheel velocities of $\dot{\varphi}_1 = 10$ radians per second and $\dot{\varphi}_2 = 5$ radians per second drive the front section of the vehicle in a circular path with a constant turning radius. From the initial pose, the rear section of the vehicle moves to an equilibrium path that trails the front section. Figure 42 details the change of the body angle γ as a function of time and is it evident that the angle between the two bodies tends towards a steady state value.

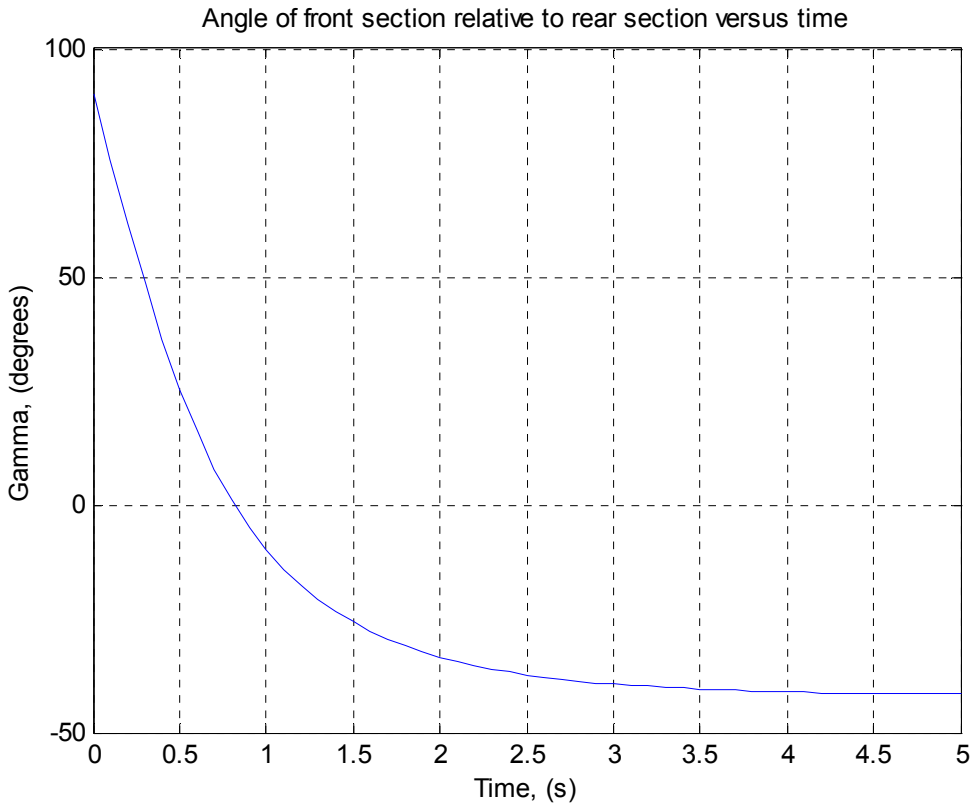

Figure 42: Angle between front and rear sections of the vehicle as a function of time for the case presented in Figure 41.

This tendency of the rear of the vehicle to follow the from section to achieve a steady state relationship based upon the speed of the front wheels is exemplified by plotting the resulting rear wheel velocities as a function of time. Figure 43 clearly indicates that the rear wheels move with variable velocity through the transient stage of motion before reaching a stable steady state velocity the provides the constant turning radius required to maintain kinematic constraints to match the motion of the front section.

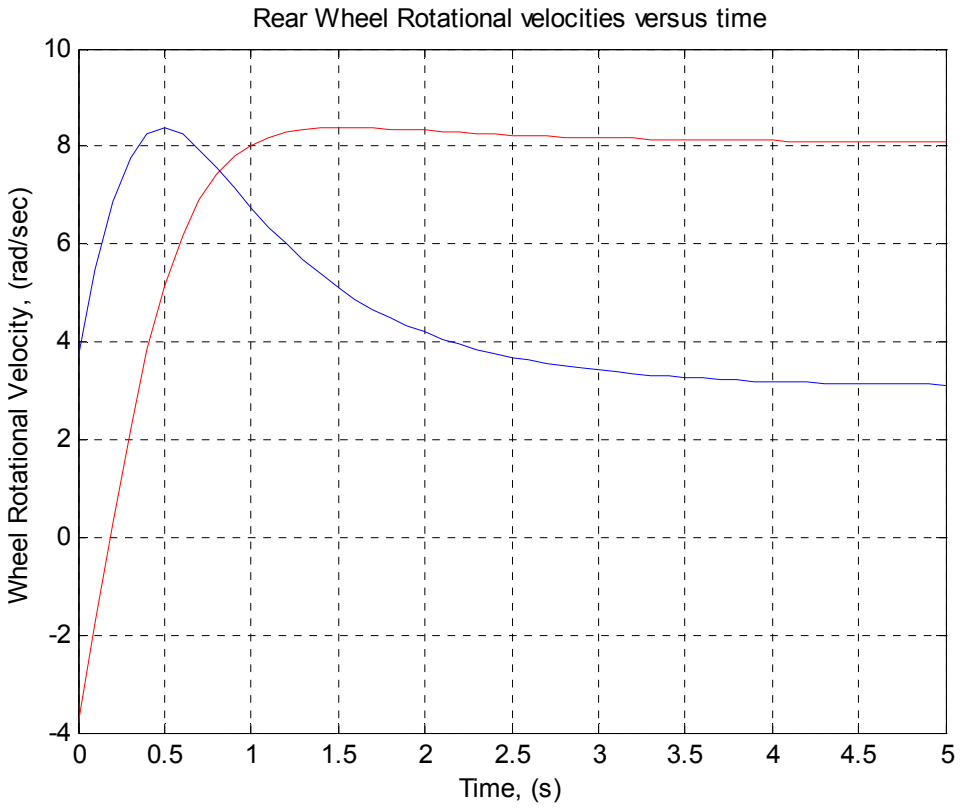

Figure 43: Rear wheel rotational velocity as a function of time for the case presented in Figure 41.

The motion of the case of platform movement shown in Figures 41, 42, and 43 indicates the rear wheel velocities stabilizing to track the front section as it travels in a path of a constant turning radius during the application of constant front wheel velocities.

For another example of the vehicle motion, consider the pose of the vehicle where $\theta = -\pi/4$ and $\gamma = -\pi/2$ and both wheel velocities are equal at $\dot{\varphi}$ = 5 radians per second. As the vehicle moves from an initial position, Figure 44 reveals that the rear section trails the front section and moves towards matching the path of the forward section as the path progresses.

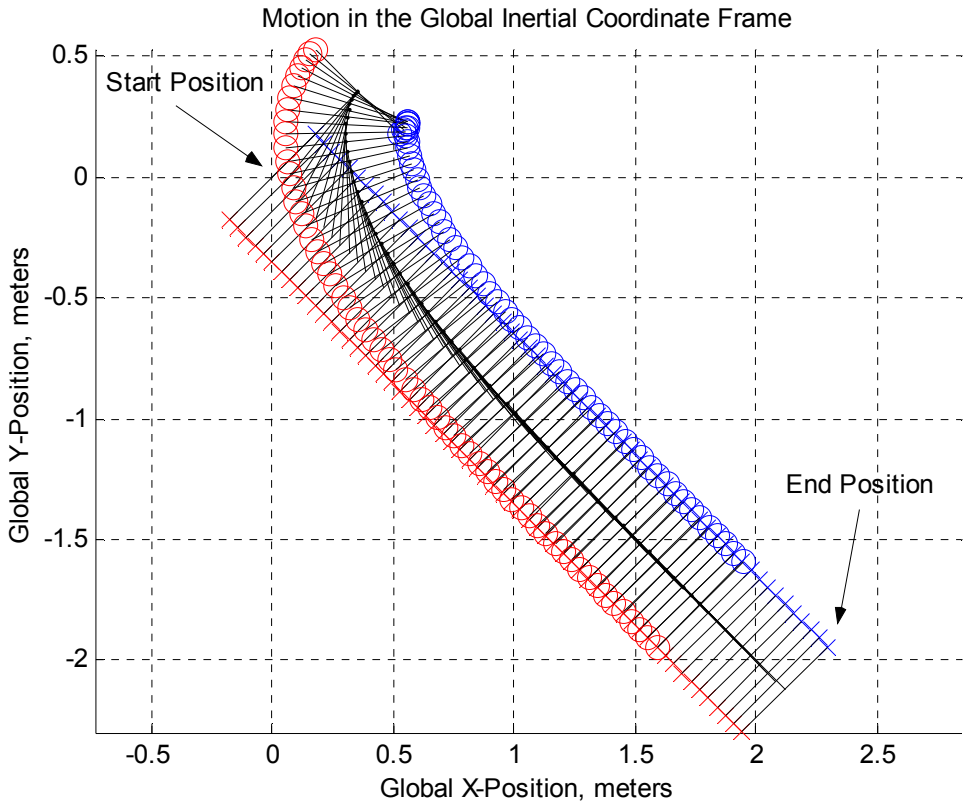

Figure 44: Motion of the two-bodied platform with the rear wheels moving to match the velocity of the front wheels.

Figure 45 details the relative angle between the front and rear sections converging on a value of zero as the simulation progresses and the rear section follows the front section.

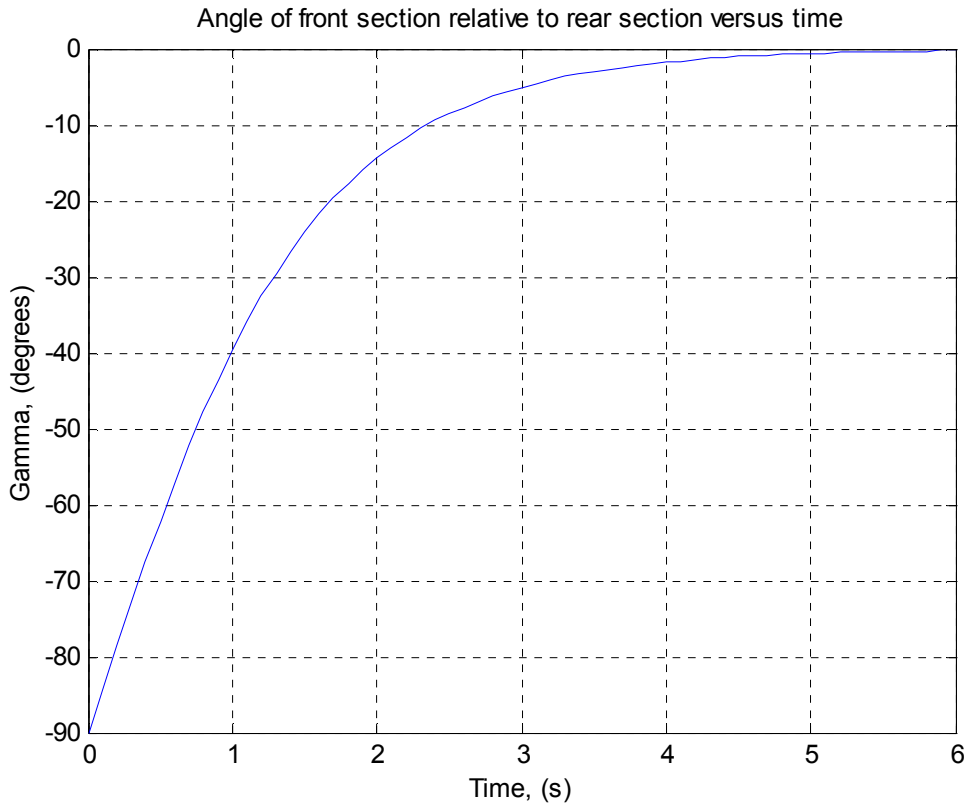

Figure 45: Plot of the angle between the front and rear section and a function of time.

More telling is the plot shown in Figure 46 of the rear wheel velocities as a function of time. It is apparent that the wheel velocities converge to a value of five radians per second to match the wheel velocities of the front section as the front and rear sections align through the course of the simulated motion. Based upon the initial pose of the vehicle it is apparent that the right rear wheel velocity must be greater than the left rear wheel to make the transition to follow the front section.

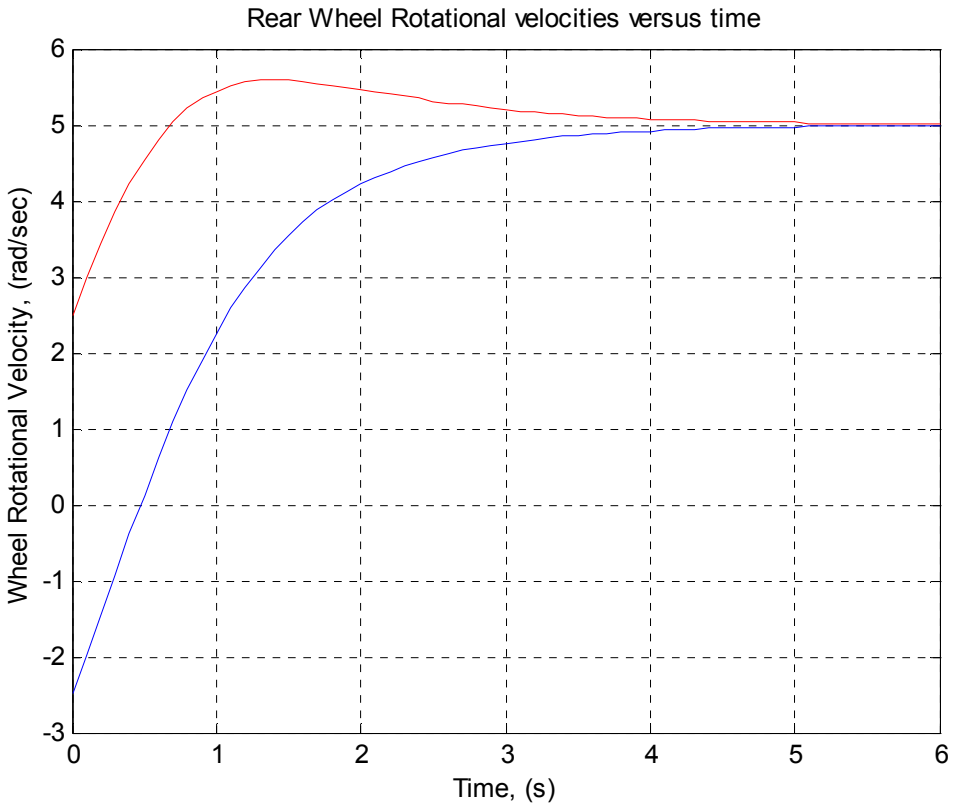

Figure 46: Plot of the rear wheel velocities as a function of time.

The results of the computer simulation of the kinematic relationships of the two-bodied mobile robotic platform leads to the ability to develop several unique features that are novel to the unique axle-articulated design proposed for the NERV platform. The utilization of this model will facilitate the enhanced dynamic control of the vehicle through the ability to apply control algorithms that will provide four-wheel drive and evasive reverse navigation capabilities.

3.1.4 Implications of the Kinematic Model

The kinematic model developed for the two-body articulated vehicle can be applied to several key areas of investigation that would extend the theoretical understanding of the mobility of the two-body platform. The implications of the kinematic model include the ability to predict an accurate value for the path allowances for the two-bodied articulated vehicle for the purpose of developing path planning algorithms. The model allows for the determination of a path swath estimate that can be used to navigate the vehicle through narrow corridors where the trailing section could become mired on an obstacle.

In addition, the model indicates that the rear wheel velocities can exceed the commanded front wheel speeds. For the mobility case presented in Figures 44 through 46, the maximum wheel speed commanded to the front wheel was five radians per second. However, Figure 46 indicates that the resulting right rear wheel achieves a speed of approximately 5.5 radians per second due to the geometric pose of the vehicle through the motion. In application, the design of the NERV platform would account for this requirement by providing rear wheel power train that can achieve maximum rotational speeds that would be compatible with the maximum speeds of the front section for all poses of the vehicle. This solution would result in the rear wheel motors having increased maximum speed capabilities while potentially sacrificing torque output. However, the speed requirements for the rear wheels based upon the case detailed in Figures 44 through 46 are nominally ten percent greater than the commanded wheel speed. This indicates that potentially there would be little required sacrifice of torque output for the rear section to achieve the necessary speeds. Alternatively, the front wheel speeds would be limited so that the rear section required wheel speeds would be compliant with the capabilities of the rear wheel motor maximum speeds.

Developing the kinematic model to include the second degree-of-freedom between the front and rear section requires further investigation into two areas: (1) the effect of the second degree-of-freedom on the induced rear wheel velocities and (2) the working envelope of motion of the front section relative to the rear section. The introduction of the second degree-of-freedom alters the assumption that the relative distances between the points of wheel contact remain constant and interact on the same plane. Extending the kinematic model to include these variables would enhance the applicability of the model in varying terrain cases. Additionally, the addition of the consideration for multi-planar points of contact demands the need to develop model constraints that can predict interference between mechanical aspects of the vehicle construction. This may take the form of developing a working envelope for the relative position of the front section. This is due to the fact that the front section has the possibility of interfering with the connecting beam of the rear section as the value of γ approaches $\gamma = \pi/2$ or $\gamma = -\pi/2$. Development of this working envelope of the front section would permit the development of further control algorithms that would prevent platform interference over a variety of surfaces and terrain conditions.

Extending the model presented for the two-body articulated vehicle, there is a distinct possibility to apply this method to developing kinematic models for other multi-body mobile robotic platforms of varying sizes. For instance, potential military applications of

autonomous convoys could benefit greatly from the development of a kinematic model of a vehicle and trailer configurations to assist in the creation of algorithms that support autonomous trailer maneuvers. The methodology developed for the NERV can be extended to determine convoy swath allowances, obstacle avoidance corridor maneuvers, and parking.

3.1.5 Four-Wheel Drive

In a configuration where only the forward wheels of a two-bodied articulated vehicle are powered, there is a distinct concern to distribute the majority of the vehicle weight towards the forward section centered over the drive wheels to improve and maintain sufficient traction. The consequences the forward section being driven wheels is not limited to the potential for loss of tractive force through poor surface conditions. Unfavorable weight distribution poses the threat of the rear section becoming mired in a surface discontinuity could leave the vehicle wholly disabled. In contrast to the Gemini platform configuration where the two forward wheels provided all of the force to drive the vehicle, the NERV provides the ability to power all four of the wheels with the application of the kinematic model for a two-bodied mobile platform. A four-wheel drive configuration allows for improved traction and stability over difficult terrain as well as increased the payload capacity of the vehicle as weight distribution can be distributed over the entirety of the vehicle chassis. The result of this leap towards four wheel power is a sport-utility robotic vehicle that maintains the maneuverability of a differentially driven vehicle (i.e. zero radius turning) while providing extended mobility and capability to more aggressive terrain situations.

Analysis of the results of the kinematic model development and computer simulation indicates that the ability to practically apply a four wheel drive system on the NERV platform. This improved capability over the two-wheel drive Gemini design is reliant on the ability to measure the angle between the front and rear sections of the vehicle as well as the front wheel velocities. In practice this is a simple capability to provide with the inclusion of an absolute position encoder on the steering joint on the vehicle platform.

This leads to the dramatic conclusion that the NERV can be simply controlled by commanding the front section wheel velocities as if the vehicle were a simple differentially driven vehicle while the rear wheels are commanded to drive so that the induced motion would be kinematically matching. This is indeed a leap forward in design due to the fact that upper-level path planning an control algorithms can consider the motion of the vehicle as a simple two wheeled differentially driven robotic platform. This simple model can then

supplemented by the kinematic model to allow for enhanced body position awareness and motion control within a lower-level control applications.

Further, the kinematic model developed for the two-body Gemini-type vehicle can be applied irrespective of which section is labeled the "front". The model is completely reversible and can also adapt to varying asymmetric geometries.

The application of this feature will be the kinematic model applied within the control software of the NERV that will synthesize the commanded wheel speeds of the front section and the current angle between the front and rear section to develop the proper rear wheel rotational velocities. The result is a wheeled mobile robotic vehicle platform with enhanced mobility capability coming from four-wheel drive locomotion without the drawbacks of tracked or wheeled skid-steer designs.

3.1.6 Adaptive Drive

The adaptive drive capabilities of the NERV exist to alter drivetrain characteristics in an effort to achieve increased performance in a variety of mobility situations as well as sustain the NERV platform through discretionary tactics that prevent damage to the vehicle during operation. This capability manifests itself through the adaptive drive techniques resulting from external conditions and internal states of the vehicle. A means for generating an accurate assessment of current terrain conditions through characterization of drive motor response yields a classification of surface conditions (e.g. grass, rocks, sand, etc.) as well as detecting wheel slippage [73]. This research indicates that through the analysis of motor performance criteria such as current, a relationship can be developed related to the shear strength of a ground surface. This shear strength can then be correlated to a particular ground covering. The NERV will utilize this capability to generally classify the surface over which it is operating. Once the surface is characterized, the drive system will adapt drive limits, parameters, and control systems to account for the particular ground conditions in an effort to maximize efficiency and effectiveness. In practice, this capability would provide means to detect wheel slippage over non-cohesive surfaces such as sand or snow and provide the justification to alter the control systems on the fly in response to the current state of the wheels to account for this change in condition. Wheel torques and speeds could be altered to increase traction or to maintain a specific vehicle velocity over a variety of terrains through the utilization of the adaptive drive capability. Further, the adaptive drive function supports the implementation of the four wheel drive NERV platform as power can be applied to specific wheels to maintain traction and mobility in much the same way as systems implemented in production all wheel drive passenger automobiles.

In addition, the implementation of a four wheel drive system adds the threat of the wheels driving the vehicle into kinematic contention. To avoid this inefficient and potentially immobilizing situation, strain gauges within the structure of the connecting rod between the two bodies will be used. The presence of strain, particularly elevated levels of strain, within the connection rod indicates that the wheels may be driving the vehicle into kinematic contention. Slight contention resulting from drive wheel mismatch would often lead to little more than small amounts of wheel slippage however, if surface conditions are not conducive to permitting wheel slippage or if the levels of contention are at an elevated level it is conceivable that the vehicle platform would be compromised through excessive stress ultimately leading to total failure. Figure 47 highlights the effects of mismatched wheel velocities leading to kinematic contention and the resulting induced tress in the vehicle frame. Monitoring the vehicle for the presence of kinematic contention in real time and adapting the drive control systems to null contributing parameters will add to the capability of the NERV system.

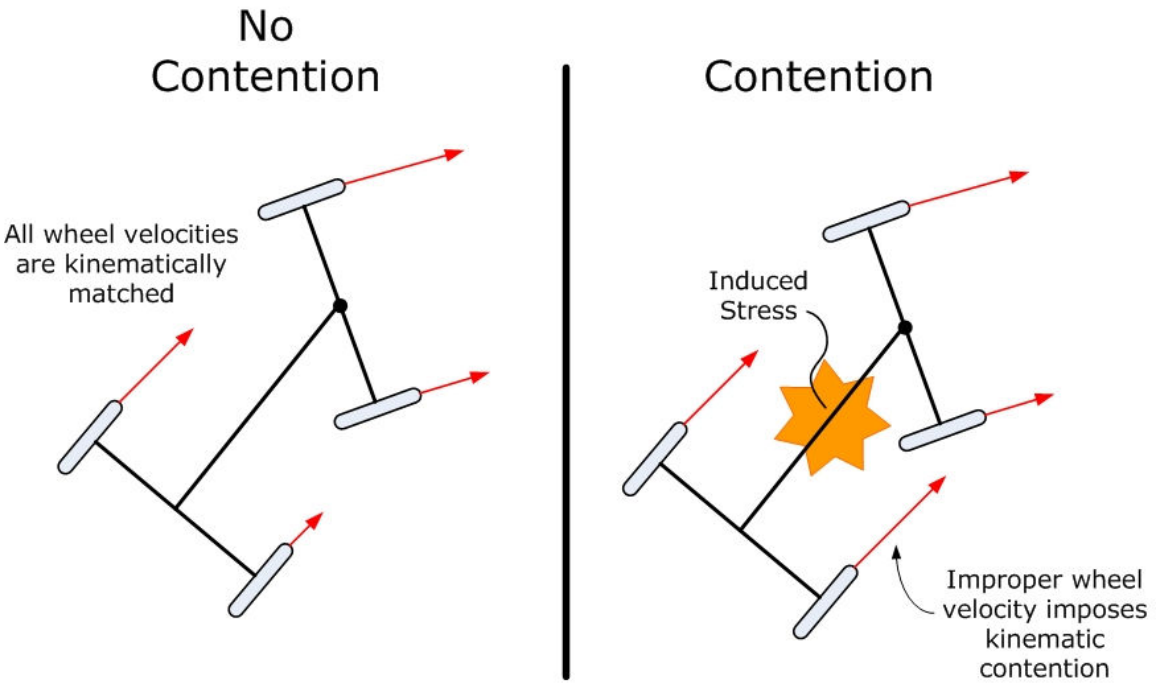

Figure 47: Wheel velocity mismatch yields kinematic contention

3.2 Power System

Batteries are the ideal option for the NERV power supply as it affords the ability to operate without an inhibiting tether and without the noise, complexity, and inherent volatility of an internal combustion engine. The NERV will rely on batteries to provide the

necessary power to attain sufficient runtimes to support unmanned systems experimentation.

A frequent request of users from testing with unmanned ground vehicles is that any batteries used on the vehicle be standardized throughout the system, that is interchangeable between the vehicle and any other system hardware such as an OCU, and that the batteries are congruent with standard cell configurations and chemistries. This desire is most notable in the requirements for the military as there is a definite advantage to limit the number and diversification of battery types used during operations. Therefore, it is desirable that the batteries used on a vehicle be a mil-spec form factor that is already in use in the field. However, this requirement is difficult to meet as the batteries available within the military inventory often lack the energy density required to meet UGV performance marks [74].

To help address this need to provide flexible and scalable power sources, the NERV incorporates a modular power system that accepts a common specification battery power supply that can be comprised of a variety of battery chemistries. The battery system is envisioned as a module that can be removed and swapped for a fresh battery bank to continue the mission. Also, the NERV vehicle includes provisions for an onboard battery charging system that can interface with AC power through an external power port and charge the onboard batteries without having to remove the battery cells from the vehicle.

In addition, the rear section of the vehicle could potentially utilize a gasoline or diesel fuel generator to feed into the battery power system to provide for sustained battery charge for extended runtimes and in situation where the complexity and noise associated with such a solution would be acceptable.

Based upon the lessons learned from the design and development of the Gemini robotic platform, the distribution of the power derived from the onboard battery banks should be carried out via solid-sate components that are mounted on custom printed circuit boards to eliminate failure modes associated with electro-mechanical distribution switches and wired terminal connections. The power system should also include current and voltage regulation to maintain the proper power ranges for specific components and to prevent damage to components and safety concerns.

3.2.1 Health Monitoring

Development of robotic vehicle autonomy necessitates the inclusion of system health monitoring capabilities. The goal of the health monitoring system on the NERV is to gather

and interpret data pertaining to the state of onboard systems in an attempt to alter system commands in response to changing characteristics of the vehicle platform. In essence, this capability seeks to replace a human operator in the capacity of making a judgment call on the state of vehicle and the appropriate course of action to maintain system integrity and accomplish mission objectives. Much like a human driver who notices that the fuel gauge on the dashboard is nearly on empty, engine temperature is creeping towards the red zone, or that the vehicle is pulling to the left; the NERV health monitoring system will suggest responses to these out of the ordinary characteristics in order to maintain overall system effectiveness much like a driver who seeks the nearest gas station, pulls over to let the engine cool down, or notices that a flat tire requires repair. The health monitoring system will alter the operational parameters such as speed and path planning in response to changes in state such as fuel level, temperature, and structural integrity. This type of systemic monitoring is unique among small unmanned ground vehicles and is a fundamental component of the next-generation of autonomous robotic systems.

The health monitoring capabilities of the NERV begins with the evaluation of the state of the vehicle power system. Instrumentation will monitor the health of the onboard power supply to assure that the mission objectives can be reliably attained and provide alert to changes in the system that may compromise the ability of the NERV to continue operation. Parameters of interest that would be included in the power system monitor include:

- Battery temperature
- Battery state-of-charge
- Power/Current/Voltage demands
- Circuit Protection Status
- Motor Temperature

In addition, the health monitoring system will provide useful feedback on the state of the mechanical platform itself. Analysis of observed strain in critical areas of the vehicle chassis would indicate the potential for self destructive conditions and would require a reevaluation of vehicle movement. The wheels and tires would be monitored to assure that tire pressure and assembly integrity is within specifications. Extending this idea further, lubricants and self-noise level detection can also be monitored to support mission objectives.

3.3 Sensor and Payload Integration Schema

The approach to the integration of sensor technologies on the NERV serves to provide a multi-level approach to progressive autonomy in accordance with the NERV design goals. This is accomplished through the use of the standard JAUS reference architecture to develop compliant software and hardware solutions. The end result support the accomplishment of the NERV design goals through the implementation of an open architecture that provides a scalable solution for unmanned systems researchers.

3.3.1 JAUS Reference Architecture

The JAUS reference architecture [75] is the basis on which the NERV system integration is designed. The entire NERV system architecture is be implemented as a JAUS compliant sub-system that is able to mesh with an external JAUS compatible host network or system. The JAUS topology is outlined in Figure 48.

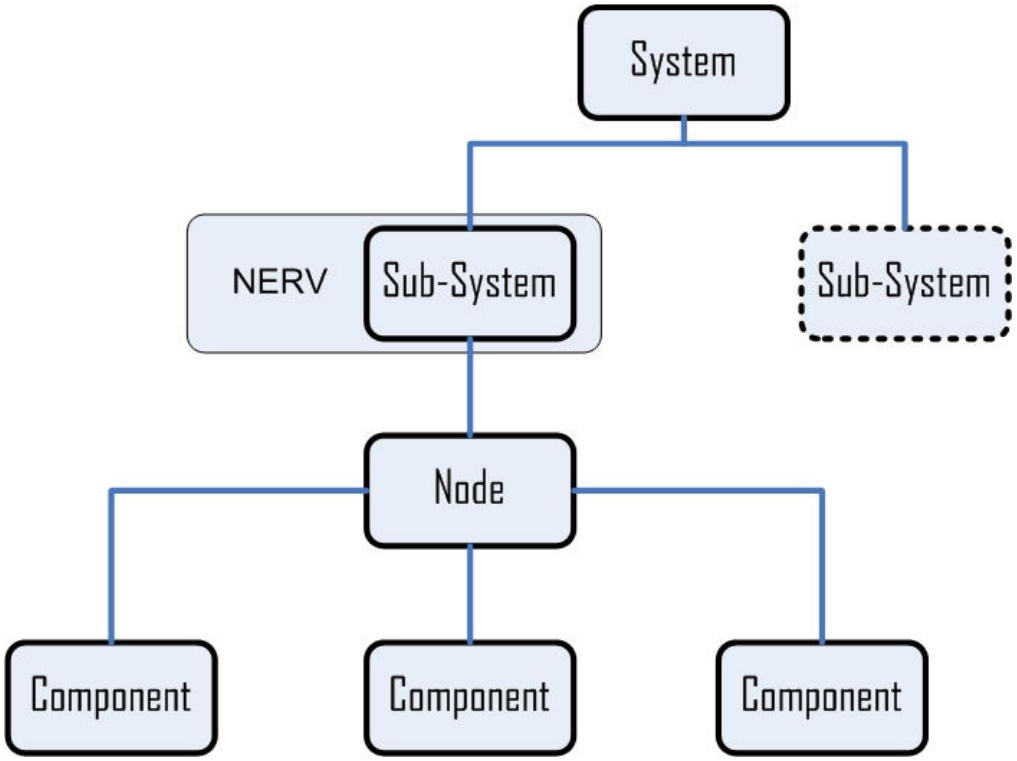

Figure 48: JAUS Topology with the placement of the NERV within the framework

The JAUS topology is described in four hierarchical terms: system, sub-system, node, and component. Barrowing the description of the JAUS topology from the JAUS reference architecture documentation, a System is a logical grouping of one or more subsystems. A system would normally be grouped in such a manner as to gain some cooperative advantage

between the constituent subsystems. An example system might group several operator control units (OCUs) and unmanned vehicles to form a large array of assets.

A subsystem is an independent and distinct unit with regards to physical and functional isolation. The unit may consist of any number of computational hardware devices and software components necessary to support its functional requirements. Specifically, the overall collection of constituent components within the subsystem, are the parts of the unit that shall comply with the JAUS reference architecture. An example of a sub-system would be a UGV that consists of hardware and software that supports the function of autonomous navigation.

A node is composed of all the hardware and software assets necessary to support a well-defined computing capability within the subsystem. Such a defined capability would be a device that handles the motion control of a UGV or the wireless communications device that links devices internal and external to the subsystem.

A component is the lowest level of decomposition in the JAUS hierarchy. A component is a cohesive software unit that provides a well-defined service or set of services. Generally speaking, a component is an executable task or process.

With the five most elementary JAUS terms defined, the JAUS working group provides a simple and direct statement that gets to the heart of how they work together —

- *A sub-system is composed of component software, distributed across one or more nodes.*

The JAUS working group notes that from a systems engineering standpoint, this last statement is significant in that it implies, yet does not specify. Since configurations can be virtually unlimited, node or component interface boundaries are not dictated. This is one of the key aspects of JAUS flexibility.

The JAUS approach to systems integration ensures a technology and computer independent solution. The platform independent approach to systems development allows for incredible latitude for designers while ensuring continuity amongst the UGV community. Although the JAUS specification maturity is an ongoing effort, this open specification is an invaluable resource on which the NERV systems topology can be developed.

3.3.2 Modular Payload System

Following the work of Armstrong [76] and Tabler [77] at the Center for Intelligent Machines and Robotics (CIMAR) and the reference architecture outlined by JAUS working group, the NERV system architecture will comprised of modular elements that are integrated via a common communication protocol independent of particular hardware or specific technologies. The entire NERV sub-system is a singular element in a larger system extending beyond the scope of this design.

Integration of system components occurs through the modular system architecture defined in Figure 49. The NERV architecture is characterized by two distinct layers of control: the Built-in Autonomous Systems Engine (BASE) layer and the intelligence layer. The BASE layer is the fundamental building block of the NERV capability set. This layer contains the Central Mobility Controller (CMC), the Sub-System Communicator (SSC), motors, and the health monitoring system. These elements provide for the ability to operate the vehicle from a remote location via command sets issued from the host network and the ability to control and monitor the NERV mobility platform.

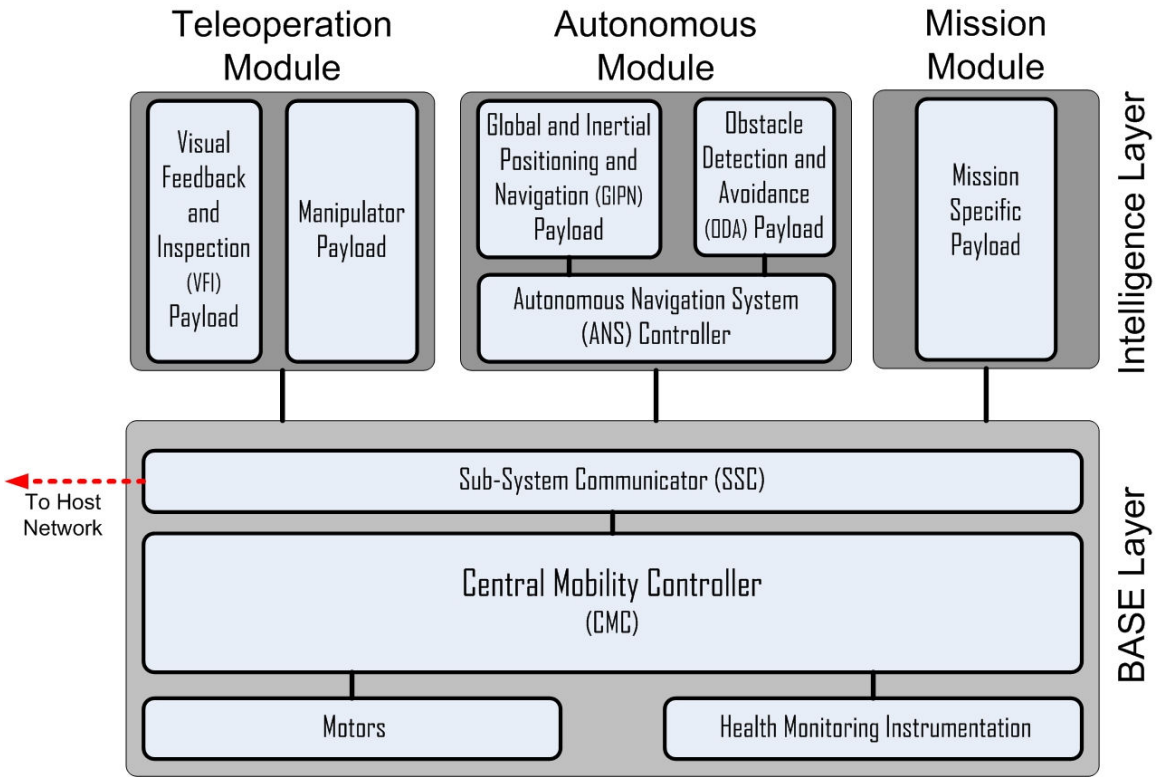

Figure 49: Modular payload system architecture

Above the BASE layer, the intelligence layer provides the expandability and flexibility for a variety of sensor and computing solutions to be integrated into the NERV system. The intelligence layer is comprised of modules which are groups of devices that enable a specific level of vehicle functionality whereby progressive intelligence is obtained by linking such modules to the BASE layer. In this manner, the NERV can scale functionality to meet specific mission objectives while retaining the flexibility to adapt to changing technologies for future missions.

The three primary modules that can be implemented in the intelligence layer are: the teleoperation module, the autonomous module, and the mission module. The teleoperation module enables the NERV to become a teleoperated UGV with the addition of instrumentation such as digital video cameras, microphones, and other devices used for inspection and data collection. This capability is contained within the Visual Feedback and Inspection (VFI) payload. The manipulator payload adds the capability of teleoperated physical interaction with the environment. These devices support the human operator during teleoperation by not only providing situational awareness but also the capabilities to perform semi-autonomous behavior to assist the operator in completing the assigned mission.

The autonomous module fuses sensors and computing elements to allow the NERV to localize, perceive, and act/react autonomously. The Global and Inertial Positioning and Navigation (GIPN) payload provides accurate absolute position data vital to any autonomous operation. The Obstacle Detection and Avoidance (ODA) payload perceives the local surroundings in an effort to provide the data necessary for the NERV to react to irregularities or threats within the vehicle's projected path. In combination, the GIPN and ODA payloads pass data to the Autonomous Navigation System (ANS) payload that fuses the available data to determine the proper course of action to complete mission objectives.

The mission module is an element of the intelligence layer that allows the NERV to be tailored to specific mission requirements. While the teleoperation and autonomous modules provide a means for the vehicle to navigate successfully, the mission module allows the vehicle to perform tasks outside the basic navigation functionality. Examples of mission specific modules would a chemical, biological, or nuclear (CBN) contaminant sensor for use in military or homeland security operations or an array of task specific sensors for analyzing crops and soil for agriculture applications.

Each module within the intelligence layer can provide a level of capability to meet specific mission goals as the teleoperation, autonomous, and mission modules can be inserted

into the NERV architecture independently. Figure 50 details this progressive approach to functionality. Remote control functionality is inherent in the BASE layer capabilities and allows the vehicle to be operated within the line-of-sight of the operator. The teleoperation module allows for operation of the vehicle out of the line-of-sight of the operator. Additional capabilities provided by the teleoperation module allow the operator to be supported by additional data collected by the NERV to better support operation at a distance. Finally, the autonomous module provides the NERV with the capability to operate completely independent of a human operator.

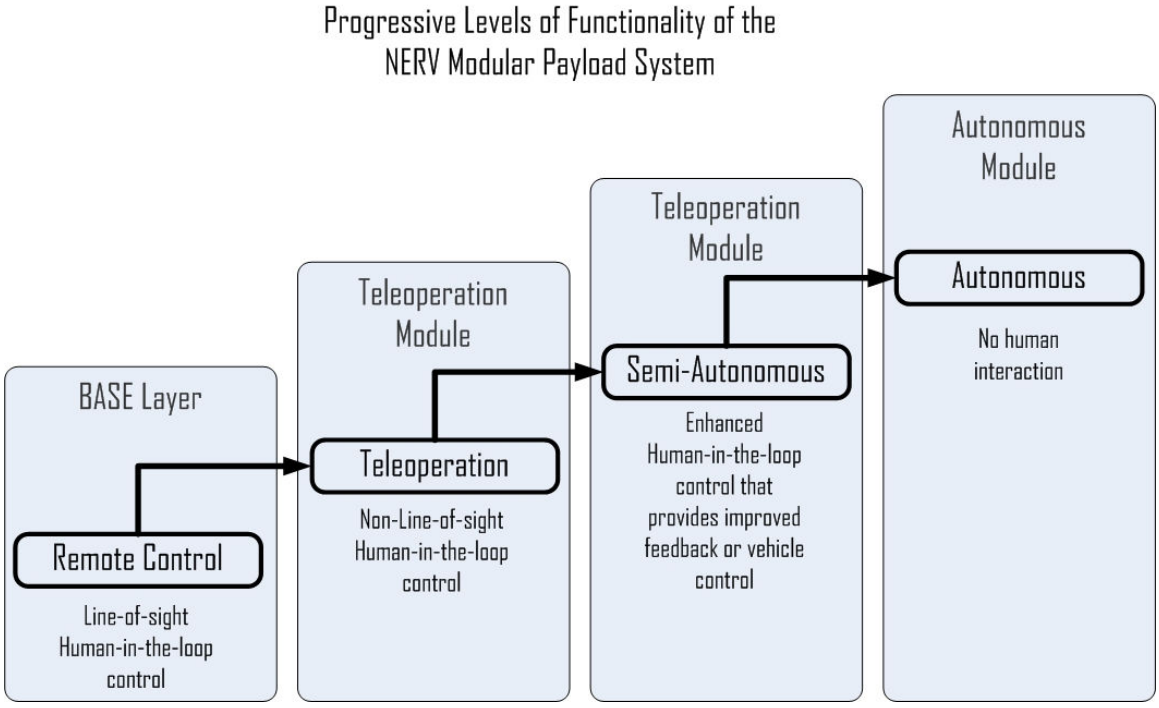

Figure 50: Progressive functionality afforded by the modular design of the NERV

If multiple modules are implemented, the modules will not be restricted to be exclusively independent as data sharing can occur. The SSC within the BASE layer facilitates the cooperation and intermingling of data and processes between the modules present in the intelligence layer. For example, while the vehicle is operating autonomously, there is no need for a human-in-the-loop that is provided by the teleoperation module. However, the instruments (cameras, microphones, etc.) incorporated in the teleoperation module can provide valuable information to the autonomous module in order to support decision making capabilities. Conversely, if the NERV is operating with a human operator via the teleoperation module assets within the autonomous module such as GPS and inertial data would supplement the operators' capabilities and situational awareness.

3.3.3 BASE Layer

The BASE layer consists of two primary components: the Central Mobility Controller (CMC) and the Sub-System Communicator (SSC). In addition, the BASE layer contains the actuators needed to support the mobility capabilities of the NERV as well as instrumentation that enable the determination of systemic health parameters of the platform. Remote control functionality, limited to line-of-sight operation, is contained within the BASE layer. The BASE layer also supports the addition of intelligence layer modules to expand upon this capability.

3.3.3.1 Central Mobility Controller

The CMC is the primitive driver for the NERV mobility platform and resides within the BASE layer of the NERV architecture. The CMC provides intelligent motion control as well as platform health monitoring maintenance. The constituent functionalities inherent in the CMC are detailed in Figure 51.

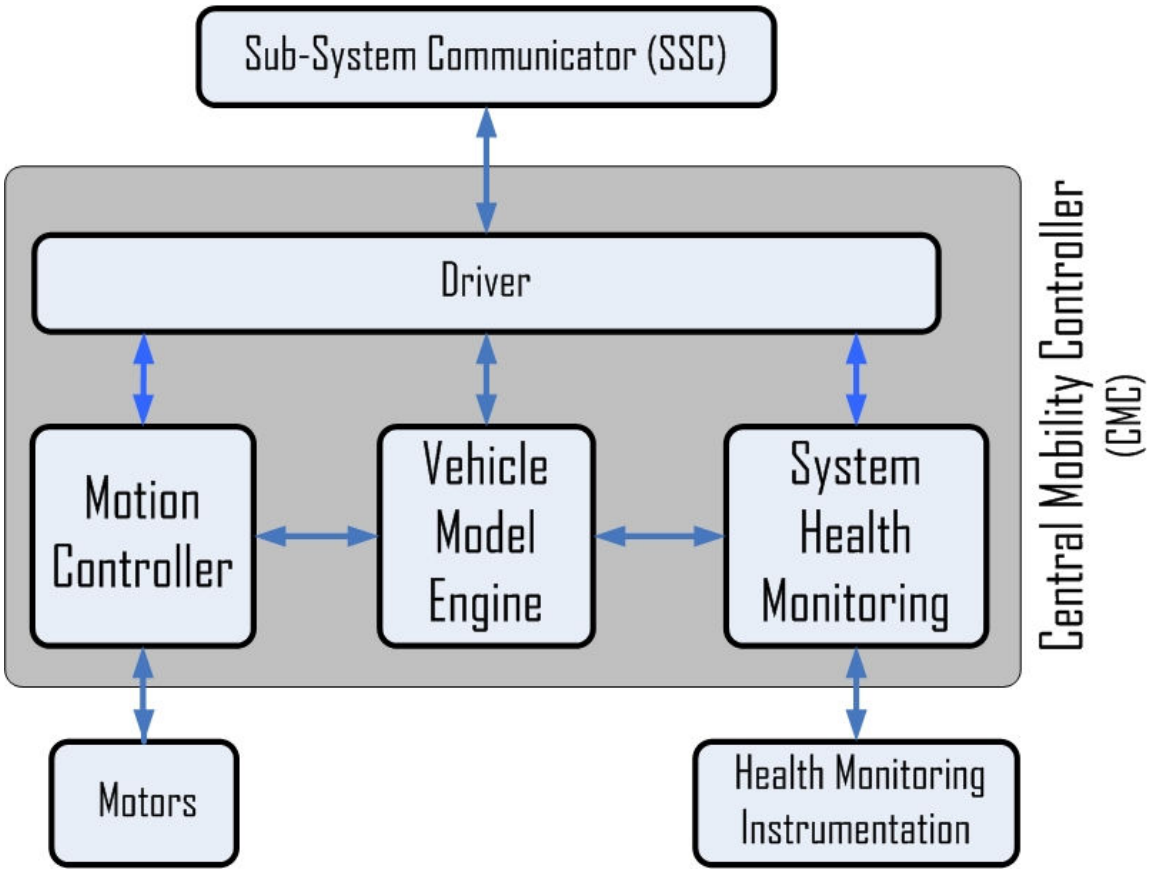

Figure 51: Components of the CMC

The CMC consists of three primary functions with a driver controlling the interaction of the functions. The vehicle model engine utilizes a descriptive analysis model of the NERV platform to determine the proper motion control commands based upon conditional or state input from the upper level controllers such as the modules intelligence layer in the system architecture. Such state based data from the intelligence layer could include manipulator positions or payload vibration levels. These additional inputs will provide a basis on which the control of the NERV can be adapted to improve platform safety and performance. The model includes a kinematic representation of the mobility platform that is fused with the data collected from the system health monitoring functional block to determine the correct motion commands to pass to the motion controller. The motion controller directs the function of the motors and ensures proper servo actuation to achieve the desired results.

3.3.3.2 Sub-System Communicator

The SSC is an integral part of the BASE layer. The function of the SSC is to provide the physical data transport capabilities to pass information between onboard components. The SSC is analogous to a network router where component data can be passed to assigned network entities. The SSC is an essential aspect of the plug-and-play technology independent design built upon the JAUS reference architecture.

3.3.4 Teleoperation Module

The teleoperation operation module provides the ability for the NERV to be operated remotely without an operator within visual range. This capability is primarily provided by the Visual Feedback and Inspection (VFI) payload. In addition, a manipulator payload serves as a means to implement a robotic actuator that can interact with the surrounding environment to perform tangible tasks such as inspecting objects by moving, lifting, and disrupting. While allowances within the NERV system architecture are made for the manipulator payload, in the interest of simplicity the payload will not be discussed in detail within this context. Considerations within the NERV framework will address a generic manipulator device without regard to specific function or technology.

3.3.4.1 Visual Feedback and Inspection Payload

The success of any robotic platform designed for the purpose of inspection [teleoperation] hinges upon the ability of an operator to quickly and reliably assess the video feedback to determine if objects in the view are of any tactical significance [78]. Through experimentation and testing of current small unmanned ground vehicles, such as the

URBOT, it was determined through user feedback there are several points regarding the usefulness of video feedback.

1. Analog video transmitters generally have too much multi-path breakup and signal degradation.

2. digital video systems need to have an update rate of at least ten frames per second.

3. mechanical jitter is a problem while the robot is moving; and

4. a high-resolution inspection camera with the ability to tilt and zoom is a necessity.

These points, while in many ways linked to a specific technology, point to the necessity to develop VFI technologies beyond the current methods. A platform such as the NERV vehicle would be well suited to the task of developing improved solutions that can address the aforementioned issues with video feedback devices.

The function of the VFI payload is to provide visual feedback to a remote location to support teleoperated control of the NERV. This capability allows a human to control the NERV via teleoperation based upon visual feedback. Audio feedback as well as alternate cameras designed to observe additional angles or spectrums outside the visual range would provide supplementary data that would support the task of teleoperation. Figure 52 details the architecture of the VFI payload.

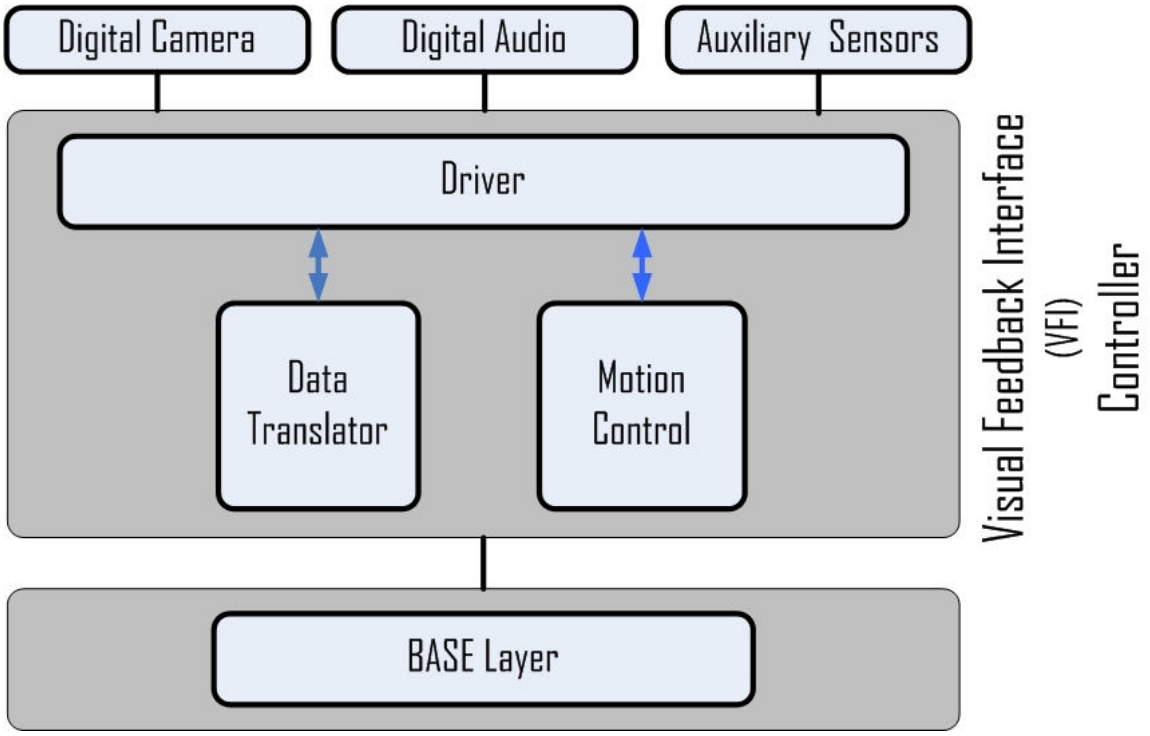

Figure 52: VFI controller architecture

The sensors that comprise the VFI are supported by two primary functions. A data translator maintains the ability to pass visual and auditory data streams to the BASE layer where they can be delivered to the operator or other NERV intelligence layer modules. The motion control function allows the mechanical aspects of the VFI to be controlled. Specifically, the motion control function interfaces the operator to such devices as a pan and tilt unit for cameras and any manipulator payload included within the teleoperation module. This information is passed into the BASE layer where the VFI controller output is passed to the operator and while payload variables (such as vibration and manipulator position) can interface with the CMC so that control of the NERV is adapted to consider the state of the associated VFI payload.

3.3.4.2 Manipulator Payload

Often it is desirable for the unmanned vehicle to interact with the surrounding environment to achieve such tasks as scientific exploration, threat assessment and neutralization, and pathway maintenance. Within the customer survey conducted for this research, the respondents identified a manipulator payload as a must have item on a research UGV. This is a logical conclusion since it is often desired for a UGV to perform tasks as an extension of human capability including manipulating surround objects.

The manipulator payload in the architecture of the NERV platform will be a generic allowance for the possibility of implementing a mechanical device on the vehicle in the sense that power and communication system allowances will facilitate the integration of such a device. Keeping the design of the NERV technology independent, the allowance for the manipulator payload will provide a secure mounting position, ample power provision, and clearances to allow a variety of manipulator payloads to be implemented.

3.3.5 Autonomous Module

The autonomous module brings together the elements required for autonomous navigation. In order to develop this autonomous capability, the Autonomous Navigation System (ANS) controller fuses data from the Global and Inertial Positioning and Navigation (GIPN) and Obstacle Detection and Avoidance (ODA) payloads.

3.3.5.1 Autonomous Navigation System Controller

The NERV will be capable of autonomous operation with the inclusion of the Autonomous Navigation System (ANS) controller. This family of payloads will be integrated onto a base NERV platform to provide the capability of autonomous navigation. The task of autonomous navigation can be described by five key sub-tasks [79]:

1. Vehicle actuator control
2. Vehicle positioning
3. Perception of the environment
4. Path Planning
5. Path Execution and Obstacle Avoidance

The CMC included on the base NERV platform will serve to implement the vehicle actuator control and vehicle positioning. The remaining higher level tasks will be addressed by the ANS controller. The ANS controller will be an add-on payload to the NERV platform that will interface with the onboard CMC and communications bus. Additional sensor payloads will interface with the ANS to provide perceptive capabilities supporting autonomous navigation.

As shown in Figure 53, the ANS controller fuses sensor data from the GIPN and ODA payload modules and passes vehicle control commands to the BASE layer. The ANS controller incorporates the navigation algorithms and computing hardware to achieve

intelligent autonomous navigation. This distributed computing approach to the ANS controller divorces the autonomous technology from the NERV mobility controller. This allows the computing intensive autonomous capabilities to be selectively incorporated on the NERV platform thus eliminating the cost and complexity associated with an integrated CMC and ANS controller solution. Moreover, the independent ANS computing platform provides the ability to quickly swap, alter, or upgrade hardware and software contained in the ANS controller without rendering the base NERV platform and the CMC inoperable. This also supports interoperability and ease of integration of a variety of GIPN and ODA payloads. Compliance with the JAUS reference architecture ensures that seamless integration of the ANS within the NERV system architecture and provides the flexibility to expand as technology progresses.

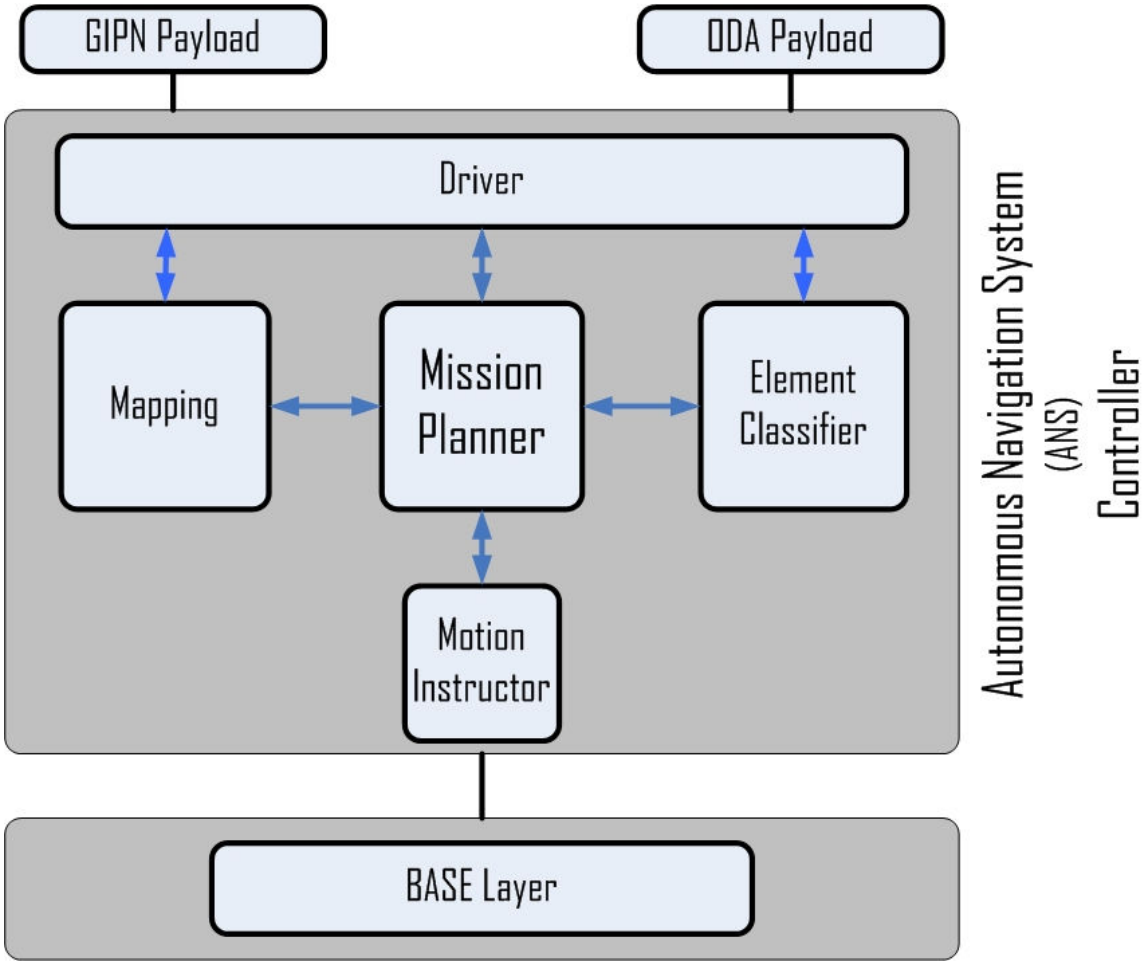

Figure 53: ANS controller architecture

The ANS controller is based upon a mission planner module that contains the software components required to develop, adapt, and execute fully autonomous mission oriented behavior. The mission planner fuses data from mapping, element classifier, and BASE layer to provide intelligent navigation capability. The mapping process component develops a map of the vehicle's surroundings that supports the mission planner by enabling vehicle localization and path planning functionality. The element classifier collects data from the ODA payload to extract and assess elements of the surroundings that pose a threat to navigation or to other mission critical objectives. The motion instructor extends the mission planning results and translates them to the BASE layer where they instruct the CMC and result in physical response of the NERV platform.

3.3.5.2 Global and Inertial Positioning and Navigation Payload

Essential to the ANS controller is accurate global position data. The Global and Inertial Positioning and Navigation payload data stream provides the basis for all the navigation tasks of the vehicle during autonomous operation. In addition, the inertial data can provide valuable input to the CMC to support the adaptive drive capabilities of the vehicle platform.

The GIPN payload can also be implemented independent of the ANS to support operations that do not require autonomous capability. If the NERV is to be applied as a teleoperated platform, the global and inertial position data can provide valuable feedback to the operator to assist in improved situational awareness.

In practice, the GIPN payload would consist of a differential global position system receiver unit coupled to an inertial measurement device. There are currently available commercial-of-the-shelf solutions for this payload that can easily be integrated into the ANS controller schema. It is also of interest to some to develop improved GIPN type payload devices. Research areas include hardware development as well as sensor fusion and filtering techniques to improve performance and accuracy. The NERV would be an ideal platform to develop and improve GIPN payload technology.

3.3.5.3 Obstacle Detection and Avoidance Payload

Real-world autonomous and teleoperated applications of a UGV require the ability to perceive the surrounding environment to accomplish navigation objectives. To accomplish this, the NERV will provide the ability to integrate an Obstacle Detection and Avoidance (ODA) payload into the system architecture to support such capabilities.

Obstacle detection currently in use includes scanning laser range finders, ultrasonic transducers, and computer vision based systems. Such systems would comprise the capabilities of an ODA payload to provide the ANS controller the ability to perceive potential obstacles or threats and to allow the vehicle to augment autonomous navigation decisions to avoid mission failure. The ODA payload would also be capable of supporting teleoperated mission profiles to increase operator situational awareness.

4 NERV Conceptual Design

The system architecture design concepts and kinematic theory supporting the design of a NERV platform is readily transferable to a variety of platforms and largely technology independent. In application, the elements of the NERV design can be applied independently or mutually to yield a variety of robotic platforms; both in form and in function.

Illustrating a conceptual design of a singular form of the fundamental NERV platform provides the ability to highlight salient features that support the ability of the vehicle to facilitate unmanned systems research. Although the design presented provides allowances for the scalable NERV payload architecture, the focus remains on the basic platform design with the CMC functionality while other payloads are not specifically included. Development of a creative sketch of the NERV concept platform was completed using Solidworks three dimensional computer aided design software.

4.1 3-D CAD Model

The conceptual sketch of the two-body articulated NERV platform is presented in Figure 54 through 56. As presented, the vehicle utilizes aluminum and carbon fiber construction to maintain a rugged mechanical construction while minimizing overall weight. A noticeable feature is the carbon fiber connecting arm that links the front and rear sections. This feature is a thin walled component that provides a means to transport cables from the front section to the rear section. Additional carbon fiber body panels bolster a light weight and minimal aluminum under body that provides a rigid frame. Large flat surfaces provide area to mount payloads and other devices to the platform to customize the vehicle to a specific mission profile.

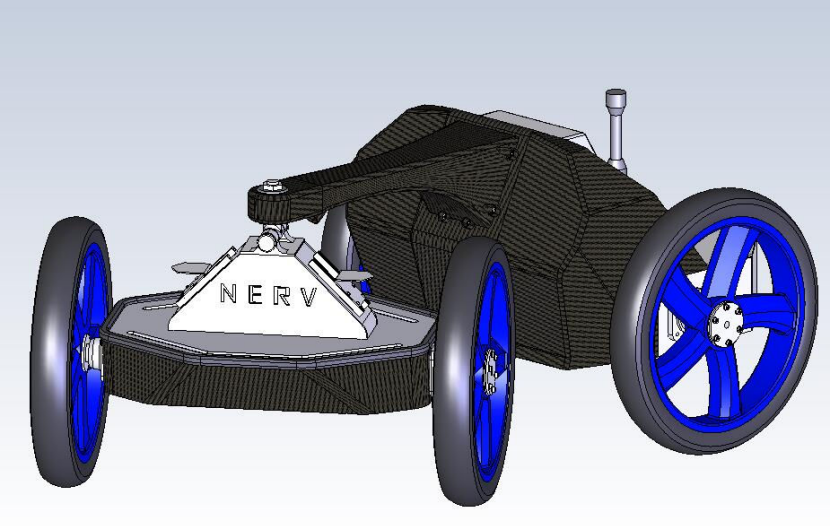

Figure 54: NERV conceptual three dimensional model

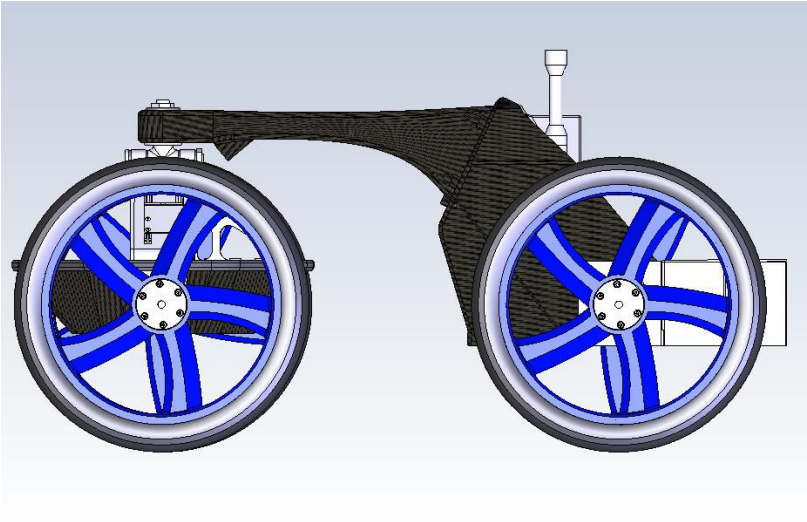

Figure 55: Right side of the NERV vehicle

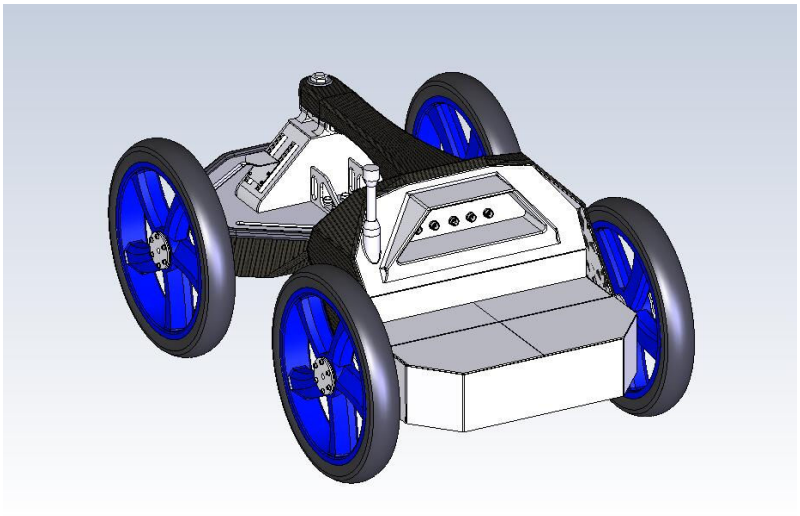

Figure 56: Back left view of the vehicle

The NERV concept platform is approximately 24 inches wide, 36 inches long, 20 inches high. Figure 57 details the overall size of the platform. The design was conceived with several elements such as the motors, batteries, and computing form factors considered based upon particular manufacturer specifications. However, the intent of the presented design is not to limit the concept to a particular set of technologies rather, it is the with the intention to provide the ability to visualize a single concept and note that it can be altered and scaled to fit particular devices.

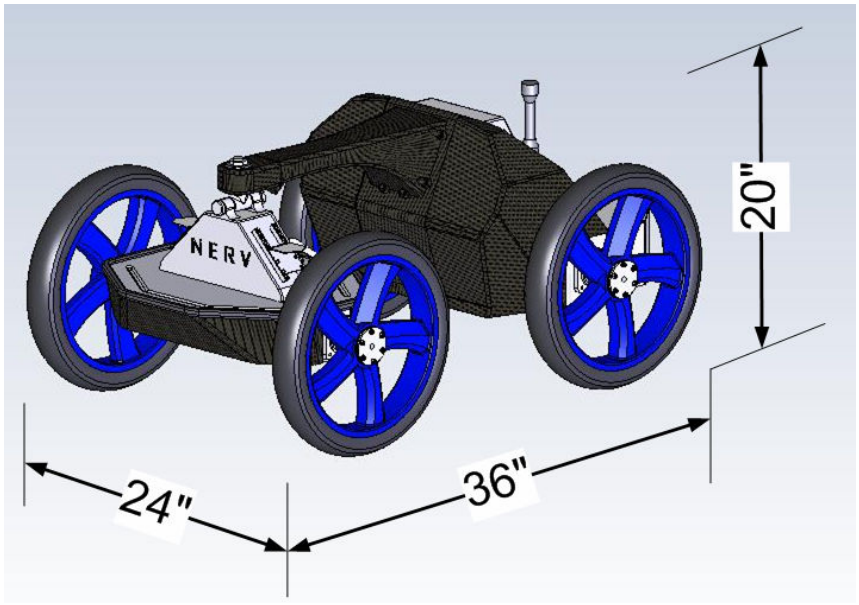

Figure 57: Dimensions of the NERV platform

Including a brushless DC motor power train, lead acid battery power supply, and mechanical components selected to be included in the conceptual design, the estimated baseline vehicle weight is approximately 98 pounds. The value for this estimate was obtained through the mass properties functionality in the Solidworks CAD package. Based upon the author's experiences developing designs within the Solidworks environment, this method of obtaining estimates of component weight has proven accurate within one to ten percent with errors depending on the complexity and material variability in the component parts. This weight will vary based upon the amount of auxiliary power supply as well as the number and type of attached payload devices.

Figure 58 details the relative size of the NERV platform concept compared to a six foot tall person.

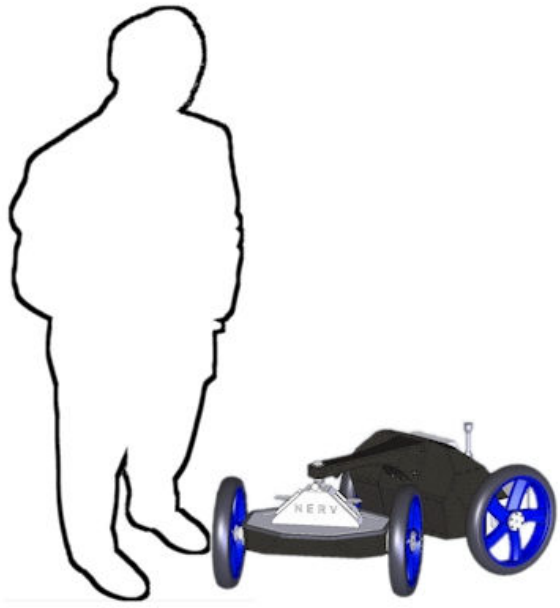

Figure 58: Relative scale of the NERV platform concept

Access to the onboard removable and swappable battery cells is provided by removing the side cover panels on the rear of the vehicle as shown in Figure 59. The battery storage compartment is designed to allow rapid access to the cells to swap the batteries during operation with a fresh set to extend the operational runtime. Also included in the battery storage compartment is a micro-processor controlled multi-stage battery charger that provides the ability to link the NERV vehicle to AC current and charge the batteries without removing the cells from the vehicle.

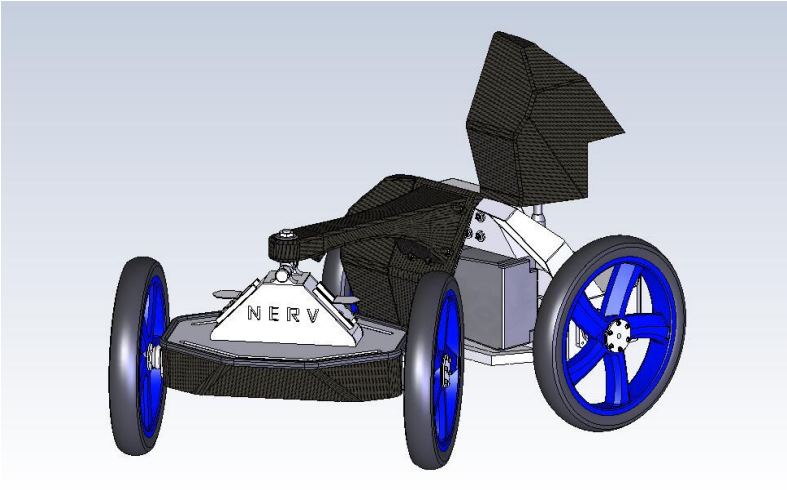

Figure 59: Access to primary battery supply

The four driven wheels are based upon the common drive train design detailed in Figure 60. The simple direct drive system is based upon two NEMA 23 frame brushless motors with drive controller hardware couple to a single stage planetary gearhead. A custom machined shaft couples the wheel to the output shaft of the gearhead and is supported by a flange mount eccentric locking bearing assembly. The scale of the conceptual design is primarily based upon the limiting factors of the component selection and layout of the drive train assembly. The result is a design that can be scaled to larger or smaller form factors by altering the specific motors and gearheads selected for the design.

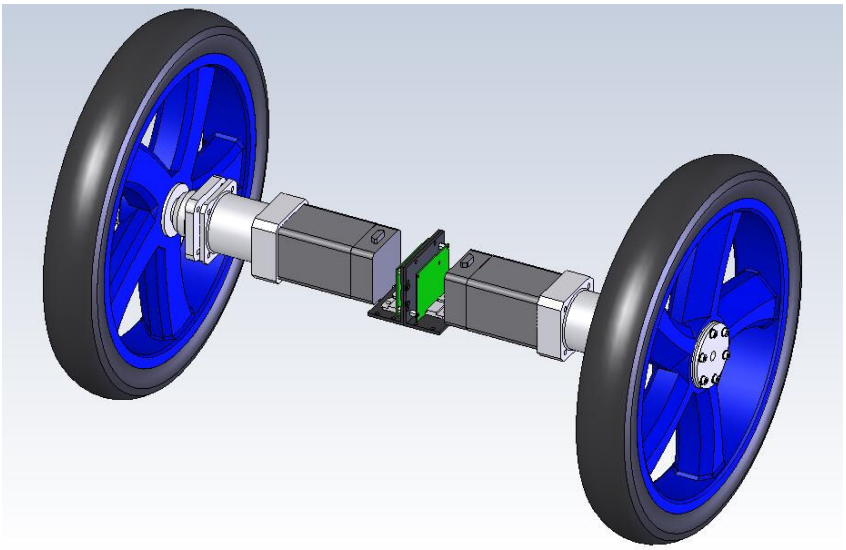

Figure 60: NERV drivetrain assembly

Connecting the front and rear sections of the vehicle is a two degree-of-freedom joint assembly which provides the ability for the front to turn and roll relative to rear. As with the Gemini type vehicle, this feature provides the ability to maintain ground contact with four wheels over variable terrain and allows for the front section to maneuver with zero-radius turning capability. Figure 61 details the joint connection.

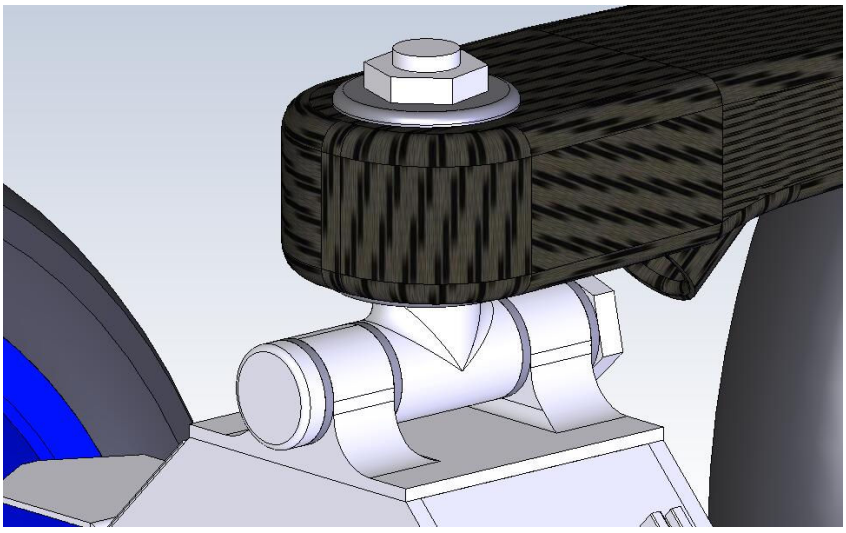

Figure 61: Two degree-of-freedom joint assembly

The construction of the connecting joint is detailed in Figure 62. Fabricated of custom machined high-strength aluminum alloy, the joint components mate together to provide the turning and rolling capabilities of the two-body vehicle. The joint pins are supported by ultra-high molecular weight (UHMW) polyethylene bushings and washers that provide a durable yet low friction surface on which the surfaces can rotate. The pins are firmly fastened with two large hexagonal nuts that thread onto each shaft and compress a spring washer to maintain joint sufficient compressive preload to maintain intimate contact of the joint assembly to avoid variability in the geometry.

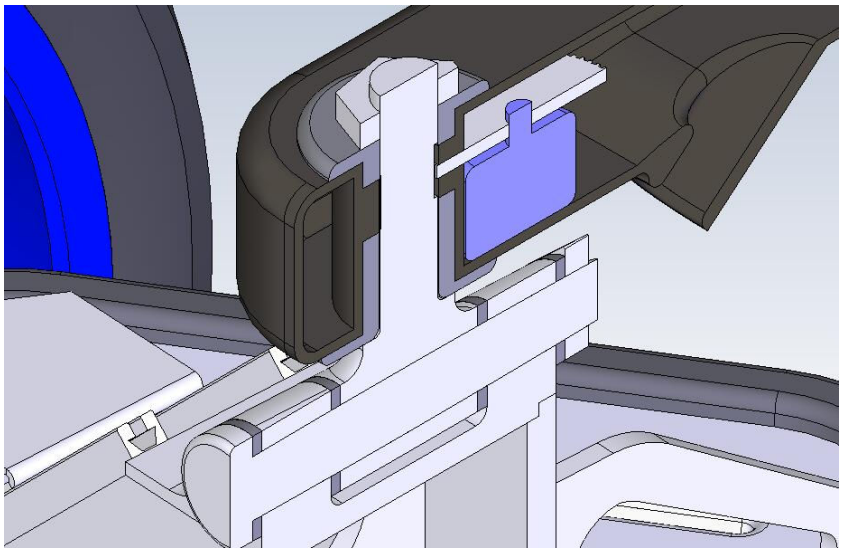

Figure 62: Section view of the two degree-of-freedom joint

The vertical turning axis of the joint assembly passes through a molded through hole in the carbon fiber connecting arm and is maintained by two UHMW bearing bushings that include bearing flanges. These bearing bushings and flanges support the compressive and rotational interface between the aluminum shaft and the carbon fiber connecting arm. Also included in the section view presented in Figure 62 is a cross-section view of the cable pass-through that is integrated into the carbon fiber connecting arm.

Not shown in Figures 61 and 62, is the connecting cable that interfaces the cable feed exiting from the connecting arm to the front section control and power systems. A similar external cable interface between the front and rear section of the vehicle was employed in the design of the Gemini platform with great success. However, providing the ability to complete a full revolution with a multi-conductor slip ring of the front section would allow the motion control software to operate without regard for twisting or mangling the connections. The drawback to the implementation of a slip ring is that it adds mechanical complexity, weight, size, and cost to the design. In an effort to reduce the impact of these drawbacks, the NERV concept does not include a slip ring in the design of the joint. This design selection is supported by the fact that the kinematic design of the two-body articulated vehicle provides for symmetrical drive capabilities with increased vehicle position awareness resulting from the absolute body angle measurement. Therefore, limiting the rotation of the front section would have limited impact on maneuverability in most situations.

A key element to the joint design that is a step forward from the Gemini-type joint design is the inclusion of an absolute angular encoding device to monitor the relative body angle between the front and rear sections. This measurement is essential to the application of the four-wheel drive vehicle concept previously mentioned. Figure 62 provides a section view to the internal encoder assembly housed in the connecting arm. In this concept of the application, the vertical turning axis of the joint assembly includes a section of the shaft that has gear teeth machined into the surface of the shaft. The encoder includes a gear that mates to the vertical turning shaft through a slot in the carbon fiber wall of the connecting arm. The interface to resolve the joint angle can vary significantly from this mechanical configuration. Other mechanical techniques such as direct connection of the encoder to the vertical turning shaft or a friction wheel interface between the shaft and encoder are also other possible solutions. Perhaps the most promising technique may be the use of magneto resistive sensors to monitor the varying joint angle without the need for mechanical interface. Further research is needed to investigate the feasibility of integrating such technology into the NERV design.

The fundamental system architecture of the vehicle is presented in Figure 63 and is based upon the system integration schema developed in Section 3. The design is comprised of two layers of functionality: (1) logic layer and (2) power layer. The logic layer provides the BASE layer functionality of the NERV design while the power layer provides the supporting control and power functions required to maintain the system. The design also spans the front and rear sections of the vehicle. Minimization of the number of connections required to link the sections together is to the benefit of system integrity and to integration concerns of running cables through the connection arm.

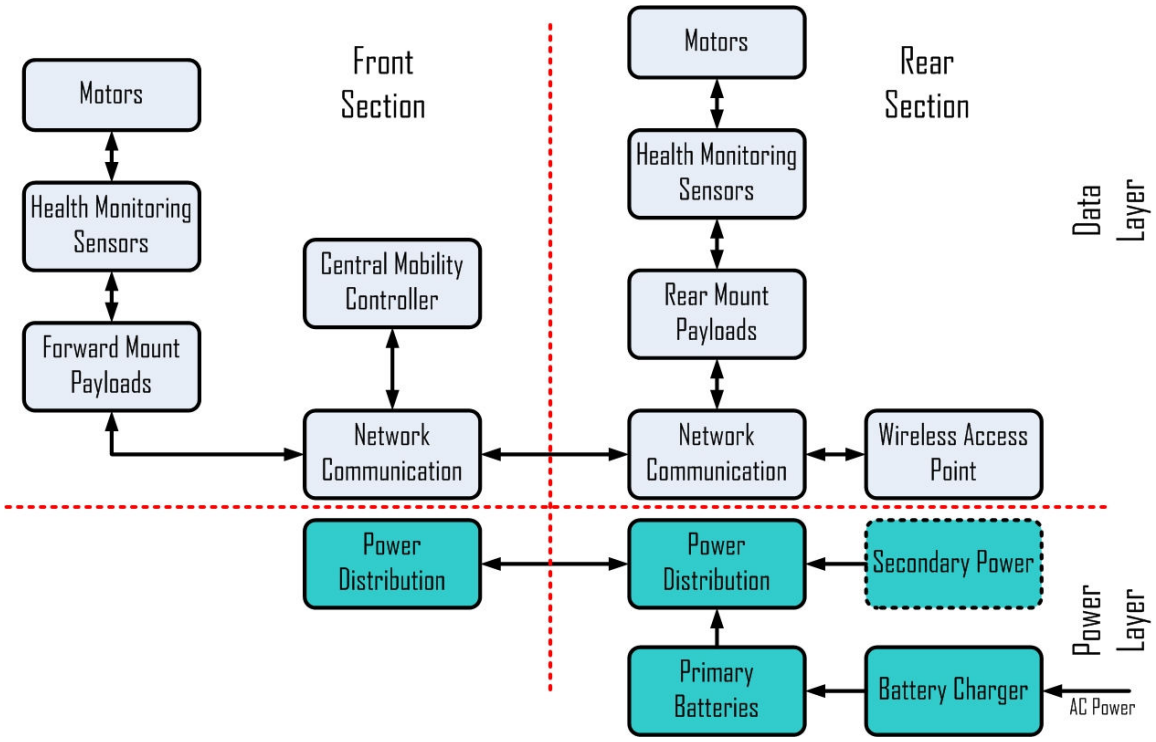

Figure 63: System architecture of NERV concept

The central mobility controller of the vehicle is located in the front section of the vehicle and is accessible by removing the protective carbon fiber body panel as shown in Figure 64. The CMC is shown as being comprised of standard PC104 computing modules that can be stacked to provide expanded functionality and capability.

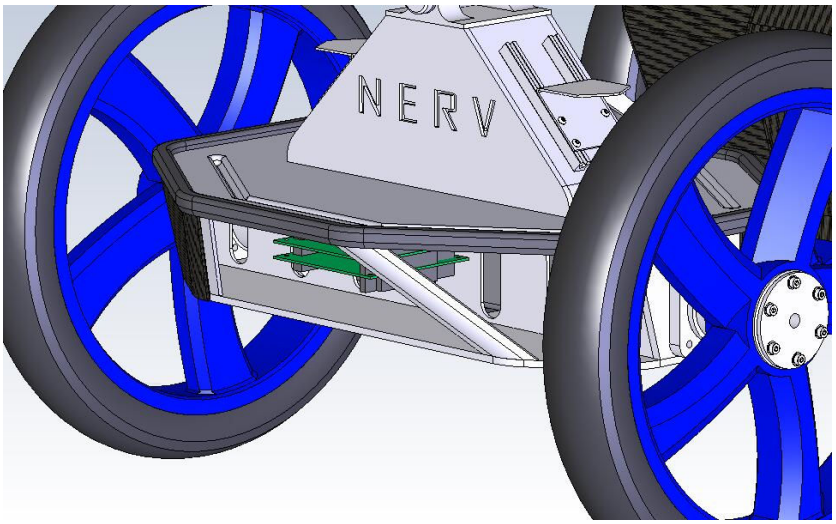

Figure 64: Central mobility controller

Likewise, as shown in Figure 65, the primary power distribution and communications hub is located in the rear of the front section and is accessible through removing the protective carbon fiber panel. In an effort to minimize size and weight while maintaining scalable and flexible functionality, these components are shown as being developed upon a standard PC104 profile PCB.

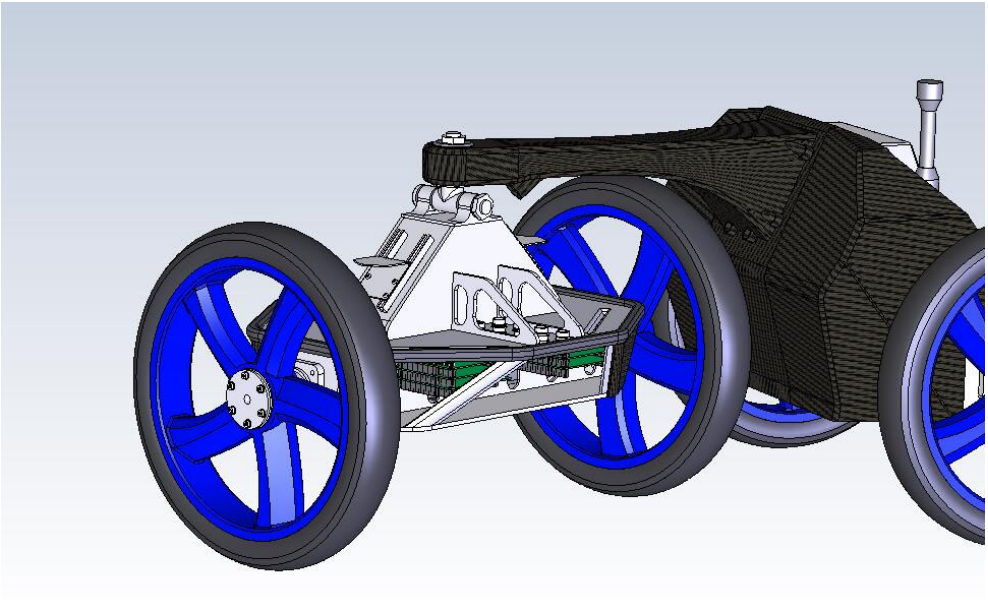

Figure 65: Power and communication hubs

The flexible system architecture is supported by the plug-and-play approach to component integration. This is made possible in large part by software design and standard communication protocols. However, common connectors that provide power and communications are essential to realize this swap and go type system. While the vehicle provides integrated solutions for power distribution, drive control, and network communication; the majority of the overall vehicle functionality is derived from the add-on components placed upon the vehicle by the user. These components can be mounted on many of the surfaces of the vehicle and interface to the onboard power and communication busses via external connectors on the front and rear section. Figure 66 highlights the power and communication connectors for the front section of the vehicle while Figure 67 details the rear connectors. The connector placement and surrounding frame components are designed to provide free access to the connectors while protecting them from accidental damage during operations where the surrounding environment may catch or snag a connector. Also shown in Figure 64 is a 802.11 wireless Ethernet omni-directional antenna that provides a high

bandwidth connection that links the onboard components to an external network for command and control purposes.

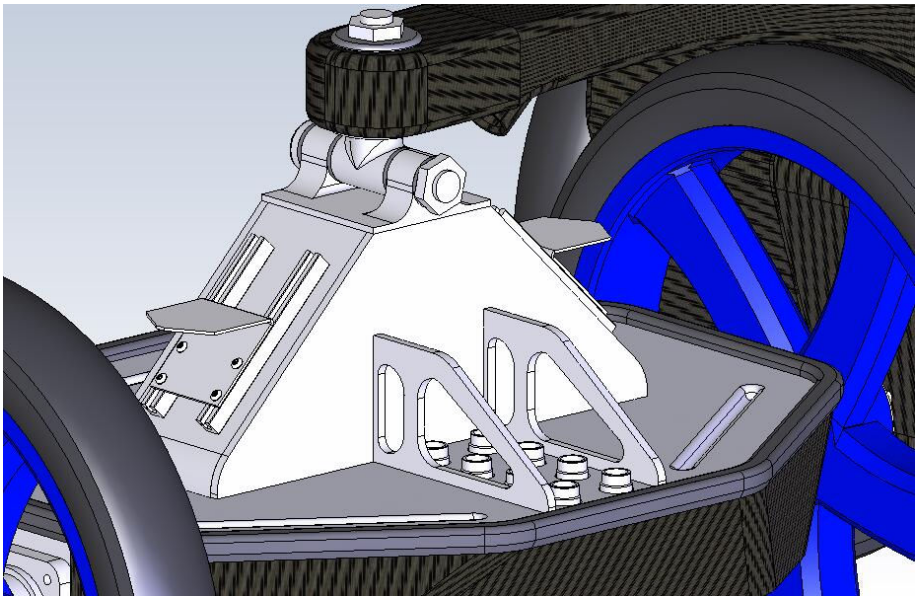

Figure 66: Power and data connections on the front section

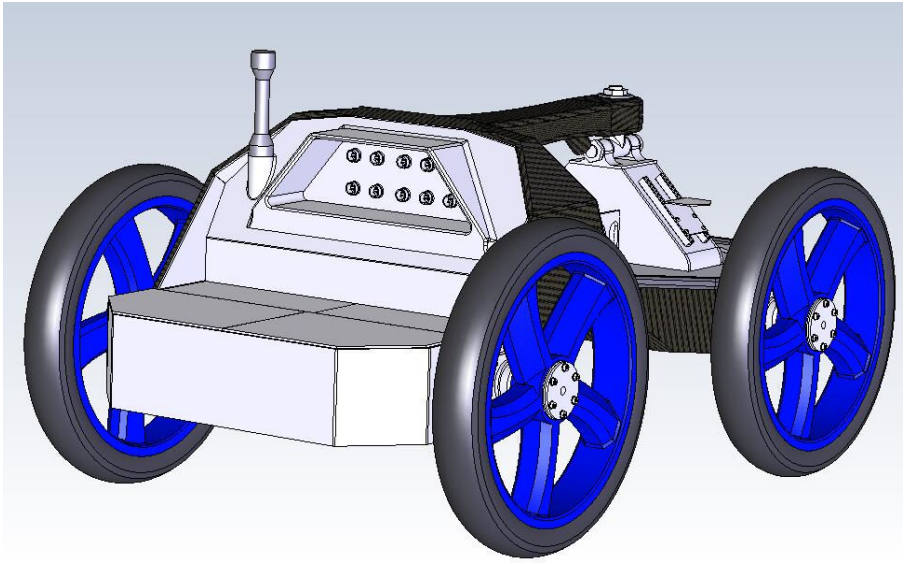

Figure 67: Power and data connections on the rear of the vehicle

The rear of the vehicle includes an auxiliary compartment that can be used for storage of additional battery cells or the inclusion of a small generator that can provide a hybrid power plant if needed. This modular battery power package is removable from the rear of the vehicle and provides the ability to swap auxiliary battery packs in the event that

extended runtimes are required. When in place it provides a flat surface on which payloads or components can be mounted.

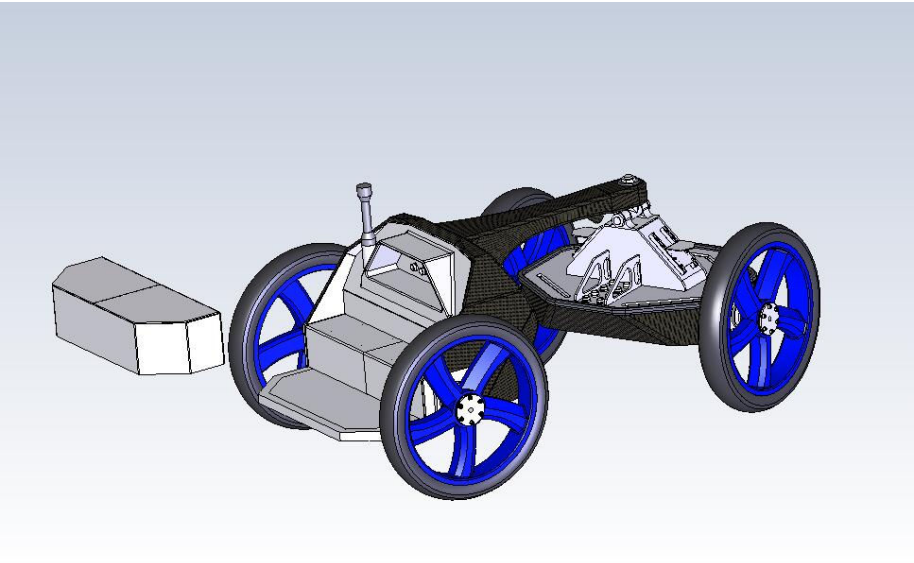

Figure 68: Auxiliary power supply

5 Proof of Concept

The Gemini vehicle platform initially established the novel two-body articulated robotic mobility design. The platform validated the practical application of such a mobile robotic vehicle for the purposes for outdoor research in autonomous and unmanned vehicle systems through successful competition at the IGVC in 2004 and 2005 as summarized in Appendix B.

A second generation of two-bodied robotic platforms was demonstrated with the development of the intelligent ground vehicle Polaris. Polaris, shown in Figure 69, was designed for the 2005 IGVC and enjoyed success in all aspects of the competition. Polaris employs the same kinematic design of Gemini while providing a hybrid power supply, an increased top speed, an improved payload capacity.

Figure 69: Polaris at the 2005 IGVC

Extending the design of the Gemini type platform into the NERV concept is aimed to serve the unmanned vehicle research community at large by providing a capable mobility platform. Proof of concept for fundamental the NERV mobility platform has been practically demonstrated with the success of two instances of the unique mobility platforms developed and tested in a real-world environment supporting autonomous research.

5.1 Kinematic Model Verification

To validate the theoretical kinematic model developed for the four-wheel drive NERV platform, experimental verification was carried out on the similar Polaris vehicle. Placing instrumentation on the Polaris platform provides the ability to provide real-world input to the theoretical model and compare the measured rear wheel speeds to the predicted theoretical rear wheel speeds. Section 3 proposed the theoretical model of the NERV kinematic platform where a two-body four-wheel drive vehicle can be controlled by simple differential drive commands of the front section while the rear drive wheels are driven to be compliant with the motion of the front section of the vehicle. If the theoretical model proves to be an accurate predictor of the rear body motion during operation of the Gemini-type platform, then the possibility of providing the control capabilities essential to four-wheel drive operation would be feasible. This additional feature is a leap forward in capability compared to the Gemini design concept as it provides increased mobility and payload capacity to support a wider range of research mission profiles.

5.1.1 Experimentation Plan of Action

The plan of action for validating the kinematic design of the NERV platform is based upon instrumentation of the Polaris mobility platform. The use of Polaris as the experimental test-bed was driven by the advantage of the ability to directly link encoding devices to rotating rear wheel axles.

The goal of the validation experiment is to determine the efficacy of the kinematic model for the two-body vehicle platform by comparing the measured to the predicted rear wheel speeds. To accomplish this task, three fundamental vehicle characteristics must be measured: (1) the front wheel rotational velocities, (2) the joint angle between the front and rear sections of the vehicle, and (3) resulting rear wheel velocities. These measurements lead to the experimental process outlined in Figure 70. The front wheel speeds will be controlled by the experimenter via a radio frequency link and joystick control. The resulting front wheel speeds will be measured along with the relative angle between the front and rear sections. With this input data, the model can be used to develop an estimated response for the rear wheel speeds. The measured rear wheel speeds will then be compared to the predicted speeds to investigate the differences between the two and provide some qualification of the kinematic model for the two-body articulated vehicle. The difference between the theoretical and experimental rear wheel velocity data sets should provide and indication of the effectiveness of the kinematic model and feasibility of the four-wheel drive NERV vehicle platform.

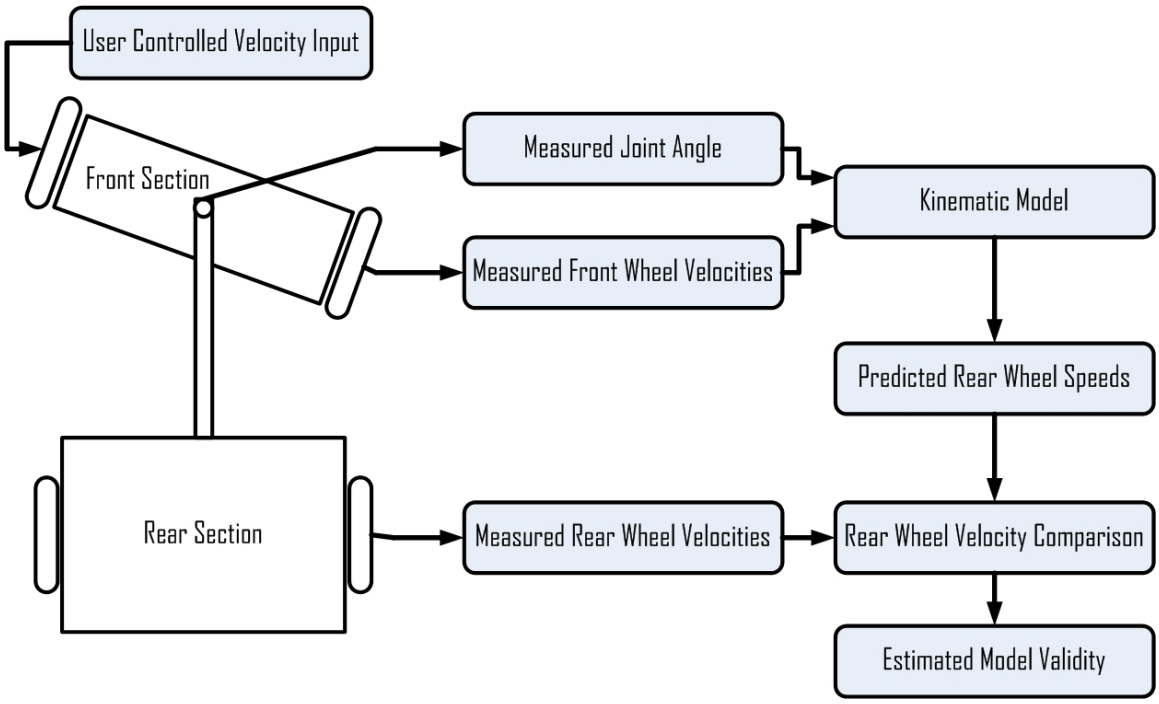

Figure 70: Experimental diagram for kinematic model validation

5.1.2 Instrumentation Selection

In order to collect reliable and accurate data for the measured parameters, the selection of the proper instrumentation hardware is essential. The data acquisition is based upon dual NI-DAQcard 6024-E PCMCIA bus data acquisition systems that links directly to a laptop computer. In total, the combined DAQ system provides 32 single ended 12-bit analog inputs, 16 digital input/output ports, and four 24-bit counters.

Appendix D details the rationale for the specification of the absolute angular encoder used to measure the relative body angle between the front and rear sections. Based upon the analysis of the effects of quantized angle inputs into the ideal kinematic model, it was determined that a 15-bit absolute angular encoder would provide an acceptable level of expected error and improved linear results for all body poses of the vehicle. The selected absolute encoder is a Sick-Stegman ARS20-6FK32768 15-bit Gray code rotary optical encoder with parallel outputs providing 0.011° of angular resolution. The parallel digital TTL outputs provide the ability to collect the angular position at a high rate of speed, as each bit of position information has a dedicated channel providing synchronous data to the DAQ system. Gray code output removes positional ambiguity when the angular motion is at a steady state that is characteristic of binary output devices. The outputs of the absolute

angular encoder interface directly to the 16 digital input/output ports on distributed between the two 6024-E DAQ cards.

For the measurement of the rear wheel velocities, Automation Direct TRD-SH2500-BD, 2500 pulse per revolution, incremental open-collector quadrature encoders were attached to the rear wheel axels of Polaris. The 2500 pulse encoders provide an angular resolution of 0.144° and provide rotational direction as well as an index position pulse. The output of the rear wheel incremental encoders interfaces with DAQ via three analog inputs per encoder for the A channel, B channel, and index channel outputs.

Measurement of the front wheel speeds is derived from 4000 pulse per revolution incremental encoders that are integrated into each of the two Quicksilver I-grade 34 frame motors that drive Polaris. Coupled to the drive wheels through 5:1 planetary gearheads, the encoders yield an effective 20000 counts per revolution resulting in a 0.018° angular resolution. The direct raw output of the encoders is provided via a high speed digital input/output port of the motor motion controller. The raw encoder output from the digital port provides A/B/Z channel quadrature output directly to the DAQ system.

5.1.3 Instrumentation Integration

The schematic layout of the instrumentation devices as installed on the Polaris platform is shown in Figure 71.

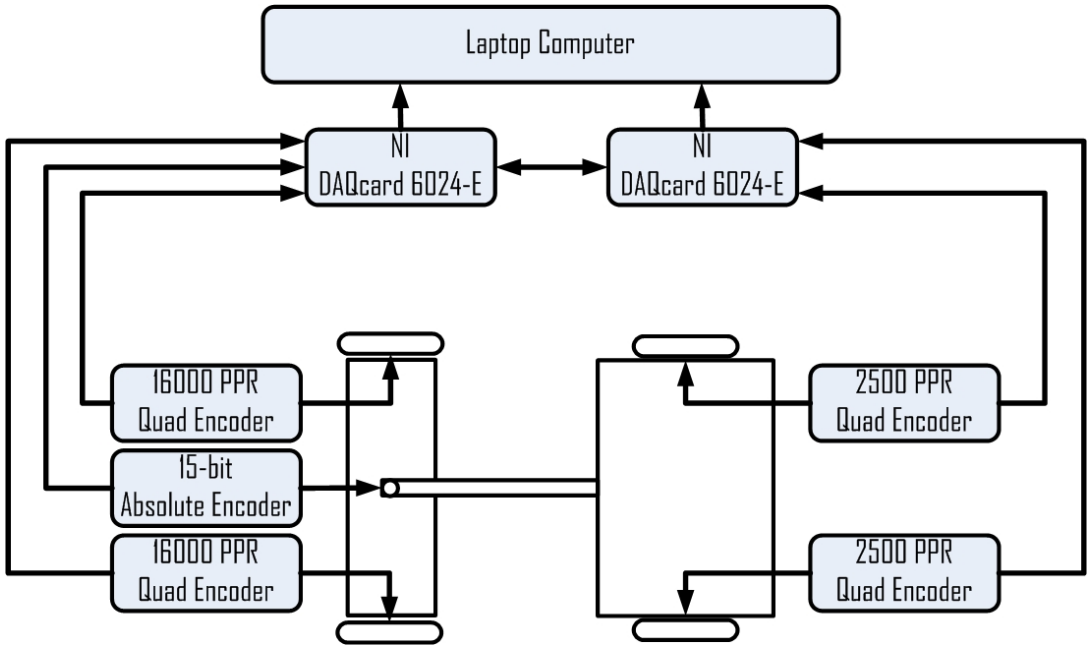

Figure 71: Schematic of the instrumentation implemented on Polaris

Figure 72 details the mechanical integration of the absolute encoder on the articulated joint. The encoder was mounted to an aluminum bracket affixed to the connecting beam between the front and rear sections allowing for the body of the encoder to remain fixed relative to the rear section. A circular aluminum plate mated the encoder shaft to the vertical joint element that remains fixed relative to the front section of the vehicle. A hole was bored into the circular aluminum plate for the shaft of the encoder and secured by means of a set screw as detailed in Figure 73. Further, the circular aluminum plate was affixed to the hexagonal bolt head that comprises the terminal end of the vertical joint shaft member by means of two square flanges and a pair of set screws. The result of this arrangement is the ability to track the relative angle between the front and rear section of the vehicle as the encoder shaft remains fixed relative to the front section and the encoder body remains fixed relative to the rear section.

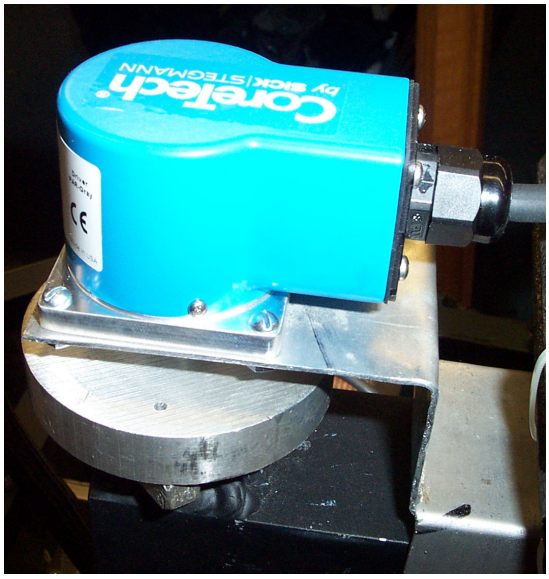

Figure 72: Integration of the absolute encoder on the joint

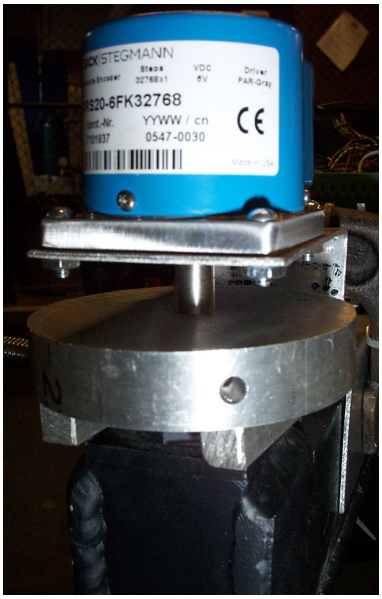

Figure 73: Side view of absolute encoder mount

Figure 74 highlights the method in which the incremental encoders were interfaced to both of the rear wheel axles. This simple installation solution was possible due to the fact that Polaris utilizes rotating shafts connected to the rear wheels that pass-through and are supported by coaxial flange mount locking hub roller bearing assemblies. The end of the rear wheel shaft was bored out to accept a steel coupling shaft that interfaced directly with the hollow shaft incremental encoder. Each end of the coupling shaft was secured by means of a set screw to maintain proper contact during operation. L-brackets supported the encoder and maintained the encoder body in a fixed position.

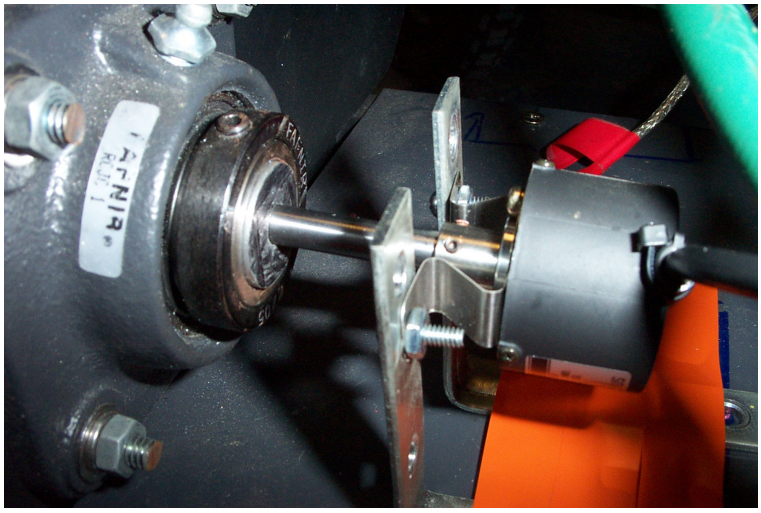

Figure 74: Detail of incremental encoder mounting solution

The data acquisition breakout boards were mounted on the connecting beam between the front and rear sections with a temporary DIN rail mounting bracket. The connections were routed to the two PCMCIA DAQ boards on the laptop computer via two shielded 68 pin cables. Figure 75 details the breakout board for the dual DAQ devices.

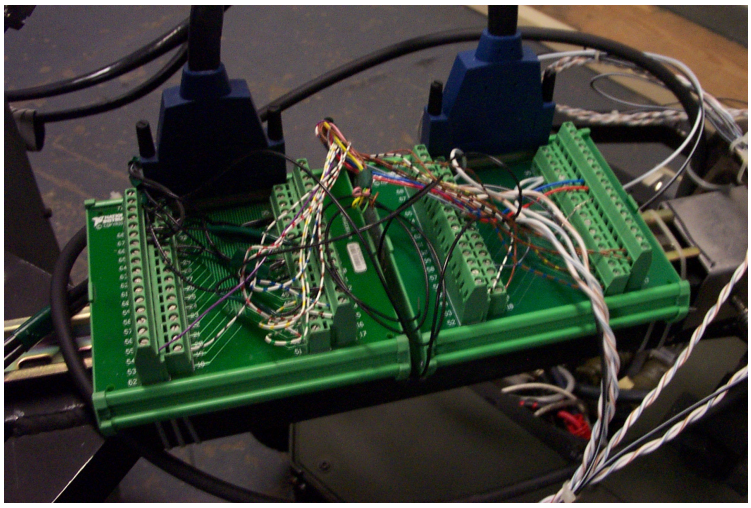

Figure 75: DAQ breakout boards

The laptop computer collecting and processing the data stream was situated on the rear of the vehicle to allow for easy access during experimentation and is shown in Figure 76.

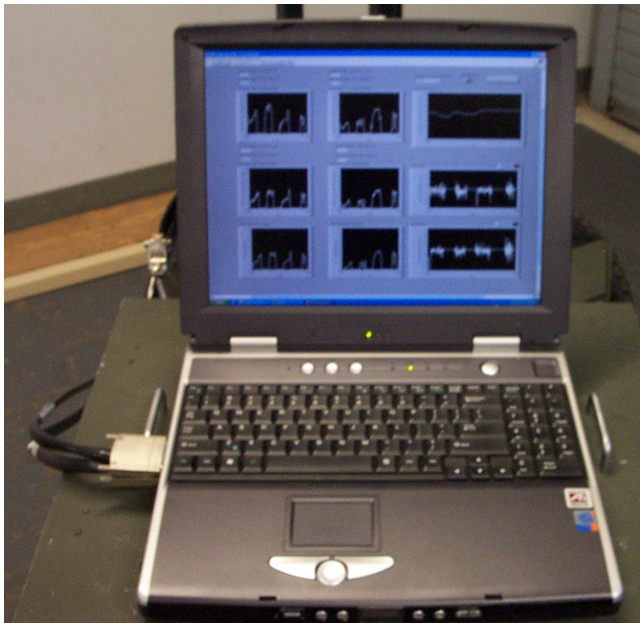

Figure 76: Laptop Computer

5.1.4 Data Acquisition Software

The software used to collect and analyze the data for this experiment was developed with National Instruments LabView software. LabView provided the means to simply interface with the NI 6024-E DAQcards and develop the virtual instrumentation functionality and a graphical user interface to gather and analyze the experimentation data.

The kinematic model originally developed for the simulation in Matlab was ported to LabView to provide the ability to determine the estimated rear wheel velocities based upon the input front wheel velocities and body position in real-time. This provided the ability to determine the theoretical results as the actual rear wheel velocities were being measured during the experiment and yield a dynamic assessment of the validity of the kinematic model.

The data collected during the dynamic experiment was logged to a data file and imported into Matlab for post processing of the results. Data was collected every 100 milliseconds or 10 Hz.

5.2 Experimental validation of the kinematic model

The validation experiment was conducted on a sealed concrete shop surface in an indoor laboratory space traversing a hallway, lobby space, and garage. Figure 77 details the layout of the area and the general path the vehicle traversed during the experiment. Remotely controlled, the vehicle completed a complete loop of the indoor space making tight turns at either end of the course. Multiple trials of the experiment were conducted with similar results. An exemplary experimental trial will be highlighted to provide validation for the kinematic model developed for the two body articulated NERV platform.

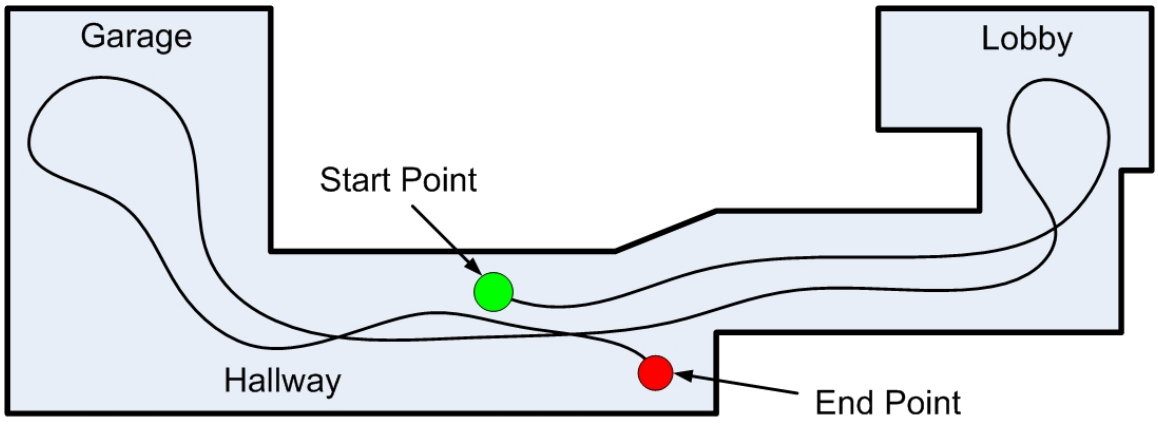

Figure 77: Experiment course

The plots presented in Figure 78 details the vehicle motion during the experimental trial. The experiment included nearly 2.25 minutes of continuous vehicle motion as it traversed a course similar to the path outlined in Figure 77.

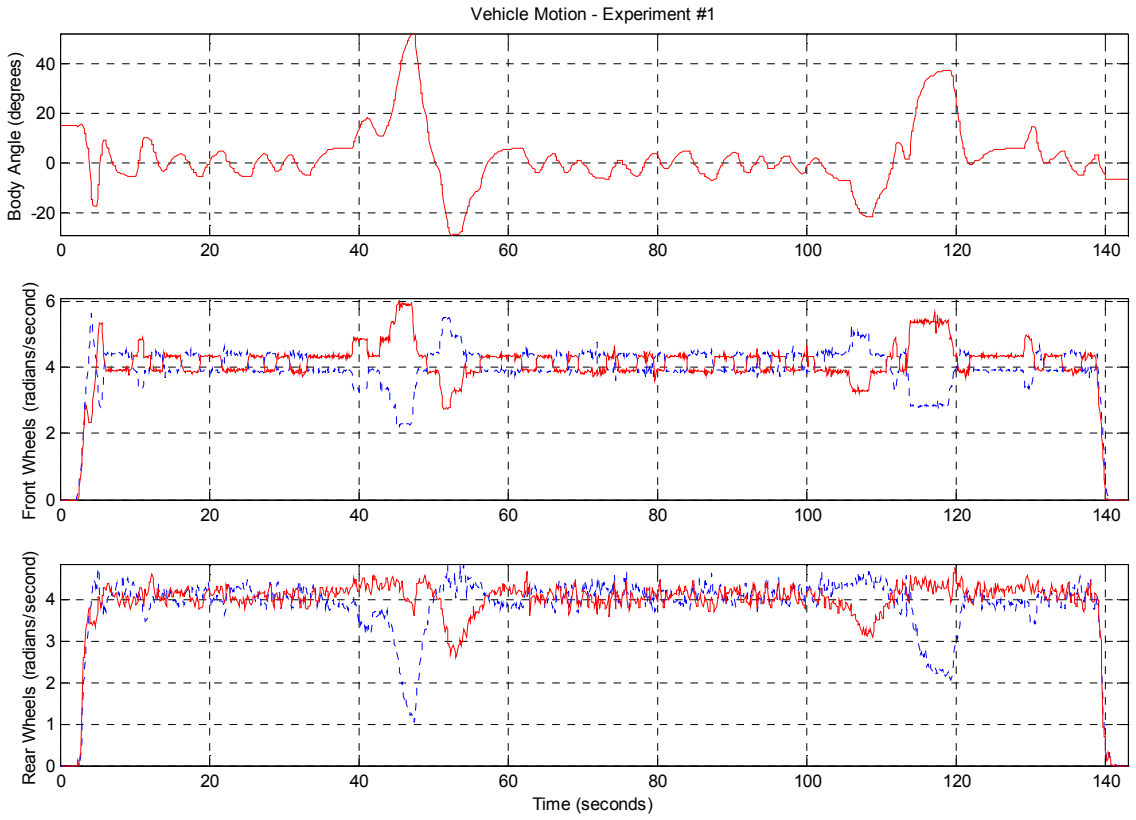

Figure 78: Vehicle motion data

The first sub plot at the top of Figure 78 presents the relative body angle during the experiment. It is apparent that there were four distinct instances where the vehicle performs a sequence of substantial turning maneuvers. These events are denoted by periods of dramatic increase in the measured valued of the relative body angle. The second subplot supports these turning motions with changes in the front wheel velocities that are indicative of a differentially driven vehicle executing a turn. For reference, the convention for multi data set plots is that the blue dashed line indicates left wheel results and the red solid line indicating right wheel results. The third subplot presents the measured values of the rear wheel velocities during motion.

A closer inspection of the front wheel speed results, shown in Figure 79, provides some insight into the characteristics of the motion of the Polaris platform. At the beginning

of the trial, the vehicle's front wheels accelerate from an initial stopped state to an average wheel rotational velocity of approximately 4.2 radians per second. Highlighted in Figure 79 are four pronounced periods of rapid turning vehicle movement that were associated with maneuvering through the garage and lobby spaces of the test area. These pronounced turning events are apparent due to the assumption that the direction and rate of the turn is determined by the differential speed between the left and right wheels. In addition, the periods where the vehicle was maneuvered to maintain a straight path down the corridor is also highlighted in the figure.

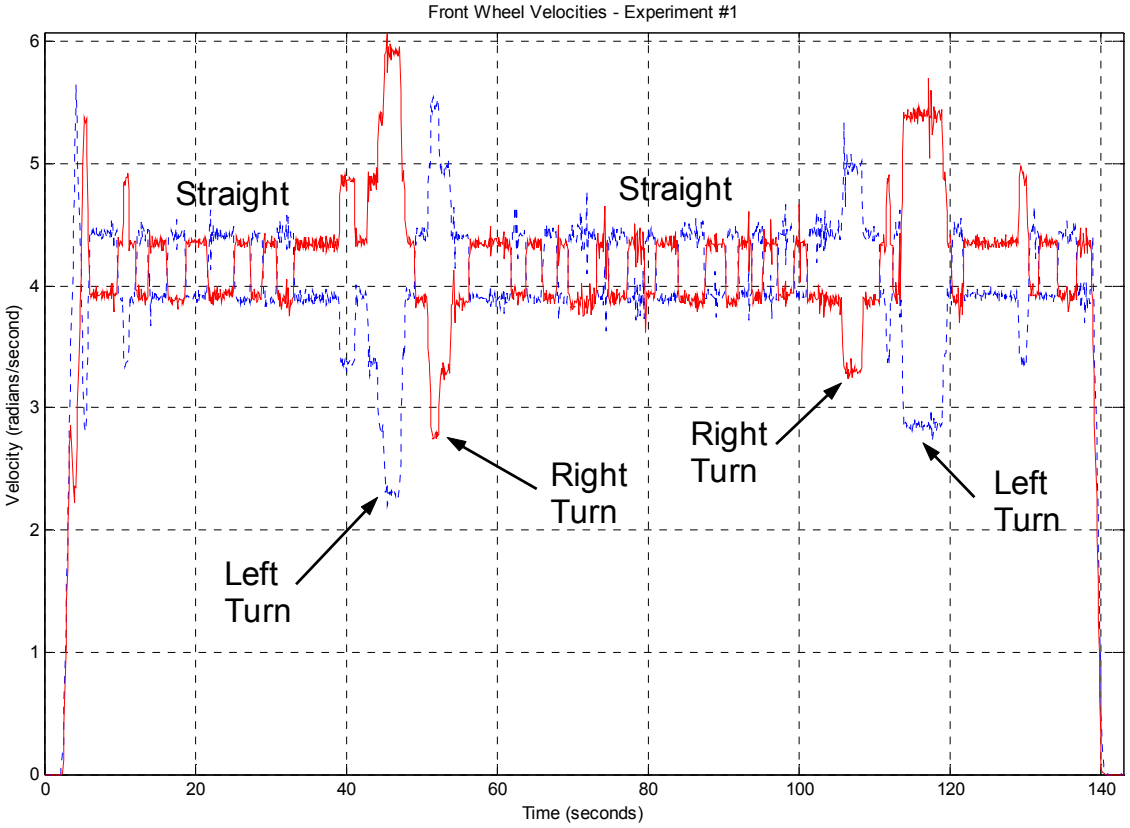

Figure 79: Front wheel velocities

The small square fluctuations in wheel speed present during the corridor navigation are the result of inaccuracies present in the remote vehicle control causing the vehicle to "swim" or oscillate back and forth as the operator attempted to maintain a straight path. These inaccuracies were the result of mechanical backlash present in the front wheel hub assembly that connected the wheels to the motor drive shaft. The significant play in the wheel connection (upwards of ± 5 degrees) resulted in the operator controlling the vehicle to

overcompensate thus requiring a continuous corrective response to maintain a straight forward path. This less than ideal vehicle characteristic demanded that the operator of the vehicle account for the variability in wheel response manifesting as an oscillating pattern present in motion of the vehicle.

Figure 80 details the relative body angle measurement collected during the trial with the major turning events highlighted. The angle measurement results validate the turn direction previously determined from inspection of the front wheel velocity plot. The oscillations present in the front wheel velocity measurement during the straight are also present in the plot of the relative body angle.

The measured rear wheel velocities presented in the lower subplot in Figure 78 ostensibly contain a significantly less pronounced effect of the vehicle control variability (e.g. "swimming"). This muted response is in part linked to the kinematic relationship between the front and rear section wheel responses. The swimming motion of the differentially driven front section has decreasing effect on the velocities of the rear wheels of the vehicle as the relative body angle remains small. However, the larger contributing factor to this result is the presence of the noticeable levels of mechanical backlash the interconnecting joint between the front and rear sections that served to absorb some of the jitter provided by the oscillating front section.

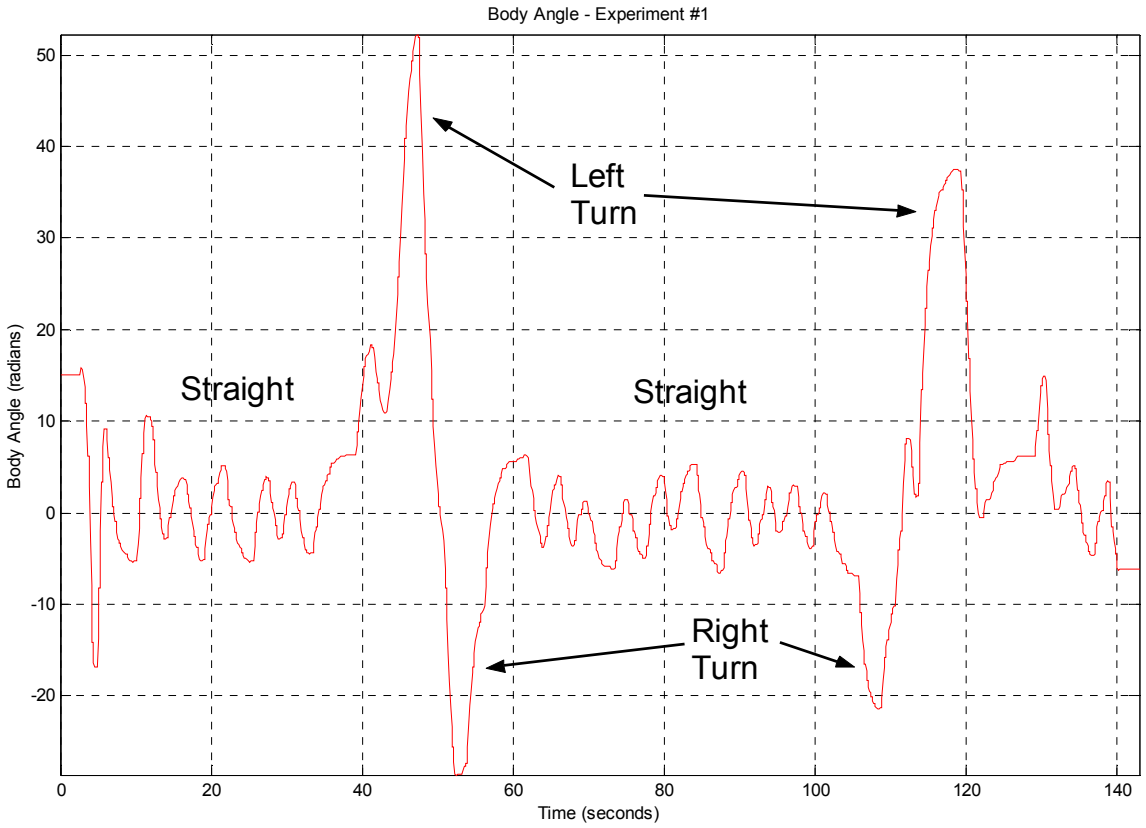

Figure 80: Relative body angle

With the measured values of the front wheel velocities and the relative body angle, it is then possible to apply the kinematic model developed for the two body articulated platform in Section 3. For each 100 ms cycle of the data acquisition system, the values obtained from the encoders for these variables can be processed via the kinematic model to predict the instantaneous expected rear wheel velocities. Figure 81 depicts the vehicle motion data presented in Figure 78 with the addition of the predicted rear wheel velocities.

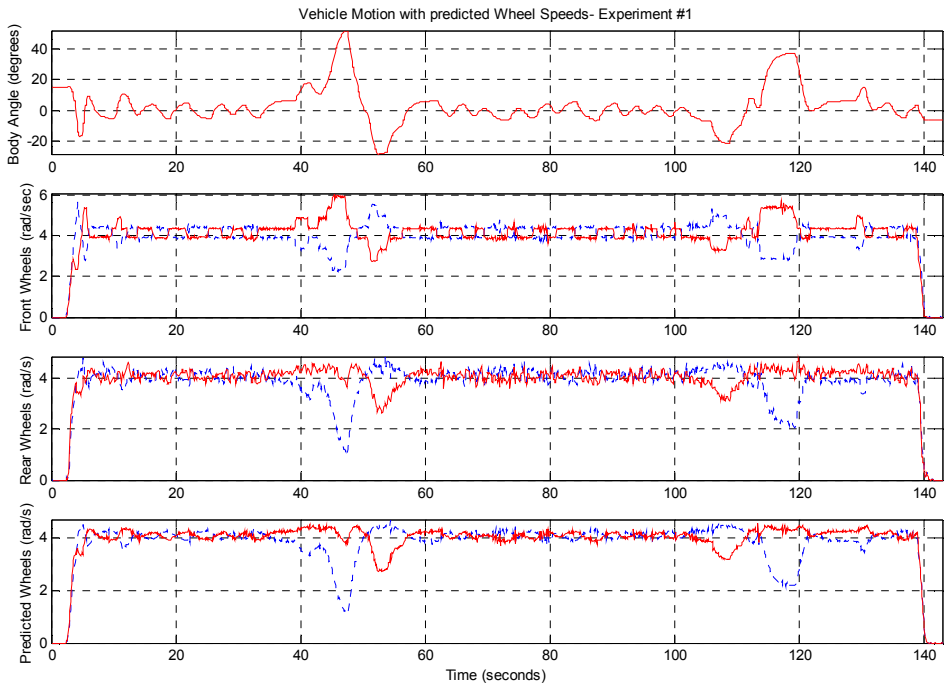

Figure 81: Measured vehicle motion with predicted rear wheel speeds

It is noteworthy that the output of the kinematic model shown in the bottommost subplot appears to track the trend of the measured rear wheel velocities with a degree of perceived accuracy. To verify this initial conclusion, residuals were calculated between the measured and predicted rear wheel speeds. These residuals for both the left and right rear wheels are presented along with the relative body angle and front wheel velocities in Figure 82. The mean value of the residuals was -0.0359 and -0.0214 radians per second for the left and right rear wheels, respectively. This bias error can be attributed to the error in vehicle constants utilized for the kinematic model as well as a small phase shift resulting from the estimation of the average wheel velocity during the measurement cycle. The range of the magnitude of the residual values was consistent over the full range of wheel speeds and relative body angles present in the trial motion. This indicates that error in predicted rear wheel speeds is a result of the random measurement error indicative inherent in the measurement of the wheel velocities and body angle.

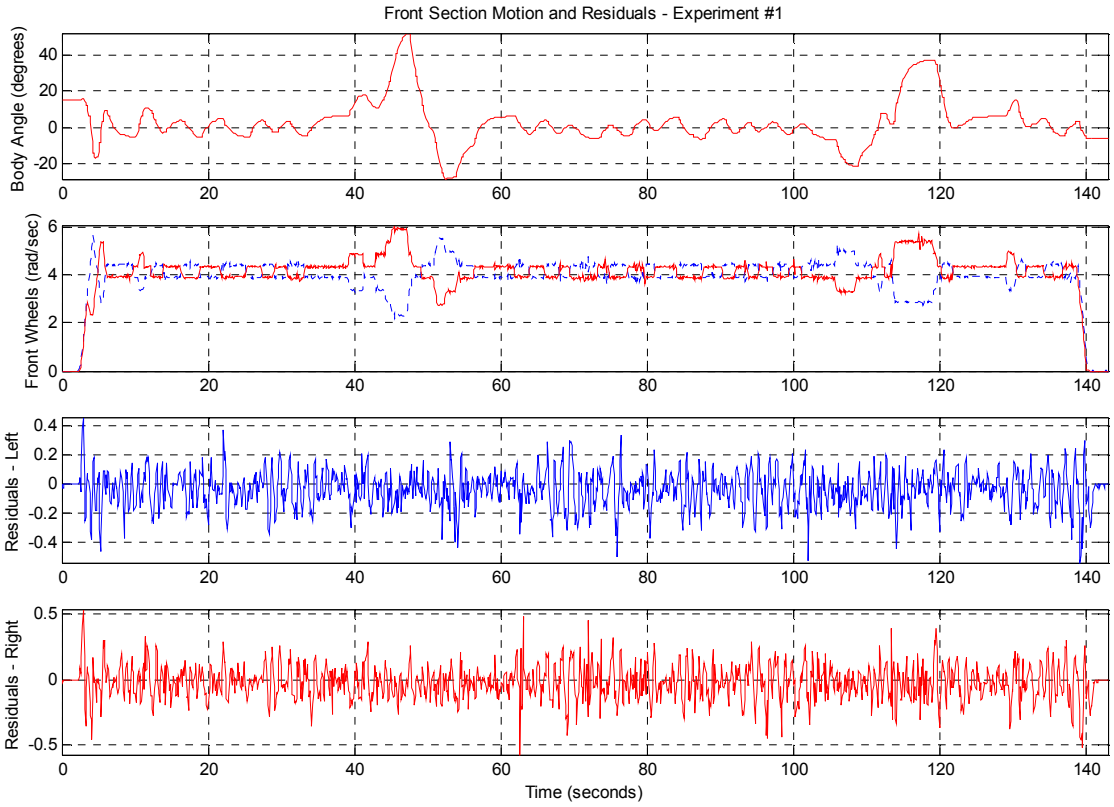

Figure 82: Residuals of rear wheel velocity

Supporting this assessment, the residual values do appear to be random in nature through the course of the experiment. To validate this, a histogram for each rear wheel velocity residual data set was developed with Figure 83 and 84 detailing the left and right rear wheel residuals, respectively. The distribution of the values contained in the histogram of both data sets appears to be similar to a normal distribution indicating random data content. The left wheel residual values had a variance of $\sigma^2 = 0.0157$ while the right residuals had a value of $\sigma^2 = 0.0173$.

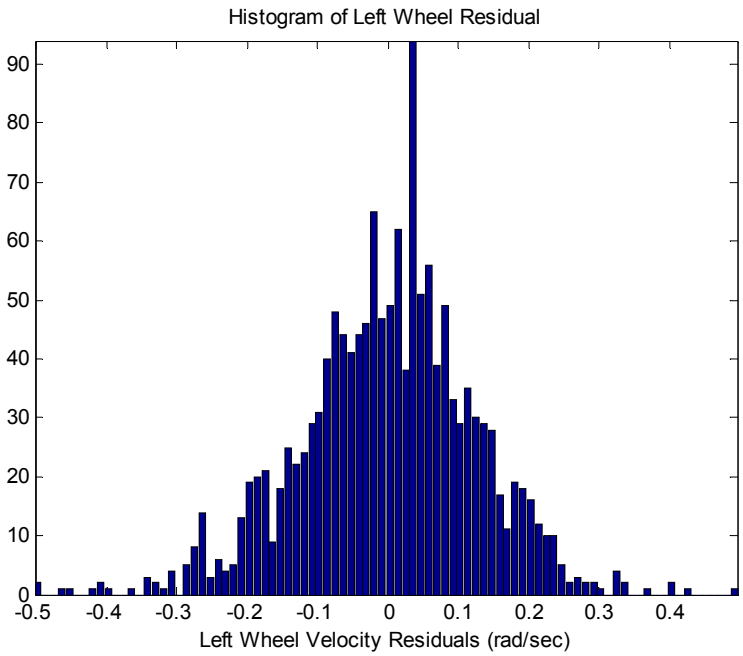

Figure 83: Left rear wheel residuals histogram

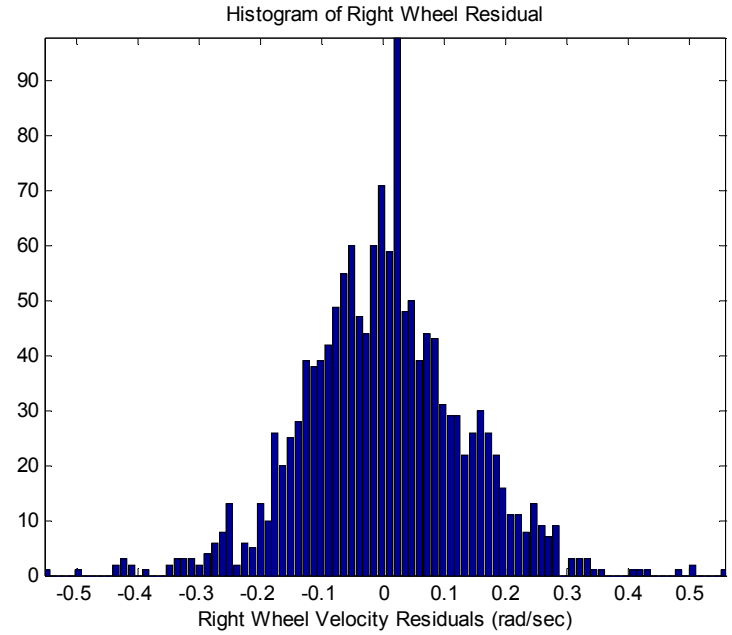

Figure 84: Right rear wheel residual histogram

To further verify that the residual values are random in nature, a quantile – quantile (Q-Q) plot comparing the distribution of the residuals to a normal Gaussian distribution of

with the same variance is generated. Figure 85 and 86 detail the Q-Q plot for the left and right rear wheel residuals, respectively. The correlation coefficient for the left rear wheel residuals was calculated to be 0.9645 and the correlation coefficient for the right rear wheel was calculated to be 0.9613. These correlation coefficient values indicate that the residual data approaches normally distributed random error values with a fair degree of accuracy.

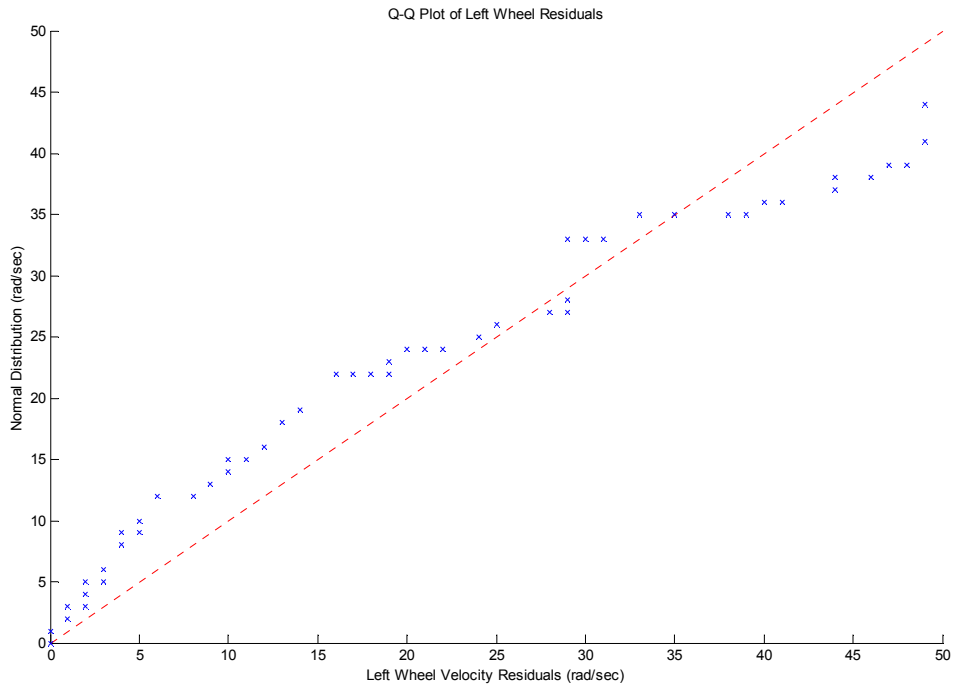

Figure 85: Q-Q plot for left rear wheel residuals

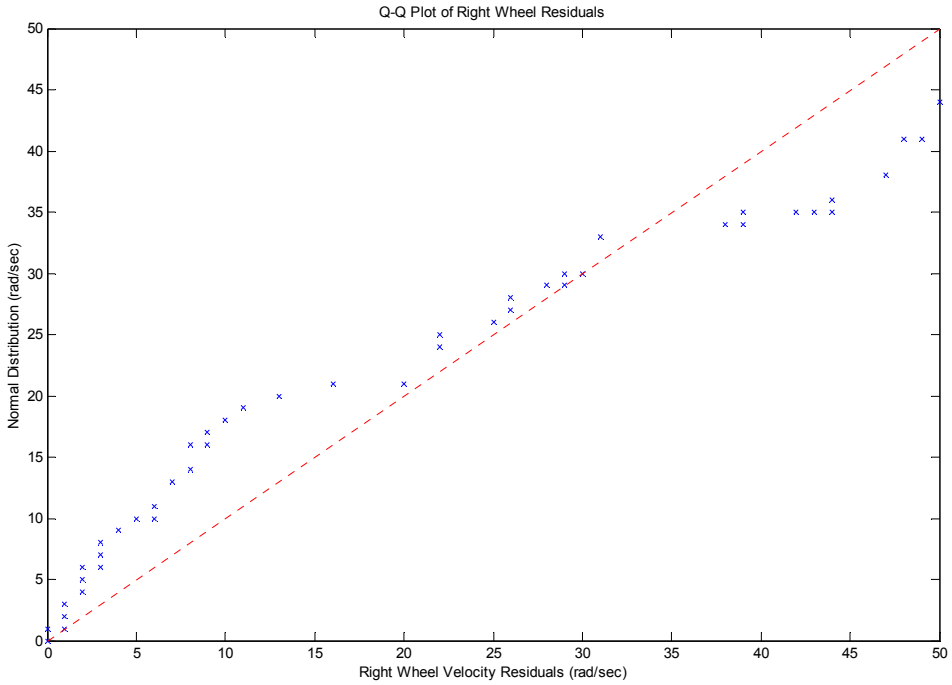

Figure 86: Q-Q plot of the right rear wheel residuals.

However, due to the variability in the histogram and Q-Q plot results further verification is desirable to conclusively substantiate that the residual data is without deterministic content. The autocorrelation of the residual data sets presented in Figures 87 and 88 indicate that the content is indeed random due to the magnitude of the correlation value being significantly less than 1 even for the zero lag condition. The results of the Q-Q plot coupled with the autocorrelation leads to the conclusion that the residuals are indeed random.

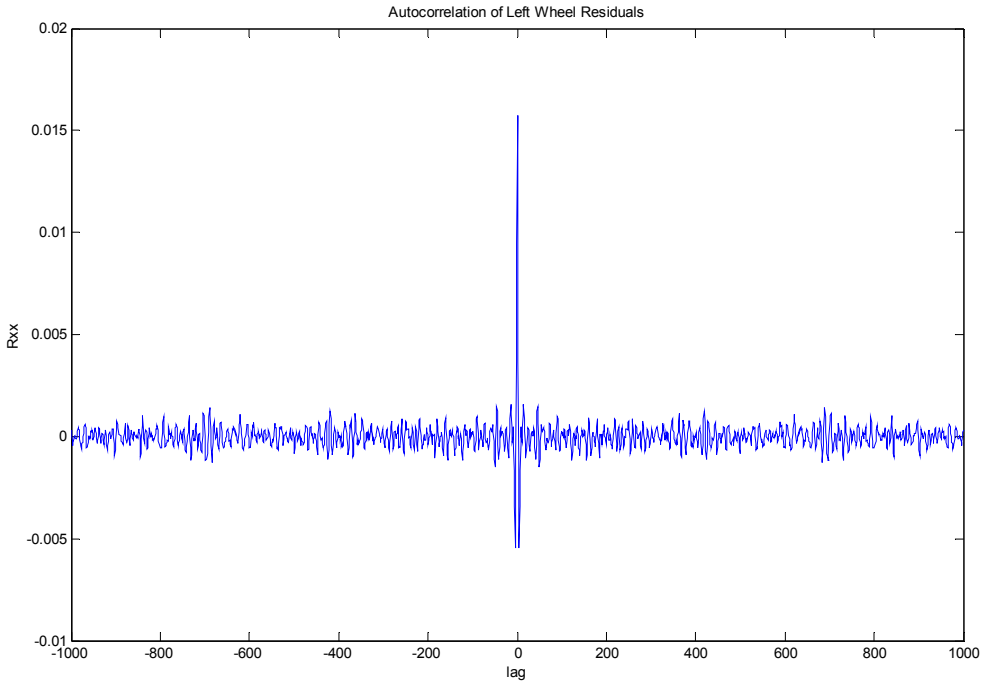

Figure 87: Autocorrelation of the left rear wheel residuals

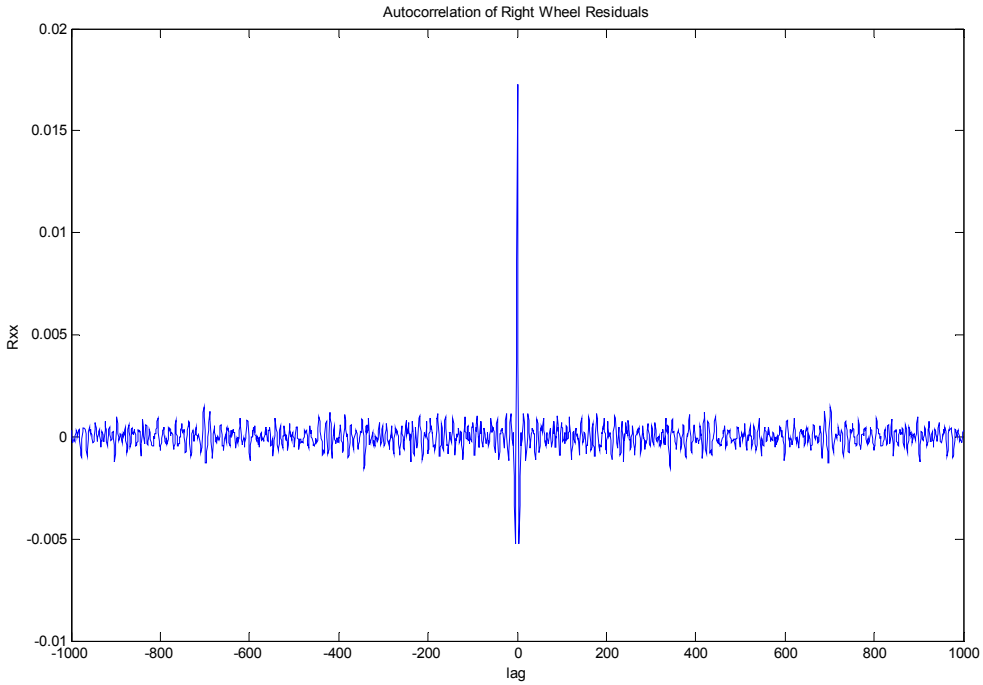

Figure 88: Autocorrelation of the right rear wheel residuals

The results indicate that the planar kinematic model developed for the two body articulated NERV platform successfully predicts the rear wheel velocities. This leads to the ability to develop and apply novel features on the NERV platform such as four-wheel drive capability. In addition, such results facilitate the development of advanced path planning and control techniques that account for multi-body planar movement. The kinematic model based upon dynamic measured inputs of front wheel speeds and relative body angle demonstrated the ability to predict the resulting rear wheel speeds without drift associated with integration errors commonly found in wheel odometery and encoding applications. The instantaneous assessment of the pose of the vehicle and the input front wheel speeds leads to the ability to accurately predict the kinematic relationships based upon concurrent feedback.

Expanding these results into a robust solution would demand further investigation into effect that acceleration, wheel slippage, and the second degree of freedom between the front and rear sections have on the observed error predicted rear wheel speed. Further, it is suggested that the effect that such levels of error observed in this experiment have on the level of kinematic contention be examined. While such deviations levels between the measured and predicted rear wheel speeds may be negligible, it is of practical interest to quantify the effect such non-ideal results have on the integrity of the vehicle structure, drive train components, and control fidelity.

6 Conclusions

The development of the next-generation experimentation robotic vehicle presented was based upon the perceived needs for supporting research in leading-edge intelligent and autonomous system technologies. It was established that a flexible and open architecture mobile robotic platform exhibiting exceptional mobility and stability in a research environment would facilitate intelligent and autonomous hardware and software development experimentation. This assertion was validated through thoughtful background research including an informal survey of unmanned system researchers.

In an effort to address the identified needs, the development of the NERV platform consisted of two largely independent yet essential design elements: (1) the kinematic platform and (2) system architecture design. The resulting kinematic platform developed for the NERV expands the understanding of multi-body mobile robotic kinematic platforms. The kinematic model provides the ability to control a multi-body robot with simple differential drive commands. The efficacy of the model was initially examined with a computer simulation of the planar motion of the robot for several cases of ideal motion. The computer simulation was then extended to include quantification error resulting from the measurement of the characteristic wheel velocities and relative body angle. The simulation determined that prediction of the motion of the vehicle was possible for the full range of vehicle poses.

Moreover, the validity of the kinematic model was supported through a proof-of-concept experiment on a full size mobile two-body articulated robotic platform in a real world setting. Despite the errors present in the construction and control of the vehicle, the kinematic model was shown to be an accurate predictor of the motion of the two-body robotic vehicle. The implications of these findings include the ability to provide four-wheel drive capability on a two-body vehicle while retaining the simple differential drive control definition for higher level vehicle control. In addition, the ability to effectively predict the motion of the rear section of the vehicle given the front wheel velocities and the state of the relative body angle allows for the ability for navigation and control algorithms to be developed that include a greater awareness of the vehicle pose. The result of this greater understanding is the ability to control the NERV to effectively maneuver through confined obstacle filled spaces as well as perform parking maneuvers. The kinematic model developed for the NERV forges the fundamental kinematics for developing multi-body autonomous vehicle including vehicle with trailers and or a train of body elements.

In concert with the development of the NERV kinematic platform, a system level design of the NERV was presented as a technology independent approach based upon the emerging JAUS standard. This open architecture design allows a variety of researchers to interface with the full functionality of the NERV platform via standard communication protocol developed by the JAUS working group. Indeed this open and forward-looking approach to system design is the defining aspect of the NERV concept by setting the NERV apart from current small UGV solutions. Leveraging a modular approach to system integration provides for a flexible integration schema that addresses the pressing need for a standard UGV solution. With such a capability, researchers will have the ability to efficiently translate novel hardware and software technology from the laboratory into real world scenarios for the purposes of validation, refinement, and benchmarking.

Altogether the fusion of a capable small UGV mobility platform and modular open system architecture defines the NERV as a practical solution that addresses the extant needs of the unmanned systems research community.

7 Appendix A: Customer Survey

A copy of the customer, UGV user, survey administered for the purpose of determining the needs for the NERV platform is presented in Section 7.1. A summary of the raw results is also included in Section 7.2. The survey was design and implemented as an "unscientific" mechanism to lend some insight into customer requirements.

7.1 Survey Questions

An unmanned ground vehicle, or UGV, is a robotic platform that operates in a real-world environment as an extension of human capability. UGV capabilities can range from remote teleoperation by a human to fully autonomous mission execution.

The purpose of this survey is to gain insight on the current and potential usage of small unmanned ground vehicles (5 to 500 lbs) within the research community. For reference, a 5 pound UGV can be considered the same size and weight of a bag of flour and a 500 pound UGV can be considered the size of a small golf cart.

Please consider these questions in terms of your own experiences and needs as a user or potential user of an unmanned ground vehicle.

Have you heard of a UGV before?

☐ Yes ☐ No

Have you ever used a small UGV before?

☐ Yes ☐ No

How would you rate your familiarity with UGV technology?

☐ not at all ☐ somewhat ☐ average ☐ more than most ☐ in-depth knowledge

If you were using a small UGV for research purposes, how important to you is the ability to have access to the inner workings (hardware and software) of the UGV?

☐ not at all ☐ somewhat ☐ average ☐ desirable ☐ required ☐ not sure

If you were using a small UGV for research purposes, how important to you is a small UGV designed with consideration for and compliance with an industry standard communications protocol?

☐ not at all ☐ somewhat ☐ average ☐ desirable ☐ required ☐ not sure

Do you feel as though the currently available small UGVs meet the needs of unmanned systems researchers?

☐ not at all ☐ a little ☐ somewhat ☐ most of them ☐ all of them ☐ not sure

Identify the UGV vehicles contained in the list with which you are familiar (i.e. observed or operated). If you are familiar with a specific platform that is not in the list, add it in the "other" field.

- ☐ "PackBot" by iRobot
- ☐ "ATRV" by iRobot
- ☐ "Talon" by Foster-Miller
- ☐ "Dragon Runner" by CMU
- ☐ "Matilda" by Mesa
- ☐ "Pioneer 2 or P3" by ActiveMedia Robotics
- ☐ "Chaos" by Autonomous Solutions
- ☐ "Spector" by Autonomous Solutions
- ☐ "ODIS" by CSOIS Utah State University
- ☐ "VGTV" by Inuktun Services
- ☐ "WiFiBot" by Robosoft
- ☐ "OmniTread" by University of Michigan

other: _____

Identify the sensor and payload devices that you feel are essential equipment that should be incorporated into the design of a small research UGV

- ☐ Camera (visual, near IR, Thermal, etc.)
- ☐ Microphone
- ☐ Manipulator (gripper, disruptor, etc.)
- ☐ Cable Spooler
- ☐ Obstacle detection (Laser range finder)
- ☐ Global Positioning System (GPS)
- ☐ Inertial Measurement Unit (IMU)
- ☐ Reconnaissance, Surveillance, and Target Acquisition (RSTA)
- ☐ Nuclear, Biological, Chemical (NBC) sensor
- ☐ Lethal weapons
- ☐ Non-lethal weapons

other: _____

What performance features and capabilities do you feel a should be a part of the design of a small research UGV?

- ☐ Carry a payload
- ☐ Tow a payload
- ☐ Interface with add-on payloads
- ☐ Climb and descend stairs
- ☐ Operate over a variety of terrain (grass,soil,sand,etc)
- ☐ Weathertight
- ☐ Submersible in water
- ☐ Shock/Drop rated
- ☐ Man-portable
- ☐ Operate without line-of-sight
- ☐ Autonomous navigation
- ☐ Teleoperation
- ☐ Small logistical footprint

other: _____

In what type of environment do you feel it is necessary for a small research UGV to be able to operate?

- ☐ Indoors
- ☐ Roadways (paved and unpaved roads)
- ☐ Grass Field
- ☐ Forest
- ☐ Swamp/Mud/Bog
- ☐ Beach
- ☐ Desert
- ☐ Ice/Snow
- ☐ Field/Crops
- ☐ Battlefield
- ☐ Urban Terrain
- ☐ Collapsed Structures
- ☐ Confined Spaces (tunnels)
- ☐ Fire
- ☐ Radiation
- ☐ Space

other: _____

What areas of UGV research do you feel require the most attention in order to foster UGV development?

- ☐ All areas require equal attention
- ☐ Mobility
- ☐ Software protocols
- ☐ Algorithms
- ☐ Computing capacity
- ☐ Sensors
- ☐ Power sources
- ☐ Communication

other: _____

What types of steering methods do you feel are the most appropriate for a small UGV?

- ☐ Skid Steer (Tank Drive)
- ☐ Differential Steering (two drive wheels)
- ☐ Omni-directional wheels
- ☐ Ackermann (car steering)
- ☐ Body articulated
- ☐ Axle articulated (like a wagon)
- ☐ not sure

other: _____

What would be a suitable runtime for a small UGV?

- ☐ 1 to 2 hours
- ☐ 2 to 4 hours
- ☐ 4 to 8 hours
- ☐ 8 to 10 hours
- ☐ 10 to 12 hours
- ☐ 12 hours +
- ☐ not sure
- ☐ other: _____

What would be a suitable top speed for a small UGV?

- ☐ 1 mph
- ☐ 5 mph
- ☐ 10 mph
- ☐ 15 mph
- ☐ 20 mph
- ☐ 20+ mph
- ☐ not sure
- ☐ other: _____

Do you prefer small UGVs with wheels or with tracks?

☐ Wheels ☐ Tracks ☐ Depends on the situation

If rechargeable batteries were used to power a UGV, would you prefer to have removable battery packs or integrated battery packs?

☐ Removable ☐ Integrated ☐ not sure

If batteries were to power a UGV, would you prefer to have rechargeable or single-use batteries?

☐ Rechargeable ☐ Single-use ☐ not sure

How important is the development of autonomous technologies to the future of unmanned vehicles?

☐ not at all ☐ a little ☐ average ☐ good ☐ required ☐ not sure

Do you feel that unmanned and autonomous vehicle research requires standards for developing and validating vehicle designs?

☐ yes ☐ no ☐ not sure

Identify your occupation (optional)

☐ Academic/Education

☐ Student

☐ Researcher

☐ Industry/Commercial

☐ Government

☐ Law Enforcement

☐ Military

☐ Self-Employed

other: _____

Please provide any additional comments regarding small UGVs (optional)

Thank you for taking the time to work through this survey!

7.2 Summary of Survey Responses

Have you heard of a UGV before?

Yes	55	(98%)
No	1	(2%)
no answer	0	(0%)

Have you ever used a small UGV before?

Yes	38	(68%)
No	18	(32%)
no answer	0	(0%)

How would you rate your familiarity with UGV technology?

not at all	1	(2%)
somewhat	10	(18%)
average	10	(18%)
more than most	22	(39%)
in-depth knowledge	13	(23%)
no answer	0	(0%)

If you were using a small UGV for research purposes, how important to you is the ability to have access to the inner workings (hardware and software) of the UGV?

not at all	0	(0%)
somewhat	1	(2%)
average	2	(4%)
desirable	20	(36%)
required	31	(55%)
not sure	2	(4%)
no answer	0	(0%)

If you were using a small UGV for research purposes, how important to you is a small UGV designed with consideration for and compliance with an industry standard communications protocol?

not at all	0	(0%)
somewhat	1	(2%)
average	3	(5%)
desirable	35	(63%)
required	11	(20%)
not sure	6	(11%)
no answer	0	(0%)

Do you feel as though the currently available small UGVs meet the needs of unmanned systems researchers?

not at all	1	(2%)
a little	5	(9%)
somewhat	22	(39%)
most of them	6	(11%)
all of them	0	(0%)
not sure	22	(39%)
no answer	0	(0%)

Identify the UGV vehicles contained in the list with which you are familiar (i.e. observed or operated). If you are familiar with a specific platform that is not in the list, add it in the "other" field.

"PackBot" by iRobot	18	(32%)
"ATRV" by iRobot	4	(7%)
"Talon" by Foster-Miller	12	(21%)
"Dragon Runner" by CMU	5	(9%)
"Matilda" by Mesa	26	(46%)
"Pioneer 2 or P3" by ActiveMedia Robotics	1	(2%)
"Chaos" by Autonomous Solutions	5	(9%)
"Spector" by Autonomous Solutions	5	(9%)
"ODIS" by CSOIS Utah State University	3	(5%)
"VGTV" by Inuktun Services	0	(0%)
"WiFiBot" by Robosoft	1	(2%)
"OmniTread" by University of Michigan	5	(9%)
other:	11	(20%)

Identify the sensor and payload devices that you feel are essential equipment that should be incorporated into the design of a small research UGV

Camera (visual, near IR, Thermal, etc.)	52	(93%)
Microphone	12	(21%)
Manipulator (gripper, disruptor, etc.)	18	(32%)
Cable Spooler	1	(2%)
Obstacle detection (Laser range finder)	46	(82%)
Global Positioning System (GPS)	42	(75%)
Inertial Measurement Unit (IMU)	31	(55%)
Reconnaissance, Surveillance, and Target Acquisition (RSTA)	20	(36%)
Nuclear, Biological, Chemical (NBC) sensor	6	(11%)
Lethal weapons	3	(5%)
Non-lethal weapons	3	(5%)
other:	5	(9%)

What performance features and capabilities do you feel should be a part of the design of a small research UGV?

Carry a payload	47	(84%)
Tow a payload	21	(38%)
Interface with add-on payloads	30	(54%)
Climb and descend stairs	26	(46%)
Operate over a variety of terrain (grass,soil,sand,etc)	49	(88%)
Weathertight	45	(80%)
Submersible in water	9	(16%)
Shock/Drop rated	41	(73%)
Man-portable	25	(45%)
Operate without line-of-sight	39	(70%)
Autonomous navigation	42	(75%)
Teleoperation	28	(50%)
Small logistical footprint	13	(23%)
other:	2	(4%)

In what type of environment do you feel it is necessary for a small research UGV to be able to operate?

Indoors	47	(84%)
Roadways (paved and unpaved roads)	50	(89%)
Grass Field	53	(95%)
Forest	35	(63%)
Swamp/Mud/Bog	21	(38%)
Beach	34	(61%)
Desert	37	(66%)
Ice/Snow	27	(48%)
Field/Crops	34	(61%)
Battlefield	32	(57%)
Urban Terrain	36	(64%)
Collapsed Structures	28	(50%)
Confined Spaces (tunnels)	38	(68%)
Fire	14	(25%)
Radiation	18	(32%)
Space	16	(29%)
other:	3	(5%)

What areas of UGV research do you feel require the most attention in order to foster UGV development?

All areas require equal attention	18	(32%)
Mobility	17	(30%)
Software protocols	19	(34%)
Algorithms	26	(46%)
Computing capacity	9	(16%)
Sensors	18	(32%)
Power sources	18	(32%)
Communication	9	(16%)
other:	0	(0%)

What types of steering methods do you feel are the most appropriate for a small UGV?

Skid Steer (Tank Drive)	26	(46%)
Differential Steering (two drive wheels)	31	(55%)
Omni-directional wheels	9	(16%)
Ackermann (car steering)	14	(25%)
Body articulated	6	(11%)
Axle articulated (like a wagon)	5	(9%)
not sure	8	(14%)
other:	1	(2%)

What would be a suitable runtime for a small UGV?

1 to 2 hours	1	(2%)
2 to 4 hours	10	(18%)
4 to 8 hours	19	(34%)
8 to 10 hours	9	(16%)
10 to 12 hours	6	(11%)
12 hours +	4	(7%)
not sure	6	(11%)
other:	1	(2%)
no answer	0	(0%)

What would be a suitable top speed for a small UGV?

1 mph	0	(0%)
5 mph	7	(13%)
10 mph	19	(34%)
15 mph	14	(25%)
20 mph	4	(7%)
20+ mph	5	(9%)
not sure	4	(7%)
other:	3	(5%)
no answer	0	(0%)

Do you prefer small UGVs with wheels or with tracks?

Wheels	13	(23%)
Tracks	2	(4%)
Depends on the situation	41	(73%)
no answer	0	(0%)

If rechargeable batteries were used to power a UGV, would you prefer to have removable battery packs or integrated battery packs?

Removable	46	(82%)
Integrated	7	(13%)
not sure	3	(5%)
no answer	0	(0%)

If batteries were to power a UGV, would you prefer to have rechargeable or single-use batteries?

Rechargeable	55	(98%)
Single-use	0	(0%)
not sure	1	(2%)
no answer	0	(0%)

How important is the development of autonomous technologies to the future of unmanned vehicles?

not at all	0	(0%)
a little	0	(0%)
average	0	(0%)
good	9	(16%)
required	45	(80%)
not sure	0	(0%)
no answer	2	(4%)

Do you feel that unmanned and autonomous vehicle research requires standards for developing and validating vehicle designs?

yes	37	(66%)
no	6	(11%)
not sure	13	(23%)
no answer	0	(0%)

Identify your occupation (optional)

Academic/Education	5	(9%)
Student	51	(91%)
Researcher	10	(18%)
Industry/Commercial	2	(4%)
Government	1	(2%)
Law Enforcement	0	(0%)
Military	1	(2%)
Self-Employed	0	(0%)
other:	1	(2%)

Please provide any additional comments regarding small UGVs (optional)
5 responses view this question view all questions

#9: 2005-11-01 15:49:31
many answers are dependent on the "type" of research being conducted.

#11: 2005-11-01 16:13:56
This survey is not an outlier. These are actual desired capabilities.

#15: 2005-11-01 18:27:10
Good luck on the Thesis!

#31: 2005-11-01 20:57:37
too much emphasis is on the platform... there needs to be a major paradigm shift toward a focus on software. how often have we gone "to see a robot"... what is there to see? its just a drive-by-wire vehicle. the software is what makes these machines unique. countless times ive heard "our platform...", "we have a platform", etc. software is often seen as more of an afterthought. this i believe is the underlying reason that current UGV development progress is slow.

#32: 2005-11-01 20:59:51
Do noh a single point conclude with a single path but a range of solutions, somewnat like a fuzzy rule.

8 Appendix B: Current small UGV database

Table 4: Currently Available Small UGV Platforms - Availability, Cost, and Size

Platform	Manufacturer	Availability	Cost (US $)	Weight (kg)	Length (cm)	Width (cm)	Height (cm)
Adam	ActivMedia robotics	COTS		200	91.5	91.5	73
AmigoBot	ActivMedia robotics	COTS	$2,395	3.5	28	33	
PatrolBot	ActivMedia robotics	COTS	$35,000	46	59	48	38
Pioneer 2 - AT	ActivMedia robotics	COTS	$5,495	10.8	51.28	46.1	27.5
Pioneer 2-DX	ActivMedia robotics	COTS	$3,295	7.65	44.87	38.46	23
P3-AT	ActivMedia robotics	COTS	$6,995	12	50	49	26
P3-DX	ActivMedia robotics	COTS	$4,195		44	38	22
PowerBot	ActivMedia robotics	COTS	$21,995	140	91	67	47
Advanced Whiskers	Angelus Research Corporation	COTS	$2,200	10.9	19.05	8.89	
ART1	Angelus Research Corporation	Prototype	$28,000	18	56.4	33.33	17.9
Intruder	Angelus Research Corporation	COTS	$22,000	11.25	43.58	35.9	17.9
Piper	Angelus Research Corporation	Prototype	$18,000	9.9	51.28	23.1	34.6
Ranger Modular Robot	Angelus Research Corporation	COTS	$28,000	24.9	81.3	40.64	30.5
Chaos	Autonomous Solutions Inc.	Prototype	$45,000	40	130.9	59.9	48.5
Spector	Autonomous Solutions Inc.	Prototype	$20,000				
VRAM	Avionic Instruments Inc.	Prototype		0.85	16.5	21.59	10.16
Dragon runner	Carnegie Mellon University	Prototype	$46,000	7.26	39.37	28.58	12.7
ODIS-I	CSOIS Utah State University	COTS	$50,000	20.4			9.52
ODIS-S	CSOIS Utah State University	COTS	$50,000	22.5	61.5	61.5	10.9

T3 ODV	CSOIS Utah State University	Prototype		54.4	50.8	66	45.7
Vanguard	EOD Performance Inc	COTS		52	91.5	43.5	40.5
Scorpion	Evolution Robotics	COTS	$9,000	20.9	44	41	45
TALON	Foster-Miller	COTS	$59,220	38.25	87.1	57.7	28.2
Max II	HDE Manufacturing	COTS	$30,000	20.25	67.69	51.28	29.2
MURV-100	HDE Manufacturing	COTS	$12,500	13.95	58.9	43.6	11.5
Micro Disruptor Vehicle	Inuktun Services	COTS	$32,222		33.33	28.2	17.9
VGTV	Inuktun Services	COTS	$28,595	3.15	32.05	19.23	6.41
Mini Distruptor Vehicle	Inuktun Services	COTS	$36,345	40.5	61.5	35.9	42.3
nanomag	Inuktun Services	COTS	$37,995	2.2	10.5	15.7	4.9
Versa Trax 100	Inuktun Services	COTS	$56,714	9		10	10
Versa Trax 150	Inuktun Services	COTS	$65,670	41		15.24	15.24
Versa Trax 300 VLR	Inuktun Services	COTS		113.4		30.48	30.48
ATRV 2	iRobot	COTS		118	105	86	65
ATRV Jr	iRobot	COTS	$19,150	49.5	78.2	64.6	49.5
ATRV Mini	iRobot	COTS		38.7	61		46.15
B14R	iRobot	COTS	$19,250	27	35.3	35.3	60.6
CoWorker	iRobot	COTS			64.1	41.1	89.7
Magellan	iRobot	COTS	$5,950	13.05	37.2	37.2	19.9
Packbot EOD	iRobot	COTS		24	69.2	41	18.3
Packbot Scout	iRobot	COTS	$39,500	18	69.2	41	18.3
ThrowBot 4 Wheels	iRobot	Prototype					
ThrowBot 6 Wheels	iRobot	Prototype					
Brat	Kentree, Ltd.	COTS	$12,000	64.43	99.9	41.58	54.6
IMP	Kentree, Ltd.	COTS	$66,000	65	80.61	42.45	
Rascal	Kentree, Ltd.	COTS	$48,000	32.76	79.69	41.53	34.8
Matilda	Mesa Robotics	COTS	$55,000	27.67	76.2	53.34	30.5
Eel	Navy	Prototype					
BombTec Responder	PW Allen & Company Limited	COTS		45	80	45	26
Bison	QinetiQ	COTS		208.35			
Ground Hog	QinetiQ	COTS		34.65			
Mini-Andros	Remotec	COTS	$10,000	84.6	107.7	61.5	94.9
Cye	Robosoft	COTS	$5,500		25.5	40	10
Pebbles	Robosoft	COTS	$12,000	11.25	41	43.6	15.4
robuCAR-TT	Robosoft	COTS	$75,900	350	184	130	61

robuROC 4	Robosoft	COTS	$67,342	90	105	80	70
RobulabPro 80	Robosoft	COTS	$48,900	70	60	48	465
WiFibot	Robosoft	COTS	$3,051	4.5	30	30	30
SUBOT	SAIC Center for Intelligent Systems	Prototype	$10,000	1.98	16.15	16.15	16.15
Casper (RATLER)	Sandia National Laboratory	Prototype	$10,000	15.75	56.4	49.998	30.768
Mini-RATLER	Sandia National Laboratory	Prototype	$10,000	2.25	20.5	20.5	15.4
Urbot	SPAWAR Systems Center	Prototype		29.25	92.3	56.4	32.1
Cyclops	The Deltic Group Limited	COTS					
ApriAlpha	Toshiba America Research	COTS		9.5			
Rhex	University of Michigan	Prototype		7.1	47.4	20.3	12
OmniTread OT-8 SnakeBot	University of Michigan	Prototype		12	116	20	20
OmniMate	University of Michigan	Prototype			180	90	

Table 5: Currently Available Small UGV Platforms – Steering, Communications, and Power Source

Platform	Wheels or tracks	Steering Method	Interior or Exterior Operation	Primary Control Mode	Communication Link Type	Communication range (m)	Power Source
Adam	Wheels	Differential	Interior	Teleop	802.11		Pb
AmigoBot	Wheels	Differential	Interior	Teleop	Wireless RF; tether	100;5	Pb
PatrolBot	Wheels	Differential	Interior	Teleop	802.11		Pb
Pioneer 2 - AT	Wheels	Skid	Exterior	Teleop/ Auton	2.4 GHz, 50 mW FHSS, 1.6 Mbps	9530	Pb
Pioneer 2-DX	Wheels	Differential	Interior	Teleop/ Auton	2.4 GHz, 50 mW FHSS, 1.6 Mbps	9530	Pb
P3-AT	Wheels	Skid	Exterior	Teleop	802.11		Batt.
P3-DX	Wheels	Differential	Interior	Teleop	802.11		Batt.
PowerBot	Wheels	Differential	Interior	Teleop	Wireless RF		Pb
Advanced Whiskers	Wheels	Differential	Interior	Teleop/ Auton	Wireless	6	Pb
ART1	Tracks	Skid	Interior	Teleop	Wireless RF	1500	Li-SO2
Intruder	Wheels	Skid	Exterior	Teleop	900 MHZ, 1 Watt, DSS, 9600 baud		
Piper	Wheels	Skid	Exterior	Teleop	tether	45.72	
Ranger Modular Robot	Tracks	Skid	Exterior	Teleop	10kHz		Batt.
Chaos	Tracks	Skid	Exterior	Teleop			
Spector	Wheels	Omni	Exterior				
VRAM	Wheels	Skid	Exterior	Teleop	2.4 GHZ, Bluetooth 1.1, Class 1	100	Li-polymer
Dragon runner	Wheels	Ackerman	Exterior	Teleop	Wireless RF		
ODIS-I	Wheels	Omni	Exterior	Teleop	Wireless RF		Ni-MH
ODIS-S	Wheels	Omni	Exterior	Teleop	Wireless RF		Ni-MH
T3 ODV	Wheels	Omni	Exterior	Teleop			Pb
Vanguard	Tracks	Skid	Exterior	Teleop	Wireless RF		Pb

Scorpion	Wheels	Differential	Interior	Teleop			Pb
TALON	Tracks	Skid	Exterior	Teleop	802.11; 900 MHz, 955 mW, SS	2001	Pb or Li-Ion
Max II	Wheels	Skid	Exterior	Teleop	Wireless RF		
MURV-100	Wheels	Skid	Exterior	Teleop	430-850 MHz, 1 W	915	Pb
Micro Disruptor Vehicle	Tracks	Skid	Exterior	Teleop	tether	100	Batt.
VGTV	Tracks	Skid	Exterior	Teleop	tether	30.5	VAC
Mini Distruptor Vehicle	Tracks	Skid	Exterior	Teleop	tether	100.65	VAC or DC
nanomag	Tracks	Skid	Exterior	Teleop	tether	30	VAC
Versa Trax 100	Tracks	Skid	Exterior	Teleop	tether	90	VAC
Versa Trax 150	Tracks	Skid	Exterior	Teleop	tether	160	VAC
Versa Trax 300 VLR	Tracks	Skid	Exterior	Teleop	tether	1830	VAC
ATRV 2	Wheels	Skid	Exterior	Teleop	802.11, 1 to 3 Mbps		Pb
ATRV Jr	Wheels	Skid	Exterior	Teleop/ Auton	2.4 GHz, 2 Mbps, DSS	1000.4	Pb
ATRV Mini	Wheels	Skid	Exterior	Teleop	2.4 GHz, 1-3 Mbps	297.375	Pb
B14R	Wheels	Omni	Exterior	Teleop/ Auton	2.4 GHz, 2 Mbps, DSS	1000.4	Pb
CoWorker	Wheels	Skid	Interior	Teleop	802.11 b	610	Batt.
Magellan	Wheels	Differential	Exterior	Teleop/ Auton	2.4 GHz, 2 Mbps, DSS	1000.4	Pb
Packbot EOD	Tracks	Skid	Exterior	Teleop/ Auton	802.11, 2.4 GHz; tether	366	Ni-MH
Packbot Scout	Tracks	Skid	Exterior	Teleop/ Auton	802.11, 2.4 GHz; tether	366	Ni-MH
ThrowBot 4 Wheels	Wheels	Skid	Exterior	Teleop			Alkaline or Lithium
ThrowBot 6 Wheels	Wheels	Skid	Exterior	Teleop	Wireless RF		Alkaline or Lithium
Brat	Wheels	Skid	Exterior	Teleop	Wireless RF		Battery
IMP	Tracks	Skid	Exterior	Teleop	Wireless RF; tether	1000	VAC or DC

Rascal	Wheels	Skid	Exterior	Teleop	458 MHz	1000	
Matilda	Tracks	Skid	Exterior	Teleop	900 MHz	800	Ni-MH
Eel	Wheels	Skid	Exterior	Teleop			
BombTec Responder	Wheels	Skid	Exterior	Teleop			Batt.
Bison	Wheels	Skid	Exterior	Teleop	Wireless RF	1000.7	
Ground Hog	Wheels	Skid	Exterior	Teleop	Wireless RF	1000.7	
Mini-Andros	Wheels	Skid	Exterior	Teleop	VHF/UHF, 2.5 W	100.04	Pb
Cye	Wheels	Differential	Interior	Teleop	Wireless RF	100	Batt.
Pebbles	Tracks	Skid	Exterior	Teleop			Ni-Cd
robuCAR-TT	Wheels	Skid	Exterior	Teleop			Pb
robuROC 4	Wheels	Skid	Exterior	Teleop	Wireless RF		Pb or Li-Ion
RobulabPro 80	Wheels	Differential	Interior	Teleop	Wireless RF		Pb
WiFibot	Wheels	Skid	Exterior	Teleop/ Auton	802.11 b/g		Ni-MH
SUBOT	Wheels	Differential	Exterior	Teleop	Wireless RF		Ni-MH
Casper (RATLER)	Wheels	Skid	Exterior	Teleop	900 MHz, 500 mW; DSS, 9600 baud	1525	Pb
Mini-RATLER	Wheels	Skid	Exterior	Teleop	900 MHZ, 1 Watt, DSS, 9600 baud	457.5	Ni-Cd
Urbot	Tracks	Skid	Exterior	Teleop	802.11	305	Ni-MH
Cyclops	Tracks	Skid	Exterior	Teleop			
ApriAlpha	Wheels	Differential	Interior	Teleop	802.11 b		Metha-nol or Batt.
Rhex	Legs	Differential	Exterior	Teleop			Pb
OmniTread OT-8 SnakeBot	Tracks	Articulation	Exterior	Teleop		10	
OmniMate	Wheels	Differential	Interior				

Table 6: Currently Available Small UGV Platforms – Runtime, Speed, and Payload

Platform	Runtime (hrs)	Top Speed (km/h)	Maximum Payload (kg)	
Adam	10	7.2		
AmigoBot	2	3.6	1	
PatrolBot	3	6.12		
Pioneer 2 - AT	5	5.23	230.76	
Pioneer 2-DX	12	5.23	128.2	
P3-AT	6	2.52		
P3-DX	24	5.76		
PowerBot	2.5	5.4	100	
Advanced Whiskers	4	4.8		
ART1	8			
Intruder	1			
Piper	inf			
Ranger Modular Robot	8			
Chaos			10	
Spector				
VRAM		0.55	0.45	
Dragon runner		32.2		
ODIS-I				
ODIS-S				
T3 ODV	16			
Vanguard	3		80	
Scorpion	1	1.8	9	
TALON	2 to 4	7.67	769.2	
Max II	1			
MURV-100	4	0.93		
Micro Disruptor Vehicle		0.54	128.2	
VGTV	inf	0.27		
Mini Distruptor Vehicle	inf	0.54	384.6	
nanomag	inf	0.09		
Versa Trax 100	inf	0.585	13	
Versa Trax 150	inf	0.585	92	

Versa Trax 300 VLR	inf	0.585	184	
ATRV 2	4	7.2	100	
ATRV Jr	6	5.37	141.02	
ATRV Mini	4	5.37	51.28	
B14R	2	3.2	112.816	
CoWorker	4	1.1		
Magellan	12	7.24	51.28	
Packbot EOD	2 to 12	13.31	64.1	
Packbot Scout	2 to 12	13.31	64.1	
ThrowBot 4 Wheels	6			
ThrowBot 6 Wheels	6			
Brat	1			
IMP				
Rascal			60	
Matilda	6	3.22	56.7	
Eel				
BombTec Responder		2.16		
Bison				
Ground Hog				
Mini-Andros	2	1.91		
Cye				
Pebbles	1	1.42		
robuCAR-TT	4	7	350	
robuROC 4		11	100	
RobulabPro 80			80	
WiFibot	2			
SUBOT	0.5	3.29		
Casper (RATLER)	5.5	3.29	51.28	
Mini-RATLER	0.75	3.29	5.128	
Urbot		7.13	115.38	
Cyclops				
ApriAlpha				
Rhex	0.8	8.11		
OmniTread OT-8 SnakeBot	inf	0.36		
OmniMate				

9 Appendix C: IGVC Results

Table 7: 12th Annual Intelligent Ground Vehicle Competition results (2004)

	Design Competition	**Autonomous Challenge**	**Navigation Challenge**	**Overall**
First Place	*Gemini,* Virginia Tech	*Johnny-5,* Virginia Tech	*Amigo 2004,* Hosei Univeristy	*Johnny-5,* Virginia Tech
Second Place	*Johnny-5,* Virginia Tech	*Amigo 2004,* Hosei Univeristy	*Johnny-5,* Virginia Tech	*Amigo 2004,* Hosei Univeristy
Third Place	*Kodiak,* University of Alberta	*Gemini,* Virginia Tech	*Optimus,* Virginia Tech	*Gemini,* Virginia Tech

Table 8: 13th Annual Intelligent Ground Vehicle Competition results (2005)

	Design Competition	**Autonomous Challenge**	**Navigation Challenge**	**Overall**
First Place	*Gemini,* Virginia Tech	*Gemini,* Virginia Tech	*Gemini,* Virginia Tech	*Gemini,* Virginia Tech
Second Place	*Polaris,* Virginia Tech	*Johnny-5,* Virginia Tech	*Polaris,* Virginia Tech	*Polaris,* Virginia Tech
Third Place	*Calculon,* *University of Central Florida*	*Polaris,* Virginia Tech	*Johnny-5,* Virginia Tech	*Johnny-5,* Virginia Tech

10 Appendix D: Kinematic Computer Simulation

10.1 Matlab Code

Matlab m-file script code for the Simulation Driver Program.

```
% Sean Baity
% 10-18-05
% NERV Kinematic Model
% Simulation Driver Program

% Flush memory
close all;
clear all;
clc;

% +++++++++  Vehicle Parameters and Initial Conditions +++++++++

rfr = 0.1; %diameter of the right wheel, meters
rfl = 0.1; %diameter of the left wheel, meters
rrr = 0.1; %diameter of the rear right wheel, meters
rrl = 0.1; %diameter of the rear left wheel, meters

theta = 45*(pi/180); %intial angle of the vehicle in world space
gamma = 0*(pi/180); %initial angle between the front section robot frame and the rear
section
CG = [0;0]; %vehicle origin in intertial space

l = 0.25; %distance between the wheel and the center point CG, meters
d = 0.5;  %distance between center point and rear axle, meters
p = 0.25; %distance between rear axle center point and wheel, meters

phi_dot_right = 10; %rotational speed of the left wheel, radians/sec
phi_dot_left= 10; %rotational speed of the right wheel, radians/sec

% ++++++ Simulation Model Parameters ++++++

delta_t = 0.1; %seconds
sim_length = 3; %number of seconds to run the sim

i = 0;
k = 1;

for i = 0:delta_t:sim_length

% Call NERV Model for Kinematic Anlaysis based on physical parameters

[x_dot, y_dot, theta_dot, gamma_dot,phi_dot_right_rear,phi_dot_left_rear]=
NERV_iterate(rfr,rfl,rrr,rrl,l,d,p,theta,gamma,CG,phi_dot_right,phi_dot_left);

%Log variables for display
gamma_deg = (180/pi)*gamma;
gamma_log(:,k)= [i;gamma_deg];
x_dot_log(:,k) = [i;x_dot];
y_dot_log(:,k) = [i;y_dot];
phi_dot_right_rear_log(:,k) = [i;phi_dot_right_rear];
phi_dot_left_rear_log(:,k) = [i;phi_dot_left_rear];

% Update parameters for iterative analysis
CG = CG + [x_dot*delta_t; y_dot*delta_t];
theta = theta + theta_dot*delta_t;
```

```
gamma = gamma + gamma_dot*delta_t;

% Update step counts
i = i + delta_t;
k = k + 1;

end

% Plot Gamma and Wheel Velocity Results
figure(2)
plot(gamma_log(1,:),gamma_log(2,:))
xlabel('Time, (s)')
ylabel('Gamma, (degrees)')
title('Angle of front section relative to rear section versus time')
grid on

figure(3)
plot(phi_dot_right_rear_log(1,:),phi_dot_right_rear_log(2,:),'r')
hold on
plot(phi_dot_left_rear_log(1,:),phi_dot_left_rear_log(2,:),'b')
xlabel('Time, (s)')
ylabel('Wheel Rotational Velocity, (rad/sec)')
title('Rear Wheel Rotational velocities versus time')
grid on
```

Matlab m-file script code for the Kinematic Solution Engine program.

```
% Sean Baity
% September 27, 2005
% NERV Kinematic Model
% Kinematic Solution Engine

function [x_dot, y_dot, theta_dot,gamma_dot,phi_dot_right_rear,phi_dot_left_rear] =
NERV_iterate(rfr,rfl,rlr,rrr,l,d,p,theta,gamma,CG,phi_dot_right,phi_dot_left)

%========== Wheel Constraint Model ================

%++++++++ Front Section ++++++++

%Geomtery
alpha1 = -pi/2;
alpha2 = pi/2;

beta1 = pi;
beta2 = 0;

%Postion Velocity Matrix
J2= [rfr 0; 0 rfl];
phi_dot=[phi_dot_right;phi_dot_left];

J2_phi=[J2*phi_dot;0];

%Rolling Constraints

J1f_1 = [sin(alpha1+beta1) -cos(alpha1+beta1) -l*cos(beta1)];
J1f_2 = [sin(alpha2+beta2) -cos(alpha2+beta2) -l*cos(beta2)];

%Sliding Constraints

C1f = [cos(alpha1+beta1) sin(alpha1+beta1) l*sin(beta1)];

%Constraint matrix

C=inv([J1f_1;J1f_2;C1f]);
```

```
rot_theta = [cos(theta) -sin(theta) 0 ; sin(theta) cos(theta) 0 ; 0 0 1];

epsilon = rot_theta*C*J2_phi;

x_dot = epsilon(1,1);
y_dot = epsilon(2,1);
theta_dot = epsilon(3,1);

%======== Rear Wheel Model ========================

psi = gamma+theta;

%determine the right rear wheel velocity

gamma_dot=(1/(d))*(-epsilon(1,1)*sin(psi)+epsilon(2,1)*cos(psi)-d*epsilon(3,1));

phi_dot_right_rear =
(1/rrr)*(epsilon(1,1)*cos(psi)+epsilon(2,1)*sin(psi)+p*(gamma_dot+epsilon(3,1)));

%determine the left rear wheel velocity

phi_dot_left_rear = (1/rlr)*(epsilon(1,1)*cos(psi)+epsilon(2,1)*sin(psi)-
p*(gamma_dot+epsilon(3,1)));

%======== Plot the resulting kinematic pose ==========

%Plot the NERV body

NERVplotting(l,d,p,theta,gamma+theta,CG)
```

Matlab m-file script code for the Solution Plotting program.

```
% Sean Baity
% August 26, 2005
%
%
% close all;
% clear all;
% clc;
% ===============  Kinematic Model of a Two-Body Articulated Planar Vehicle
=============
%
%
function []= NERVplotting(Df,Da,Dr,theta,beta,P)
%
% ===============  Body Orientation parameters  ==============

theta = theta-(pi/2); % The angle between the robot frame of the front section and and
intertial frame

beta = beta-(pi/2); % the angle of the robot frame of the rear section and the intertial
frame

% ===============  Define a z-axis rotation matrix  ===========

rotZ_theta =[cos(theta),-sin(theta);sin(theta),cos(theta)];

rotZ_beta = [cos(beta),-sin(beta);sin(beta),cos(beta)];

% rotZ_theta_beta = [cos(theta+beta),sin(theta+beta);-
sin(theta+beta),cos(theta+beta)];

% The vehicle is defined with two coordinate systems: front space and rear space
```

```
% Front space is the coord system attached to the front section of the vehicle
% Rear space is the coord system attached to the rear section of the vehicle

% Define the location of the front wheels in front space

Fr_dp = [Df;0];
Fl_dp = [-Df;0];

% Define the rear wheels in rear space

Rr_p = [Dr;-Da];
Rl_p = [-Dr;-Da];

R_p = [0;-Da];

% Map front wheel positions to rear space

Fr_p = rotZ_theta*Fr_dp;
Fl_p = rotZ_theta*Fl_dp;

% Map front wheel positions to robot space

Fr = Fr_p;
Fl = Fl_p;

% Map front wheel positions to world space

Fr_w = Fr + P;
Fl_w = Fl + P;

% Plot the position of the front wheels in world space

hold on;
%axis([-2 2 -2 2])
axis equal
plot(Fr_w(1,1),Fr_w(2,1),'rx','MarkerSize',10)
plot(Fl_w(1,1),Fl_w(2,1),'bx','MarkerSize',10)

% Map rear wheel positions to robot space

Rr = rotZ_beta*Rr_p;
Rl = rotZ_beta*Rl_p;

R = rotZ_beta*R_p;

% Map rear wheel positions to world space

Rr_w = Rr + P;
Rl_w = Rl + P;

R_w = R + P;

% Plot the position of the rear wheels in world space


plot(Rr_w(1,1),Rr_w(2,1),'ro','MarkerSize',10)
plot(Rl_w(1,1),Rl_w(2,1),'bo','MarkerSize',10)

plot(R_w(1,1),R_w(2,1),'k','MarkerSize',5)

% Plot the position of the front axle in robot space

plot([Fr_w(1,1),Fl_w(1,1)],[Fr_w(2,1),Fl_w(2,1)],'k')

% Plot the position of the rear axle in robot space
```

```
plot([Rr_w(1,1),Rl_w(1,1)],[Rr_w(2,1),Rl_w(2,1)],'k')

% Plot the position of the connecting rod in robot space

plot([R_w(1,1),P(1,1)],[R_w(2,1),P(2,1)],'k')

grid on

xlabel('Global X-Position, meters')
ylabel('Global Y-Position, meters')
title('Motion in the Global Inertial Coordinate Frame')
```

Matlab m-file script code for the Instrumentation Simulation Driver Program.

```
% Sean Baity
% 10-18-05
% NERV Kinematic Model
% Instrumented Kinematic Simulation Driver Program

% Flush memory
close all;
clear all;
clc;

t=1;
for t=1:1:4;

j=0;
for j=0:5:360
% ==================== Ideal Kinematic Model  ================

% +++++++++  Vehicle Parameters and Initial Conditions +++++++++

rfr = 0.1; %diameter of the right wheel, meters
rfl = 0.1; %diameter of the left wheel, meters
rrr = 0.1; %diameter of the rear right wheel, meters
rrl = 0.1; %diameter of the rear left wheel, meters

theta = 90*(pi/180); %intial angle of the vehicle in world space
theta_int=theta;
gamma = (j)*(pi/180) %initial angle between the front section robot frame and the rear
section
gamma_int=gamma;
CG = [0;0]; %vehicle origin in intertial space
CG_int = CG;

l = 0.25; %distance between the wheel and the center point CG, meters
d = 0.5;  %distance between center point and rear axle, meters
p = 0.25; %distance between rear axle center point and wheel, meters

phi_dot_right = 2; %rotational speed of the left wheel, radians/sec
phi_dot_left= 2-t; %rotational speed of the right wheel, radians/sec

plot_flag = 0; %Produce Plots Flag: 'Yes' = 1  'No' = 0

% ++++++ Simulation Model Parameters ++++++

delta_t = 0.1; %seconds
sim_length = 4; %number of seconds to run the sim

i = 0;
k = 1;

for i = 0:delta_t:sim_length
```

```
% Call NERV Model for Kinematic Anlaysis based on physical parameters

[x_dot, y_dot, theta_dot, gamma_dot,phi_dot_right_rear,phi_dot_left_rear]=
NERV_iterate(rfr,rfl,rrr,rrl,l,d,p,theta,gamma,CG,phi_dot_right,phi_dot_left,plot_flag);

%Log variables for display
gamma_deg = (180/pi)*gamma;
gamma_log(:,k)= [i;gamma_deg];
gamma_dot_log(:,k) =[i;gamma_dot];
x_dot_log(:,k) = [i;x_dot];
y_dot_log(:,k) = [i;y_dot];
phi_dot_right_rear_log(:,k) = [i;phi_dot_right_rear];
phi_dot_left_rear_log(:,k) = [i;phi_dot_left_rear];

% Update parameters for iterative analysis
CG = CG + [x_dot*delta_t; y_dot*delta_t];
theta = theta + theta_dot*delta_t;
gamma = gamma + gamma_dot*delta_t;

% Update step counts
i = i + delta_t;
k = k + 1;
end
%     ====================          Instrumented     Joint     Angle     Model
================

%Determine the angular resolution of the joint measurement based upon the bit resolution
of the
%instrumentation used to measure the joint angle.

res=10;
x=1;

for res = 12:2:18;

abs_encoder_res = res; %Digital resolution of the absolute encoder that is used to
determine the body angle gamma, bits
angle_res = (2*pi)/(2^abs_encoder_res); %The angular resolution of the absolute
encoder, radians

variance_angle = ((angle_res^2)/12)*(180/pi);
std_dev_angle = sqrt(variance_angle)*(180/pi);

% +++++++++  Vehicle Parameters and Initial Conditions +++++++++

%reset intial angle conditions
theta = theta_int; %intial angle of the vehicle in world space
gamma_er = (round(((gamma_int))/angle_res))*angle_res; %initial angle between the
front section robot frame and the rear section
CG=CG_int;
i = 0;
k = 1;

for i = 0:delta_t:sim_length

% Call NERV Model for Kinematic Anlaysis based on physical parameters

[x_dot, y_dot, theta_dot, gamma_dot,phi_dot_right_rear,phi_dot_left_rear]=
NERV_iterate(rfr,rfl,rrr,rrl,l,d,p,theta,gamma_er,CG,phi_dot_right,phi_dot_left,plot_flag);

%Log variables for display
gamma_deg_er = (180/pi)*gamma_er;
gamma_log_er(:,k)= [i;gamma_deg_er];
gamma_dot_log_er(:,k)= [i;gamma_dot];
x_dot_log_er(:,k) = [i;x_dot];
```

```
y_dot_log_er(:,k) = [i;y_dot];
phi_dot_right_rear_log_er(:,k) = [i;phi_dot_right_rear];
phi_dot_left_rear_log_er(:,k) = [i;phi_dot_left_rear];

% Update parameters for iterative analysis
CG = CG + [x_dot*delta_t; y_dot*delta_t];
theta = theta + theta_dot*delta_t;
gamma_er = (floor((gamma_er + gamma_dot*delta_t)/angle_res))*angle_res;

% Update step counts
i = i + delta_t;
k = k + 1;
end

% Calculate the residuals between the kinematic model and the simualtion including
instrumentation results

res_rl = phi_dot_left_rear_log(2,:) - phi_dot_left_rear_log_er(2,:);
res_rr = phi_dot_right_rear_log(2,:) - phi_dot_right_rear_log_er(2,:);
res_gamma = gamma_log(2,:)-gamma_log_er(2,:);
res_gamma_dot = gamma_dot_log(2,:)-gamma_dot_log_er(2,:);

%determine the average residual error

res_rl_avg(j+1,x) = abs(sum(res_rl)/length(res_rl));
res_rr_avg(j+1,x) = abs(sum(res_rr)/length(res_rr));
res_gamma_avg(j+1,x) = abs( sum(res_gamma)/length(res_gamma));

res = res+1;
x=x+1;
end
j=j+1;
end

figure

hold on
subplot(1,3,1),plot(res_gamma_avg,'*')
ylabel('Average Residual, degrees')
title('Gamma')
grid on
hold on
axis tight
legend('12 bit','14 bit','16 bit','18 bit')
subplot(1,3,2),plot(res_rl_avg,'*')
ylabel('Average Residual, radians/second')
title('Rear Left Wheel Speed')
grid on
axis tight
subplot(1,3,3),plot(res_rr_avg,'*')
ylabel('Average Residual, radians/second')
title('Rear Right Wheel Speed')
grid on
axis tight
suplabel('Inital Angle of Gamma, degrees','x')
t=t+2;
end
```

10.2 Example Motion Simulation Cases

Simulation results for a number of supplementary cases for motion of the two-bodied robotic vehicle platform.

Case #1: Zero radius turn

Table 9: Simulation parameters for case #1

Parameter	**Value**	**Units**
$\dot{\varphi}_1$	-5	rad/sec
$\dot{\varphi}_2$	5	rad/sec
θ	$\pi/2$	radians
γ	0	radians
CG	[0,0]	meters
R_1	0.1	meters
R_2	0.1	meters
R_R	0.1	meters
R_L	0.1	meters
l	0.25	meters
d	0.5	meters
p	0.25	meters
Δt	0.1	seconds
t	2	seconds

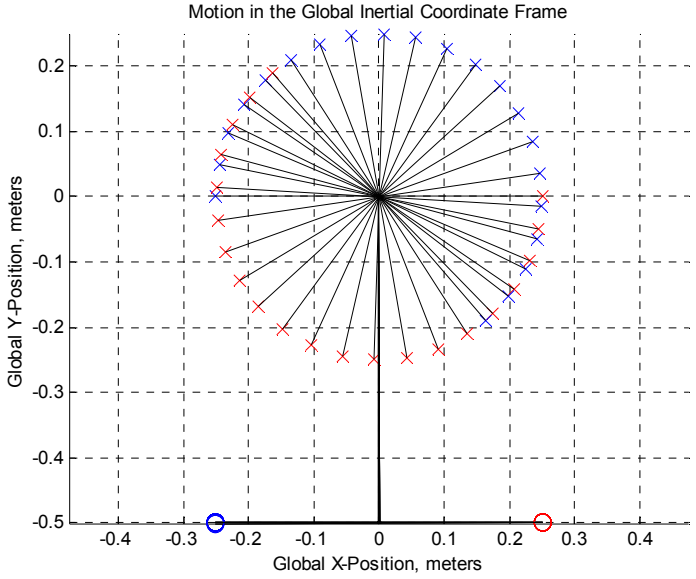

Figure 89: Simulation results for case #1 executing a zero radius turn

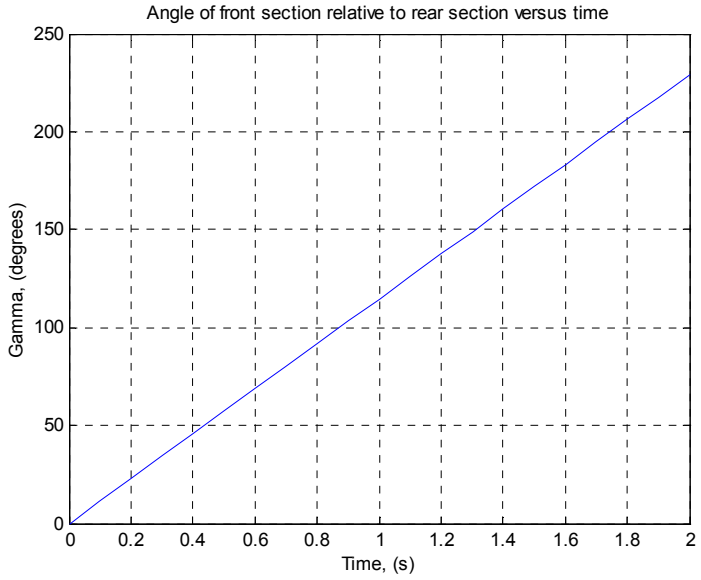

Figure 90: Body angle gamma as a function of time for case #1.

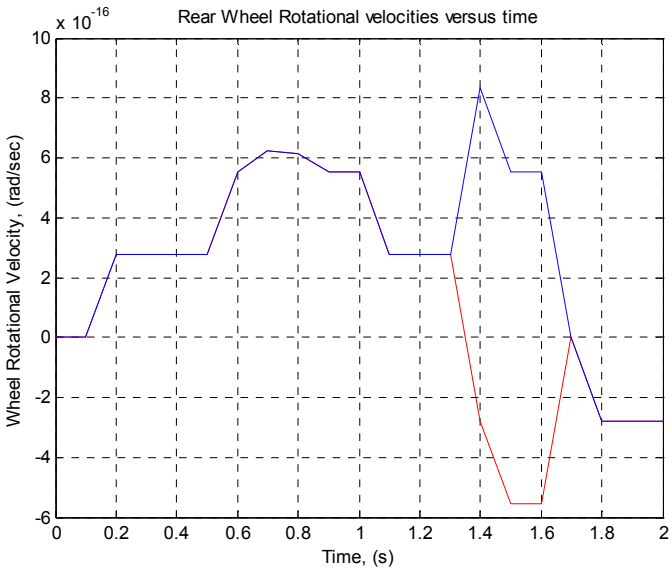

Figure 91: Rear wheel velocities for case #1

Case #2: Driving both front wheels in the negative direction.

Table 10: Simulation parameters for case #2

Parameter	Value	Units
$\dot{\varphi}_1$	-5	rad/sec
$\dot{\varphi}_2$	-2	rad/sec
θ	$\pi/2$	radians
γ	0	radians
CG	[0,0]	meters
R_1	0.1	meters
R_2	0.1	meters
R_R	0.1	meters
R_L	0.1	meters
l	0.25	meters
d	0.5	meters
p	0.25	meters
Δt	0.1	seconds
t	5	seconds

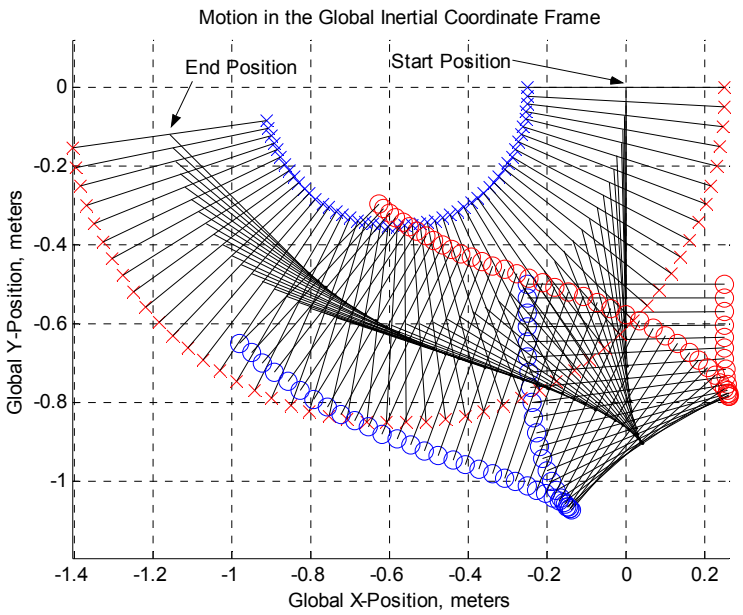

Figure 92: Resulting position for case #2.

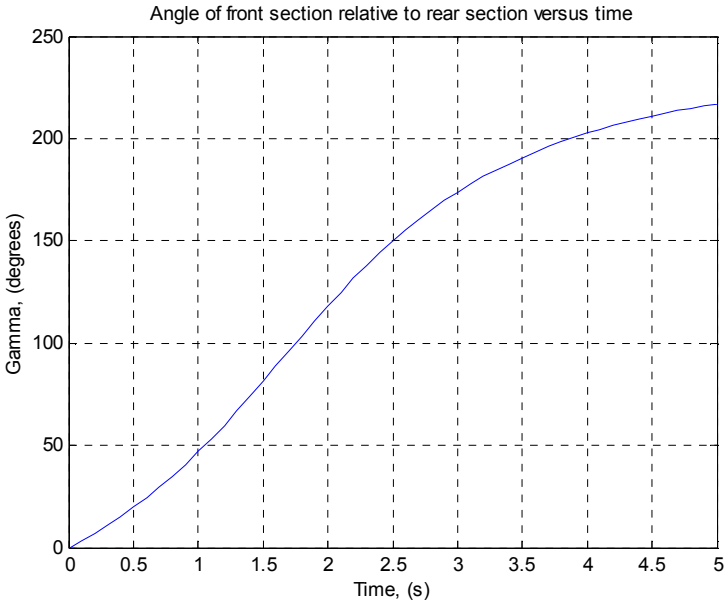

Figure 93: Body angle as a function of time for case #2.

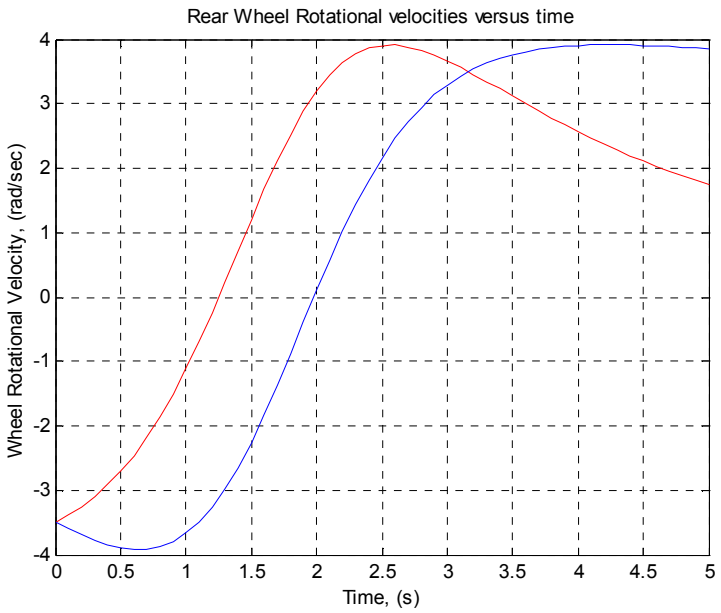

Figure 94: Rear wheel velocities for case #2.

Case #3: Orthogonal initial pose

Table 11: Simulation parameters for case #2

Parameter	Value	Units
$\dot{\varphi}_1$	5	rad/sec
$\dot{\varphi}_2$	5	rad/sec
θ	$\pi/2$	radians
γ	$-\pi/2$	radians
CG	[0,0]	meters
R_1	0.1	meters
R_2	0.1	meters
R_R	0.1	meters
R_L	0.1	meters
l	0.25	meters
d	0.5	meters
p	0.25	meters
Δt	0.1	seconds
t	4	seconds

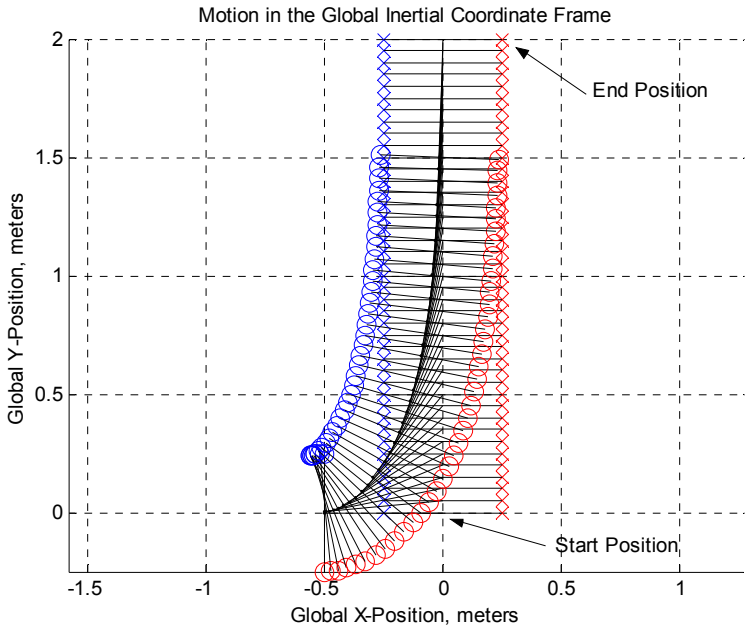

Figure 95: Resulting motion for case #3

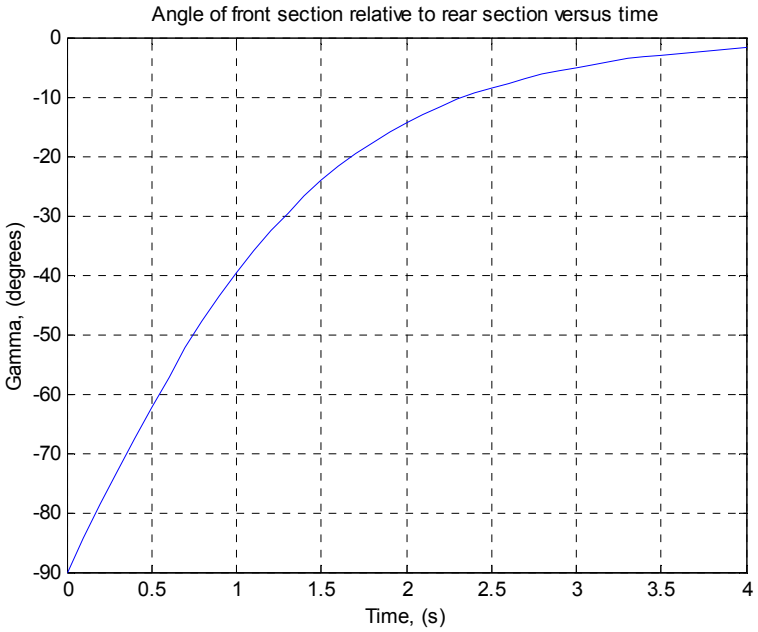

Figure 96: Body angle as a function of time for case #3

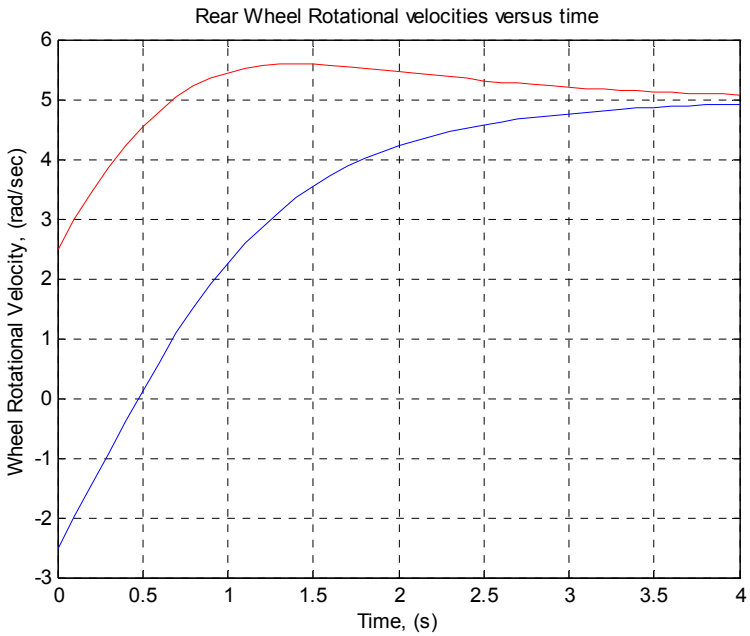

Figure 97: Rear wheel velocities for case #3. Red indicated right rear wheel while blue is the left rear wheel.

10.3 Instrumented Body Angle Model versus Ideal Model

In an effort to specify the absolute encoder that would be required to implement a four-wheel drive NERV platform, it was necessary to investigate the impact of utilizing a discrete measurement system as the feedback device to measure body angle between the front and rear sections of the two-body vehicle platform.

Utilizing the Matlab code generated to develop the ideal kinematic model presented in developed in Section 3.1.2 and detailed in Sections 3.1.3, 10.1 and 10.2, it was possible to compare the results of an ideal case where the body angle is known precisely to the case where the angle measurements are quantized as a result of analog-to-digital conversion or discrete encoding methods.

For the application of measurement of the joint angle between the front and rear sections of the vehicle, it is necessary to know the angle measurement absolutely within a single complete revolution. Generally, the error of an absolute encoder measurement is ± ½ LSB with the variance of the measurement determined by Equation 23, with N being the number of bits of resolution of the encoder. The assumption being that the probability of the angle measurement being between two of the discrete values is a uniform distribution of 100 percent.

$$\sigma^2 = \frac{1}{12} * \left(\frac{2\pi}{2^N} \right)^2 \quad (23)$$

With the theoretical error known for a specific absolute encoder at a particular bit resolution, it is then possible to modify the ideal kinematic model to investigate the impact of the measurement error on the calculated motion of the rear wheels. Excessive error within the kinematic calculations will prohibit proper locomotion or possibly damage the vehicle particularly if the vehicle is driving all four wheels.

To analyze the movement error of the vehicle model when the angular position feedback is non-ideal, the kinematic simulation software was altered to run the simulation with the value of the body angle γ conforming to the discrete values of angular measurement resulting from a particular effective bit resolution. This model is referred to as the instrumented model indicating that the results include allowances for error arising from practical measurement of the body angle. For a particular initial value of γ and front wheel rotational velocities, the instrumented simulation results were compared to the ideal model results. To quantify the amount of observed error resulting from the implementation of a particular measurement device with a specific bit resolution, the residuals between the ideal and instrumented motion were calculated. For each set of γ and wheel speed initial conditions, a series of common bit resolutions were applied to investigate what bit resolution would be required to maintain a particular threshold of performance. Initial simulation results indicated a range of encoder bit resolutions that would provide reasonable results. Encoder resolutions below eight bits yielded readily apparent discontinuous motion. The resulting motion of a simulation with an eight bit encoder implemented to measure the angle between the front and rear sections with a resolution of 1.4° as shown in Figure 98. It is apparent the resulting motion lacks the curvilinear result of the ideal kinematic simulation and that if an eight bit encoder were to be used in practical application that the resulting motion would not be acceptable.

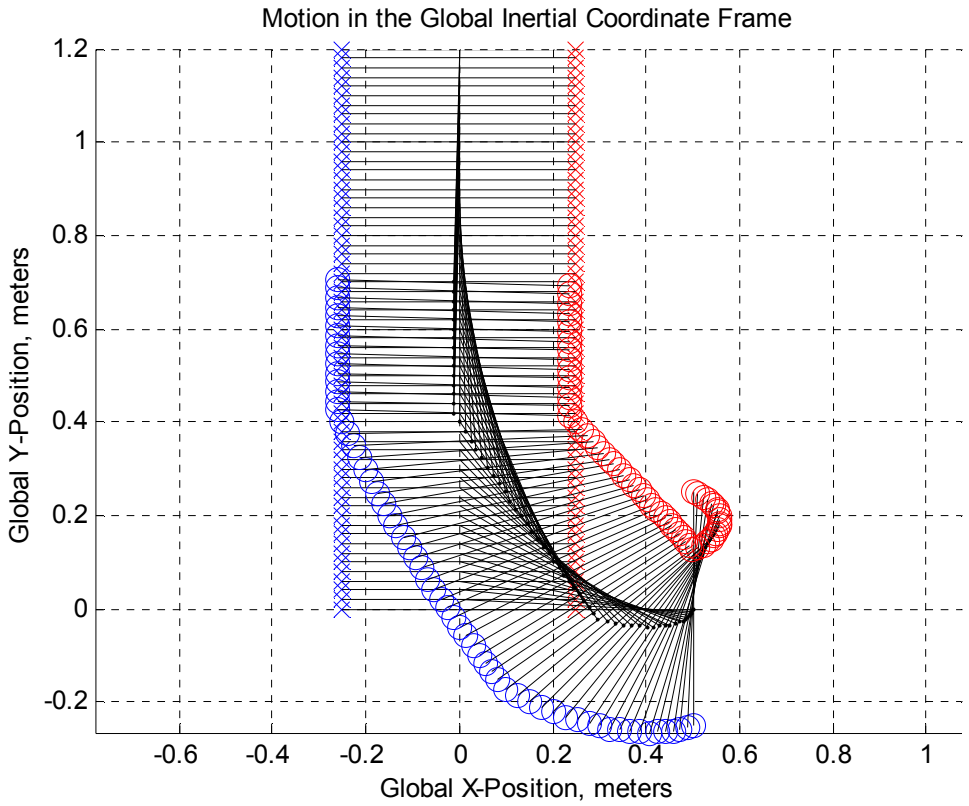

Figure 98: Discontinuous motion as a result of an 8 bit encoder to measure body angle

The results of the instrumented simulation indicated that predicted motion with encoders of resolutions less than twelve bits included readily apparent discontinuities. Table 12 summarizes the bit resolutions under consideration.

Table 12: Summary of the encoder bit resolutions under consideration.

Bit Resolution
12 bits
14 bits
16 bits
18 bits

For the calculation of the residual errors for each bit resolution under consideration, the simulation was run for a range of values of $0 \le \gamma \le 2\pi$. The value of θ was held constant as it was assumed that the orientation of the front section relative to the inertial coordinate frame had no bearing on the error induced by the discrete measurement of the

relative angle between the front and rear sections. In addition, the process of running the comparative simulation for the full range of γ for each possible bit resolution was run multiple times for a range of front wheel speed combinations. These combinations simulated several cases where the front section vehicle moved with varying turning radii to analyze the impact of motion on the error observed in the angular measurement. Table 13 summarizes the combinations of front wheel speeds used for the analysis cases.

Table 13: Summary of the encoder bit resolutions under consideration.

Simulation Case	Left Front Wheel Speed (radians/sec)	Right Front Wheel Speed (radians/sec)
#1	2	2
#2	1	2
#3	0	2
#4	-1	2
#5	-2	2

The results of the analysis are presented in three graphs for each wheel speed case. The first graph shows the average residuals between the ideal and instrumented values of γ for each bit resolution under consideration for the range of $0 \le \gamma \le 2\pi$. The simulation was run for a total of four seconds at a time step of 0.1 seconds. The simulation length of four seconds provided for the vehicle to achieve steady state for a given set of input speeds and provides a reasonable estimate for the transient errors observed during short turning motions. The second graph similarly details the average residuals for the left rear wheel rotational velocity for each bit resolution case through the full range of γ. Likewise, the third plot details the average residuals for the right rear wheel. The results for the first wheel speed case are detailed in Figure 99.

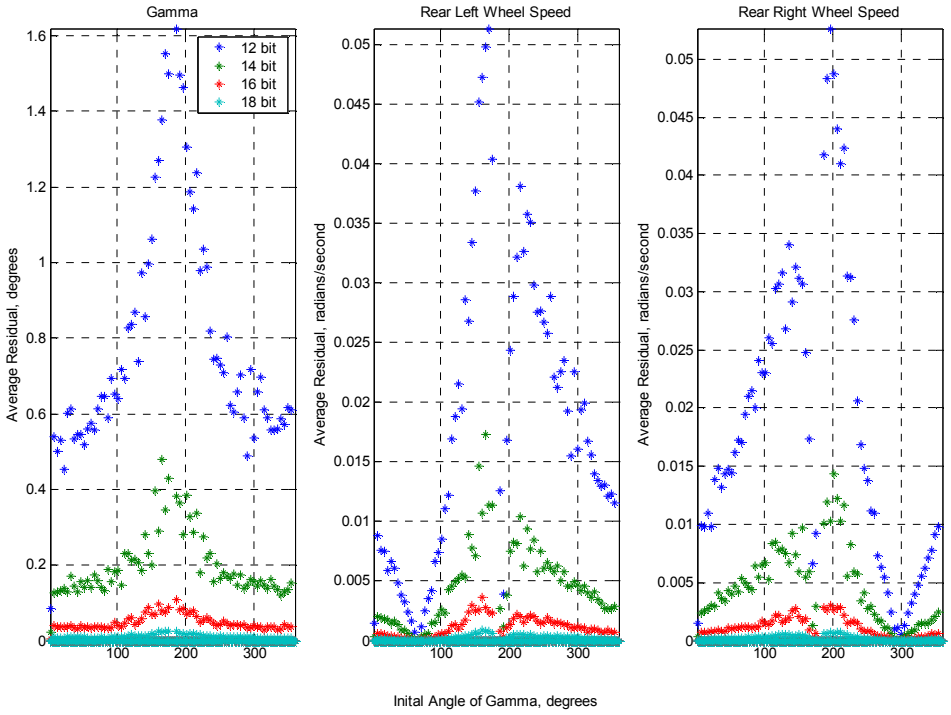

Figure 99: Absolute value of the residuals for the first wheel velocity case.

The results for wheel speed cases are detailed in Figures 100 through 103. Figure 103 details the error present in the zero radius turn case.

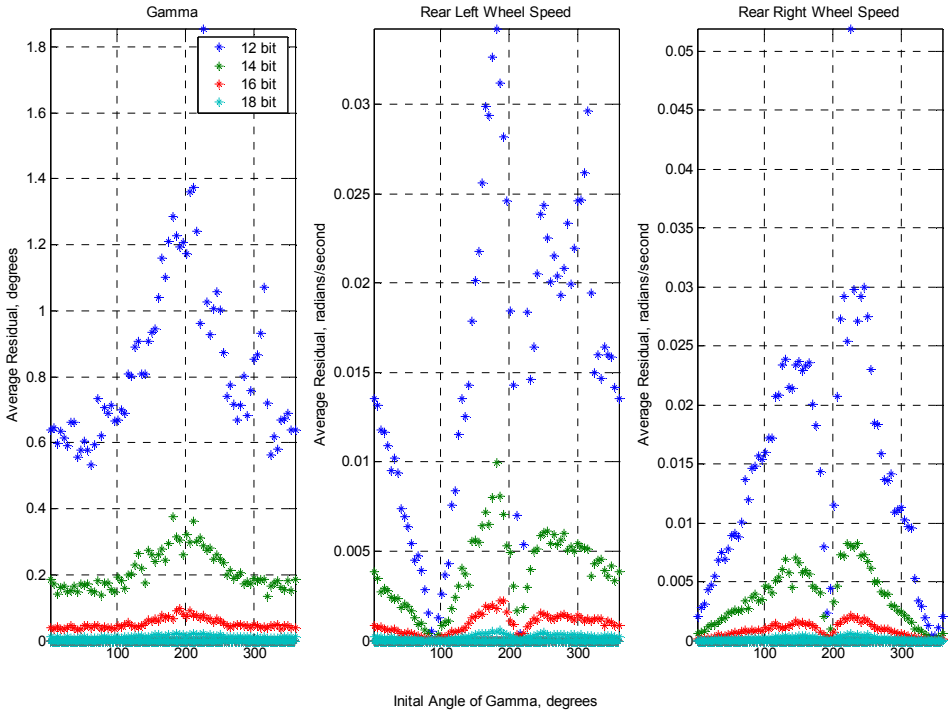

Figure 100: Absolute value of the residuals for the second wheel velocity case

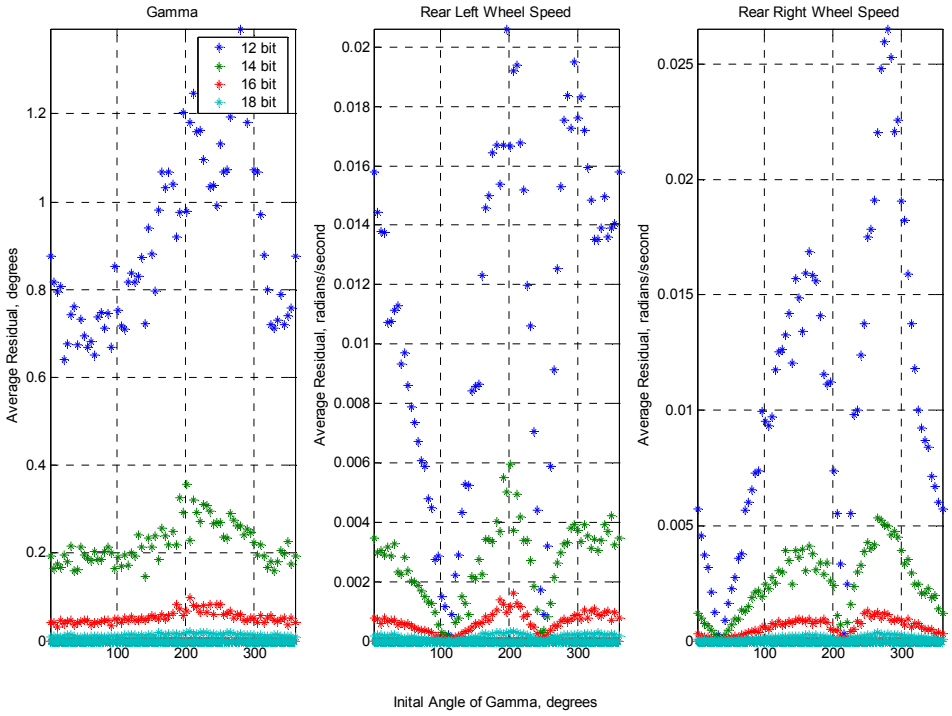

Figure 101: Absolute value of the residuals for the third wheel velocity case

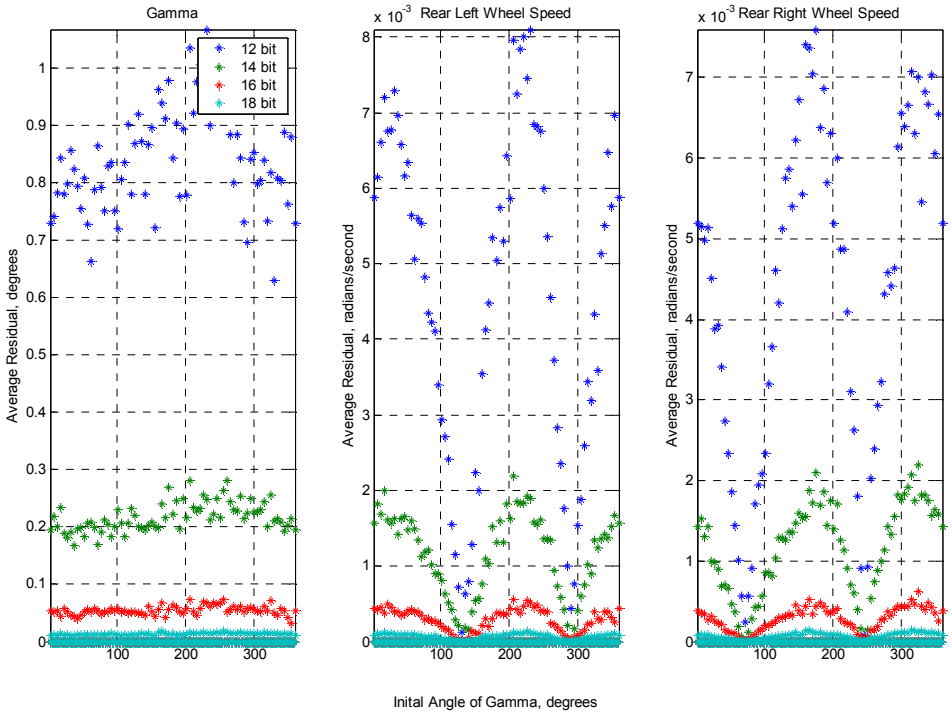

Figure 102: Absolute Value of the residuals for the fourth wheel velocity case

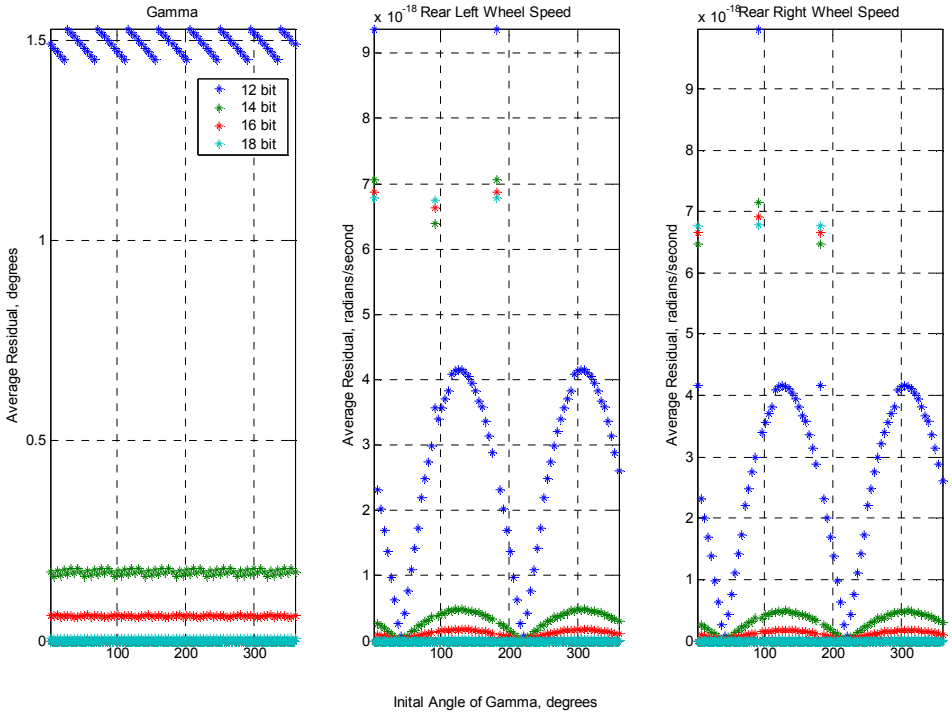

Figure 103: Absolute value of the residuals for the fifth wheel velocity case

It is interesting to note that the error in the measured value of γ increases at specific configurations of the initial value of γ used for the simulation. It is also apparent that the point at which the increased error occurs shifts depending on the wheel velocity case. For the first velocity case the peak in the average residuals for the measured value of γ is approximately when the initial value of γ is equal to 180 degrees. For second and third wheel velocity cases, the initial angle of γ that yields the peak error shifts to roughly 200 and 220 degrees, respectively. This peak in residual measurement occurs for each bit resolution examined in the simulation but it is apparent that the increased angular resolution diminishes the peak values of error.

The source of the increased error can be attributed to the pose of the vehicle during the simulation. The point at which the error peaks is linked directly to the vehicle pose where the front section is essentially "pushing" the rear section rather than the normal operation mode where the front "pulls" the rear trailing section, illustrated in Figures 104 and 105 respectively. This "pushing" motion is analogous to pushing a caster wheel rather than pulling it. When a caster wheel is pulled it naturally tends to swing around to follow the pulling action, which is the vertical axis of caster turning leads the axis of wheel rotation. When a caster wheel is pushed straight forward it is very difficult to maintain a perfectly straight path as the tendency of the wheel is to swing around to the natural following position.

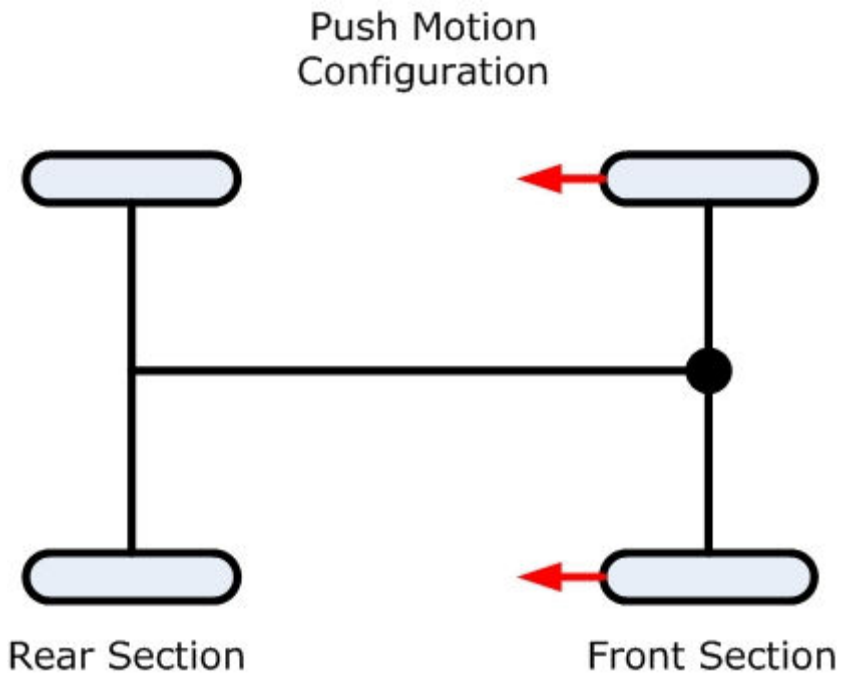

Figure 104: "Push" configuration of the two-body vehicle design

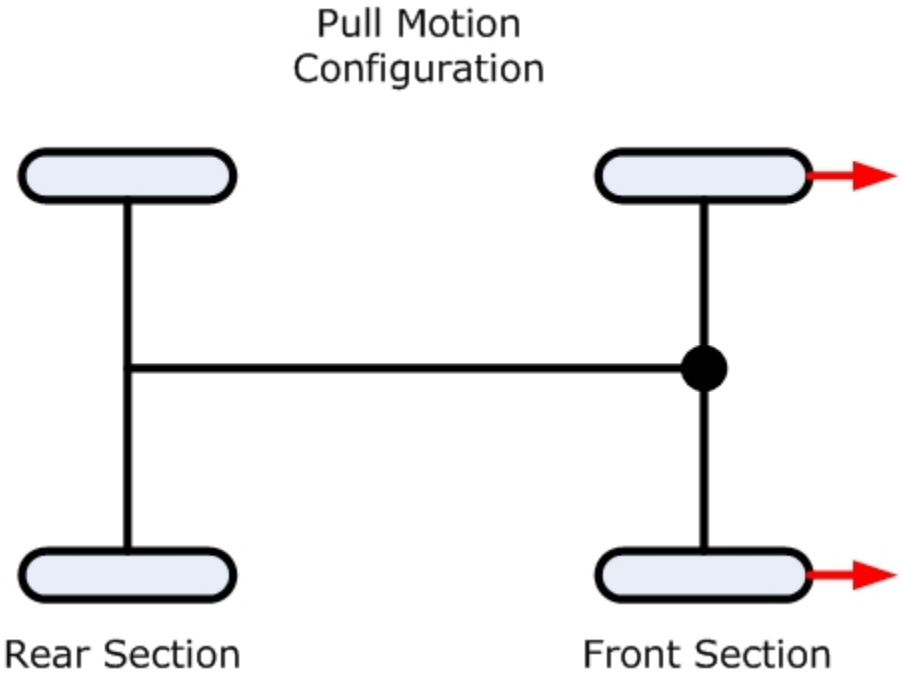

Figure 105: "Pull" configuration of the two-body vehicle design

The magnitude of the increased error in the simulation results were more pronounced in the first wheel velocity case where the vehicle front section was driven with

both wheels rotating in at the same speed. The resulting motion of the front section was a straight path essentially pushing the rear section. The yielded the situation where the relative angle γ was theoretically predicted to maintain a value of zero. However, the introduction of the quantized angular measurement from the joint angle measurement encoder caused the value to shift away from a value of zero by a small amount. In the pushing configuration, this small deviation has a significant impact on the motion of the rear section. Much like the caster wheel being pushed, the rear section of the vehicle would strive to swing around to follow the front section rather than be pushed. A small angular deviation would induce a rapid change in angular rotation rate of the rear section relative to the front to achieve a kinematically balanced position. This rapid change in magnitude of the value of $\dot{\gamma}$ would induce a large error in the calculated rear wheel speeds and thus begin to deviate from the theoretically model and could become unstable as the value could shift further and further away from the desired result.

This source of error in the angular measurement is of less concern as the vehicle is oriented in the natural pull orientation as small changes in the relative body angle γ do not lead to large values of $\dot{\gamma}$. This effect is observed in the plot of the residuals as the errors trail off from the peak values and when the front wheel speeds move the front section in a circular path avoiding the pushing configuration for extended periods of time.

With consideration to time and money constraints of the experiment of applying this method on the Gemini two-body articulated platform for the purpose of validating the kinematic model and it's application to the NERV platform, it was determined that a 15 bit absolute encoder was the most readily available solution that would yield acceptable results. The instrumented simulation was performed again to compare the errors resulting from the 15 bit encoder compared to the 16 bit results. Figure 106 details the results of the simulation for the first wheel velocity case as this velocity case had the largest peak residual error.

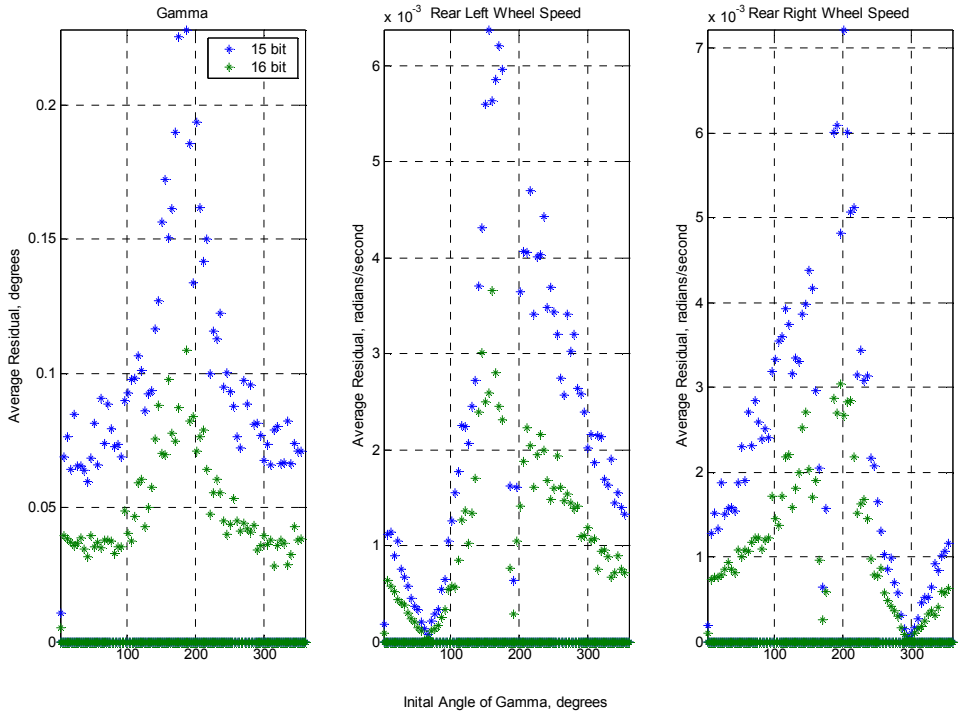

Figure 106: Absolute value of the residuals for the instrumented simulation for a 15 and 16 bit encoder.

While the 15 bit encoder appears to have significantly more error in the body angle measurement application, the levels of error are not excessive as the average residual for the value of γ is less than 0.1° with peak errors less than 0.25°. These angular measurements yield a deviation in the expected rear wheel velocities of less than approximately 0.007 radians per second. The impact of these errors will be investigated in the practical application of the encoder system to measure the relative body angle.

11 References

[1] http://www.darpa.mil/grandchallenge04/sponsor_toolkit/congress_lang.pdf

[2] Department of Defense, "DOD Robotics Master Plan for Unmanned Ground Vehicles", 2 June 1989

[3] Williams, F., "U.S. Military funding boost to bring robots into the home", Financial Times, 21 October 2004

[4] Williams, F., "U.S. Military funding boost to bring robots into the home", Financial Times, 21 October 2004

[5] Frost and Sullivan, "Technological Advances Needed for Future Combat Systems", Business Wire, 2005

[6] Frost and Sullivan, " U.S. Future Combat Systems Markets", MarketResearch.com, 2004

[7] Joint Robotics Program (JRP) Fiscal Year 2004 Master Plan

[8] The Joint Architecture for Unmanned Systems, "Strategic Plan", Version 1.5, April 2005, www.jauswg.org

[9] Kortenkamp, D., "Integrating Robotics Research", Autonomous Robots, Volume 6, pg 243-245, 1999

[10] Ulrich, K.T., Eppinger, S.D., 2000, *Product Design and Development*, Irwin McGraw-Hill, Boston

[11] Durrant-Whyte, H., "A Critical Review of the State-of-the-Art in Autonomous Land Vehicle Systems and Technology", Sandia National Laboratories, SAND2001-3685, November, 2001

[12] Photograph taken by Dr. Charles Reinholtz. Used with permission.

[13] http://www.calwild.org/photos/content/desert/avawatz2b.jpg

[14] http://www.ftech-net.co.jp/robot/maze01.jpg

[15] http://www.cs.duke.edu/~parr/dpslam/pic3.jpg

[16] http://people.howstuffworks.com/robot2.htm

[17] http://www.sunnewsonline.com/images/Rubbl-19-07-2005.gif

[18] http://images.pennnet.com/articles/mae/thm/th_153659.jpg

[19] http://www.fas.org/man/dod-101/sys/land/m1.htm

[20] http://shiro.wustl.edu/pictures/arizona/arizona-Images/13.jpg

[21] http://srvtb.appliedphysics.swri.edu/asphalt.htm

[22] http://www.sevenlinksranch.com/oldhay.JPG

[23] Alberts, D.S., "Code of Best Practice: Experimentation", DoD Command and Control Research Program, Information Age Transformation Series, July 2002.

[24] Rose, M.F., et al, "Technology Development for Army Unmanned Vehicles", Committee on Army Unmanned Ground Vehicle Technology, National Research Council, National Academy of Sciences, ISBN 0-309-08620-5, 2002.

[25] Gombar, B., Terwelp, C., Fleming, M., Wicks, A. L. and Reinholtz, C.F., "JOUSTER: Joint Unmanned Systems Test, Experimentation and Research Facility," *International Test and Evaluation (ITEA) Journal*, December 2004/January 2005, pp. 9-13.

[26] JAUS Overview Reference Documentation, www.jauswg.org

[27] Coombs, D., Murphy, K., Lacaze, A., Legowik, S., "Driving Autonomously Offroad up to 35 km/h", Proceedings of the 200 Intelligent Vehicles Conference, the Ritz-Carlton Hotel, Dearborn, MI, USA, October 4-5, 2000.

[28] Bellutta, P., Manduchi, R., Matthies, L., Owens, K., Rankin, A., "Terrain Perception for DEMO III", Proceedings of the 200 Intelligent Vehicles Conference, the Ritz-Carlton Hotel, Dearborn, MI, USA, October 4-5, 2000.

[29] Manduchi, R., Castano, A., Talukder, A., Matthies, L., "Obstacle Detection and Terrain Classification for Autonomous Off-Road Navigation", Autonomous Robots, 18, pg 81-102, 2005

[30] http://robot.spawar.navy.mil/

[31] "iRobot's Future Combat Systems Contract Grows to Over $51 Million; Additional Funds Accelerate Development of Small Unmanned Ground Vehicle", Business Wire, May 31, 2005.

[32] McBride, B., Longoria, R., Krotkov, E., "Measurement and Prediction of the Off-Road Mobility of Small Robotic Ground Vehicles", Performance Metrics for Intelligent Systems PerMIS '03, NIST Special Publication 1014, September 16 - 18, 2003

[33] http://www.army-technology.com/contractors/mines/i_robot/

[34] http://www.irobot.com/sp.cfm?pageid=146

[35] http://www.foster-miller.com/projectexamples/t_r_military/talon_robots.htm

[36] http://www.army-technology.com/contractors/civil/foster_miller/foster_miller3.html

[37] http://www.foster-miller.com/projectexamples/t_r_military/talon_robots.htm

[38] Ibid.

[39] Ibid.

[40] http://www.globalsecurity.org/military/systems/ground/talon.htm

[41] http://www.military.com/soldiertech/0,14632,Soldiertech_DragonRobot,,00.html

[42] http://www.sciencedaily.com/releases/2004/06/040629013646.htm

[43] http://www.automatika.com/downloads/319740.stm_files/20040521ho-dragon_230.jpg

[44] http://www.defenselink.mil/transformation/factsheets/Dragon%20Runner.pdf

[45] http://www.military.com/pics/SoldierTech_DragonRunner1.jpg

[46] http://www.activrobots.com/ROBOTS/p2at.html

[47] www.igvc.org

[48] Murphy, R.R., "Introduction to AI Robotics", MIT Press, Cambridge, MA, 2000, pg 165.

[49] Baity, S.M., Gombar, B.A., Fleming, M.R., Reinholtz, C.F., "Design for the Intelligent Ground Vehicle Competition", 5th Annual Intelligent Vehicle Systems Symposium, TARDEC's National Automotive Center and Vetronics Intelligent Systems Technical Review, Traverse City, MI, June 13th-16th, 2005.

[50] http://www.igvc.org/deploy/rules.htm, retrieved by Baity, S., March 25, 2005

[51] Baity, S.M., et al., "Gemini Design Report – 2005", Virginia Tech, 2005 http://www.igvc.org/deploy/design/reports/dr124.pdf

[52] Baity, S.M., et al., "Gemini Design Report – 2004", Virginia Tech, 2004 http://www.igvc.org/deploy/design/reports/dr97.pdf

[53] Rose, M.F., et al, "Technology Development for Army Unmanned Vehicles", Committee on Army Unmanned Ground Vehicle Technology, National Research Council, National Academy of Sciences, ISBN 0-309-08620-5, 2002

[54] Blackburn, M.R, Bailey, R., Lytle, B., "Improved Mobility in a Multi Degree of Freedom Unmanned Ground Vehicle", Office of the Secretary of Defense Joint Robotics Program Coordinator

[55] Durrant-Whyte, H., "A Critical Review of the State-of-the-Art in Autonomous Land Vehicle Systems and Technology", Sandia National Laboratories, SAND2001-3685, November, 2001

[56]Theisen, B.L., DeMinico, M.R., Gill, G.D., "The Intelligent Ground Vehicle Competition – Team Approaches to Intelligent Driving and Navigation", 5th Annual Intelligent Vehicle Systems Symposium, TARDEC's National Automotive Center and Vetronics Intelligent Systems Technical Review, IVSS-2005-UGV-07, Traverse City, MI, June 13th-16th, 2005

[57] Blackburn, M.R, Bailey, R., Lytle, B., "Improved Mobility in a Multi Degree of Freedom Unmanned Ground Vehicle", Office of the Secretary of Defense Joint Robotics Program Coordinator

[58] Robert F. Unger, "Mobility Analysis for the TRADOC Wheeled Versus Track Vehicle Study, Final Report," Department of the Army, Geotechnical Laboratory, Waterways Experiment Station, Vicksburg, Mississippi, (Sept 1981)

[59] Rafter, D., "Tires versus Tracks", Grading and Excavation Contractor, January/February 2005

[60] Hornback, P., "The Wheel Versus Track Dilemma," *Armor Magazine* (March-April 1998).

[61] www.defensereview.com/1_31_2004/Packbot.jpg

[62] Patel, N., Ellery, A., "Performance Evaluation of Autonomous Mars Mini-Rovers", Surrey Space Center, University of Surrey, Guildford, Surrey GU2 7XH

[63] www.activrobots.com

[64] Patel, N., Ellery, A., "Performance Evaluation of Autonomous Mars Mini-Rovers", Surrey Space Center, University of Surrey, Surrey GU2 7XH

[65] Carlson, J., Murphy, R., "How UGVs Physically Fail in the Field", Center for Robot-Assisted Search and Rescue, University of South Florida, 2004

[66] http://www.dansdata.com/images/pershing/climbing560.jpg

[67] http://www.elecdesign.com/Files/29/8076/Figure_02.jpg

[68] Hornback, P., "The Wheel versus Track Dilemma", ARMOR, March-April, 1998

[69] Zahn, B.R., "The Future Combat System: Minimizing Risk While Maximizing Capability", USAWC Strategy Research Project, May 2000.

[70] Carlson, J., Murphy, R., "How UGVs Physically Fail in the Field", Center for Robot-Assisted Search and Rescue, University of South Florida, 2004

[71] Siegwart, R., Nourbakhsh, I.R., "Introduction to Autonomous Mobile Robots", the MIT Press, Cambridge, MA, 2004, pg. 61 - 64

[72] Ibid.

[73] Ojeda, L., Borenstein, J., Witus, G., "Terrain Trafficability Characterization with a Mobile Robot", Proc. Of the SPIE Defense and Security Conference, Unmanned Ground Vehicle Technology VII, Orlando, FL, March 28th to April 1st, 2005

[74] Bruch, M.H., Laird, R.T., Everett, H.R., "Challenges for Deploying Man-Portable Robots into Hostile Environments", *SPIE Proc. 4195: Mobile Robots XV,* Boston, MA, November 5-8, 2000

[75] Joint Architecture for Unmanned Systems, *Reference Architecture Specification,* Volume II, Part 1, Version 3.2, August 13th, 2004

[76] Ibid.

[77] Tobler,C., "Development of an Autonomous Navigation Technology Test Vehicle," M.S. Thesis. Department of Mechanical and Aerospace Engineering, University of Florida, August 2004

[78] Bruch, M.H., Laird, R.T., Everett, H.R., "Challenges for Deploying Man-Portable Robots into Hostile Environments", *SPIE Proc. 4195: Mobile Robots XV,* Boston, MA, November 5-8, 2000

[79] Armstrong, D., Crane, C., Novick, D., Wit, J., English, R., Adsit, P., Shahady, D. "A Modular, Scalable, Architecture For Unmanned Vehicles," Proceedings of the Association for Unmanned Vehicle Systems International (AUVSI) Unmanned Systems 2000 Conference, Orlando, Florida, July 2000